



Politecnico di Torino

Master's degree in Biomedical Engineering

Academic year 2024/2025

Graduation Session December 2024

Study applicability of a BCI system

based on EEG signals

for the recognition of imagined movements

Supervisors:

Prof.ssa Valentina Agostini

Prof. Marco Knafnitz

Dott. Marco Ghislieri

Candidate:

Gabriele Penna 267811

© 2024
Gabriele Penna
ALL RIGHTS RESERVED

Abstract

Brain-computer interfaces (BCI) are systems capable of interpreting the neural activity of a subject and translating it into a digital output signal. BCIs are recognized by the scientific community as a potential remedy for restoring the motor functions of physically impaired patients.

The long-term goal of this study is to restore tetraplegic patients' motor abilities. As they have lost the ability to correctly execute movements, only imagined or attempted movements can be performed. ElectroEncephaloGram (EEG) based BCIs allow for the decoding of imagined movements through a non-invasive approach.

The drawback of these systems is their limited clinical application. While they achieve good performance within a laboratory, they are rarely built to work in a real-life setting and when they do, they can hardly achieve acceptable performances.

The study aims to identify what limitations prevent an EEG-dependent BCI system from being applied in a real-life situation and tries to propose how these limitations can be overcome both from the point of view of the configuration of the experimental protocol and from the point of view of the models applied.

The work is therefore divided into two: an initial study of a classification model, applied to an already existing dataset, and secondly, the development of our own experimental protocol, the data acquisition, and the application of the previously tested models on the new dataset.

The online dataset used is the BCI Competition IV dataset 1, containing EEG signals taken using a 59-electrode helmet from seven healthy subjects executing a Motor Imager (MI) task.

To overcome the limitations of laboratory BCIs, two points have been identified to be applied to the protocol: firstly, to make the BCI subject-independent, so that it does not need to be calibrated on each subject. Second: make the BCI self-paced, thus allowing the subject to freely execute movements asynchronously, without a cue. The acquired dataset consists of the EEG signals taken using a 21-electrode helmet from four healthy subjects executing a MI task.

The models applied are based on different combinations of processing steps and are validated by cross-validation using a fixed training window and a sliding testing window. The signals have been pre-processed with passband time filters in the alpha and beta range, and a Common Average Reference (CAR) filter. To extract useful features a CSP filter has been applied. Two different types of classification algorithms have been used, (LDA and SVM).

On the subject-dependent calibration phase of dataset I of BCI competition IV, the applied models show an accuracy that varies between 76% and 92% when classifying the two

Intentional Control (IC) classes. When classifying between IC and No Control (NC), the accuracy varies between 73% and 84%.

Slightly modified models have been applied to the acquired dataset. The performance results of these models have been in line with the other dataset when classifying between NC and IC while the results dropped when classifying between IC classes. Only the first subject achieved acceptable results, with an accuracy of 67%. The other 3 subjects reported random classification with an accuracy of 50%.

Possible causes are the different kinds of MI tasks performed and errors or inaccuracies in data acquisition and protocol definition.

Future continuations of the study could focus on finding better-performing classification models and revising the experimental protocol by trying to identify its limitations and flaws.

Table of Contents

Abstract.....	1
Table of Contents.....	3
Introduction	6
The brain and its electrical activity	7
Neuroanatomy.....	7
The neuron	10
Brain activity measures.....	12
BCI	14
Definition and History	14
Applications	16
Type of brain signal input.....	17
EEG signal.....	18
Definition and History	18
Properties of EEG signal.....	18
Instrumentation	20
Sampling rate	21
Electrode positioning	22
Referencing.....	24
EEG artifacts.....	26
EEG-dependent BCI.....	27
Typical BCI experiment.....	29
Different BCI systems	31
Characteristics of EEG dependent BCI.....	32
Classes	32
Movements.....	32
Task movement.....	33
Calibration and Validation.....	35

Subject-dependency	36
Synchrony	37
Paradigm	37
Literature Analysis	40
The study's objective	46
Materials and Methods	47
Sample population tested	47
Description Dataset 1 BCI competition IV	49
Acquisition system	49
Hardware.....	50
Recording Software	50
Visual stimulus software.....	51
Analysis Software	53
Experimental protocol.....	54
Calibration phase	56
Validation phase	57
Synchronization of stimuli and data	58
Electrode positioning	60
Recording setting	62
Subject's Questionnaire	62
Experimental protocol aim.....	63
PoliTo ^{BIO} Med Lab Data Visualization.....	64
Processing steps	67
Subject Independent BCI steps	69
Pre-processing.....	70
Epoch Division	74
Feature extraction	74
Classification	78
Performance evaluation.....	79

Statistical testing	82
Results	83
Questionnaire answers	83
Experimental Notes	85
Data Results	85
Dataset 1 BCI competition IV	85
PoliTo ^{BIO} Med Lab data results	97
Discussions	104
Appendices	107
Data Acquisition protocol	107
Introduction.....	107
Amplifier configuration	107
Electrode Cap Configuration	109
Software configuration	113
EEG cleaning	117
Experimental Instructions	118
General principles of good experimentation	119
List of Tables	120
List of Figures.....	122
List of Abbreviations	126
References	127
Acknowledgements	133

Introduction

Neuromuscular disorders are developmental diseases that can occur at different ages. They cause damage to the motor unit, i.e., motor neuron, nerve fiber, muscle, and fibromuscular plate, and can also involve the central nervous system (CNS). Those affected may partially or totally lose the ability to use certain muscles. This loss of motor capacity may involve control of finer movements, such as those of the fingers of the hand, to more extensive movements, such as the use of the lower and upper limbs. Neuromuscular disorders can be of various types, among them we mention genetic disorders, spinal trauma, and ischemic brain injury [1].

The occurrence of these diseases has in many cases devastating physical, economic and psychological effects for the patient [2] [3].

Brain computer Interfaces (BCI) are tools for capturing a patient's neural activity and translating it into movement and are a potential remedy for restoring lost motor skills of patients with neuromuscular diseases [4]. The disadvantage of these systems is their limited clinical application. While they perform well in a laboratory, they are rarely built to work in a real-life setting, and when they do, they can hardly provide acceptable performance [5].

The study aims to identify what limitations prevent a BCI system from being applied in a real-life situation and tries to suggest how these limitations can be overcome to restore the motor output of physically impaired patients, both from the point of view of the configuration of the experimental protocol and from the point of view of the models applied.

The work done in this thesis follows the workflow in Figure 1. Initially, a literature search was performed with the aim of understanding the state of the art of these technologies in application to our goal: to restore the motor output of physically impaired patients. Following the literature search, an experimental protocol for data acquisition was drafted. The data were acquired on healthy patients. However, the protocol was designed for patients with motor impairments and was made so that it could be performed by both healthy patients and patients with motor disabilities. Concurrently with the literature search and protocol drafting work, models were developed to classify imaginary hand movements. The models were initially constructed and tested on BCI competition IV dataset 1 [6], and then applied to our dataset with appropriate modifications.

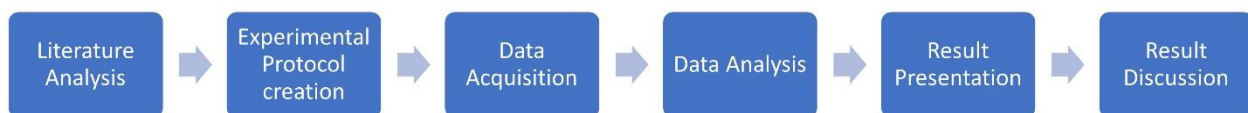


Figure 1: Thesis workflow.

The brain and its electrical activity

Neuroanatomy

The nervous system is divided into 2 parts:

1. The brain and the spinal cord form the Central Nervous System (CNS). Its function is to react to events produced by the outside world or by its own organism and to respond with outputs that meet the body's needs;
2. The Peripheral Nervous System (PNS) carries the messages towards and outside of the CNS. It is in turn divided into two different components: an afferent component, which is responsible for transmitting information from the organs to the CNS, and an efferent component, which is responsible for transmitting information from the CNS to the organs.

The brain is composed of three major parts: the cerebrum, the cerebellum, and the brain stem. Both the brain and the spinal cord are covered by three protective layers called meninges. In order from the outermost to the innermost layer, there is the dura mater, the arachnoid, and the pia mater. The latter layer is rich in veins and arteries [7]. Further layers of bone (the skull), periosteum, and skin cover the brain.

Another characteristic of the brain is that it is divided into 2 paired cerebral hemispheres: the right hemisphere and the left hemisphere. Each hemisphere consists of different layers. The cerebral cortex is the outer layer, also called gray matter. The gray matter is between 1.5 and 4 mm thick and it is convoluted into folds made of gyri and sulci. In the brain, the white matter is beneath the gray matter, while it is the opposite in the spinal cord (Figure1). The gray matter contains mainly neuronal soma (i.e., cell body) and unmyelinated axons, while the white matter mostly contains myelinated axons that interconnect the various cortical and subcortical areas.

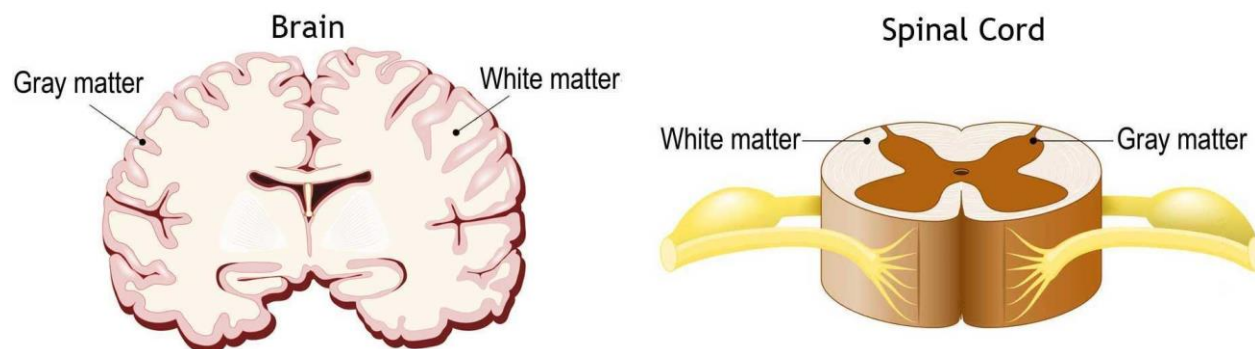


Figure 2: Gray and white matter distribution in the brain (left side) and spinal cord (right side). From "<https://www.hopkinsmedicine.org>".

The cerebral cortex can be divided into 4 main parts or lobes (Figure 2):

1. The Frontal lobe: located in the front part of the brain, includes the motor cortex, involved in the control of motor activity, and other areas involved in language and personality determination;
2. The Parietal lobe: located immediately behind the frontal lobe, comprises the somatosensory cortex, implicated in the processing of sensory information associated with sensations of touch, temperature, and pain;
3. The Occipital lobe: located still behind the parietal lobe and includes the visual cortex, which is implicated in the processing of visual processes;
4. The Temporal lobe: located inferior to the other lobes and comprises the auditory cortex, which is involved in the processing of auditory processes.

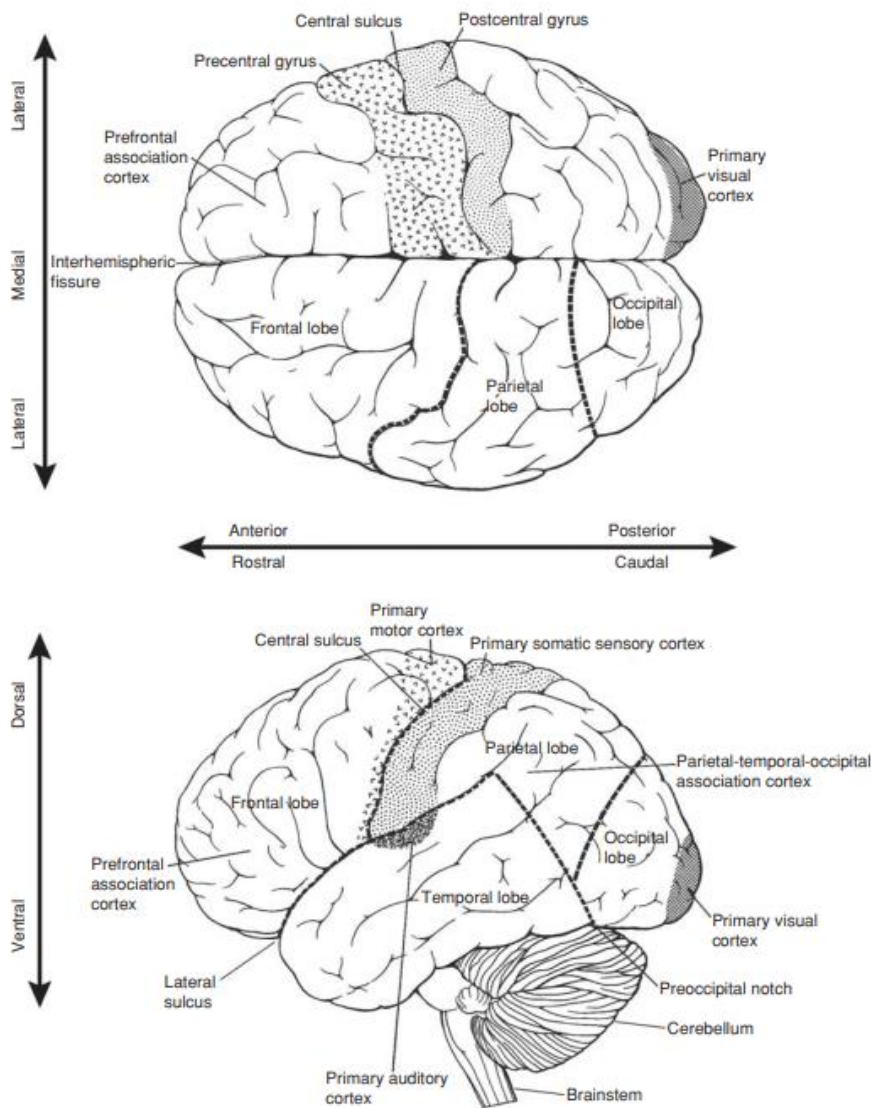


Figure 3: The division of the brain into lobes, the main sulci, and the mapping of certain functions performed by the cortex. From Wolpaw (2012).

Of particular interest to this thesis is the positioning of the motor and somatosensory cortex.

The primary motor cortex lies along the anterior wall of the brain and continues into the precentral gyrus. The primary somatosensory cortex lies along the posterior wall of the brain and continues onto the postcentral gyrus.

Those areas have been first mapped at the beginning of the last century by the work of neurosurgeon Wilder Penfield [8]. His studies led to the well-known map of the motor homunculus (Figure 3). This map shows a distorted human figure, the homunculus, where each body part is associated with an area dedicated to its motor or somatosensory function. The mapping was made possible by direct electrical stimulation of the brain [9].

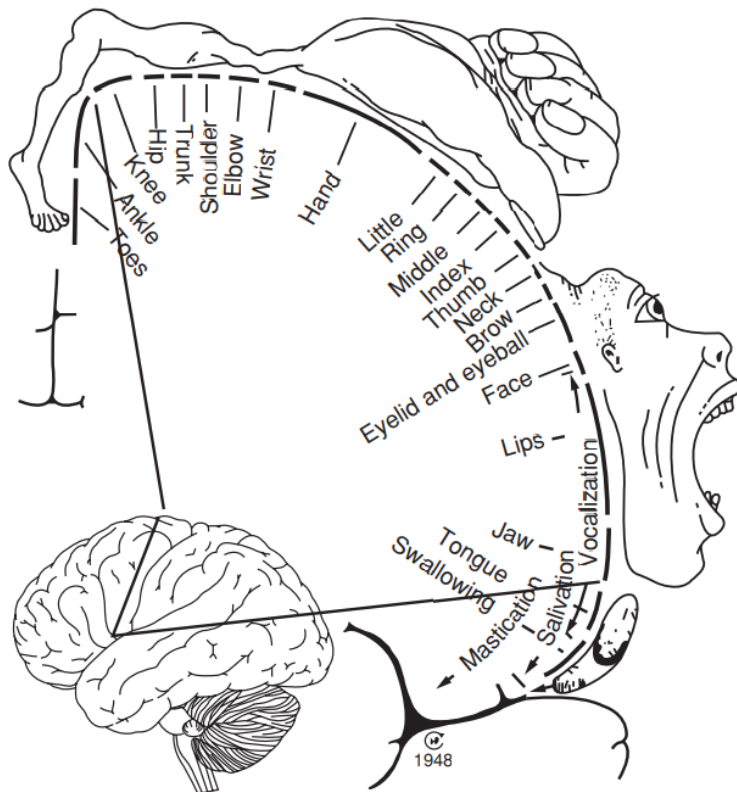


Figure 4: The motor homunculus derived by Wilder Penfield illustrating the effects of electrical stimulation of the cortex of human neurosurgical patients. Adapted from Nolte (2002).

The cortex contains three distinguishable parts which are: the neocortex, the paleocortex, and the archicortex. While the last two are connected to more instinctual and emotive functions, the neocortex is responsible for more complex cerebral functions, such as memory, language, and learning. The neocortex is in turn divided into 6 layers, each layer connected to the other layers and containing a distinctive distribution of neuronal cell types [10].

The neuron

The nervous system is composed of 2 different kinds of cells:

1. Neurons;
2. Glial cells.

Neurons are excitable cells that communicate with each other by transmitting electrical impulses. Glial cells are much more than neuronal cells and perform structural and metabolic support functions for neurons.

The neuron is the basic unit of the brain and each neuron forms 1000 to 10000 connections with other neurons.

Neurons can be classified by function into three groups:

1. Sensory neurons: transmit information from the receptors. Those are afferent neurons;
2. Motor neurons: transmit the information from the CNS to effectors. Those are efferent neurons;
3. Interneurons: connect sensory and motor neurons, do information processing, and participate in the execution of complex cerebral functions such as memory and emotions.

The neurons contain three components (Figure 4):

1. the cell body;
2. the dendrites;
3. the axon.

The cell body contains the nucleus of the neuron. The dendrites branch off the cell body and have the function of receiving information from other neurons. The axon is another branch that develops in the opposite direction to the dendrites and has the function of sending information to other neurons.

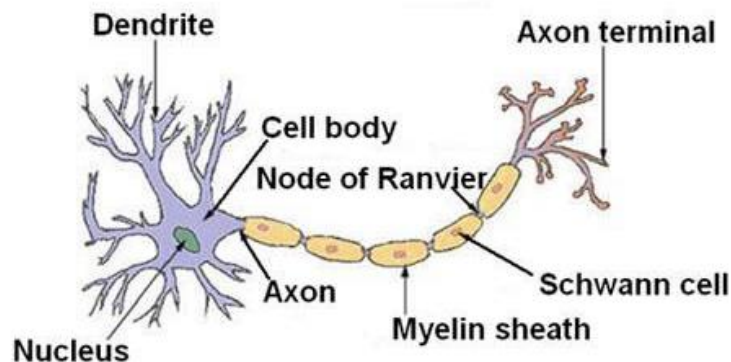


Figure 5: Structure of a typical neuron. From: “www.training.seer.cancer.gov/brain/”

Neurons communicate with each other by generating electrical signals. These electrical signals propagate along axons and are called action potentials. The action potentials transmit information from one neuron to the next one through synapses.

The action potential is a modification of the membrane potential that propagates without attenuation (Figure 5).

There is an “analogic” part of the neuron and a “digital” part. There can be many excitatory and inhibitory postsynaptic potentials from the pre-synaptic neurons (analogic part). The inputs are summed depending on the strength and type of synapse both in time (temporal summation) and space (spatial summation). In the end, the action potential starts only if the depolarization of the

neuron exceeds the threshold, it is either in or out (digital part). Once generated, an action potential propagates without attenuation along the entire axon.

The propagation mechanism of action potentials differs depending on whether myelin or amyelin axons are involved.

Myelin axons allow a faster propagation of the action potential through a mechanism called saltatory conduction. Myelin creates a high resistance to the passage of ionic currents. In the tracts where the myelin is present the membrane depolarization, and thus the propagation of action potentials, only occurs near the nodes of Ranvier. Those are the areas where the myelin sheath enclosing the neurons is interrupted and where all voltage-dependent channels are concentrated. Without myelin the conduction slows down, decreasing the travel of information speed.

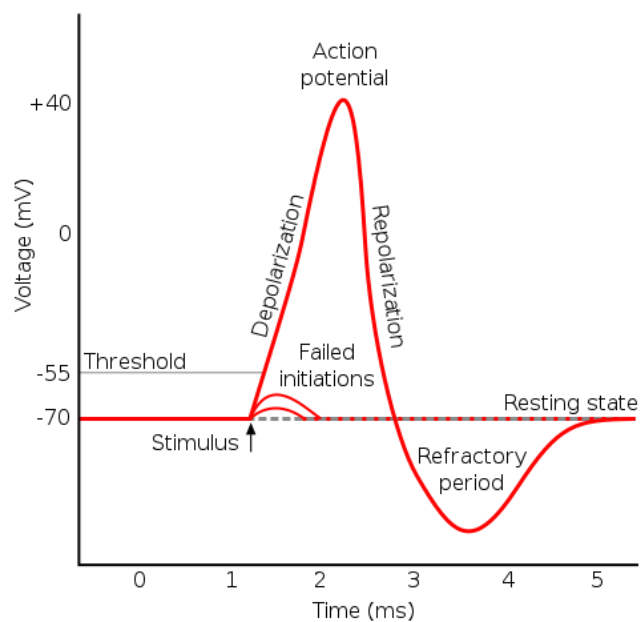


Figure 6: Phases of an action potential in relation to membrane voltage over time. From: "www.teachmephysiology.com"

Brain activity measures

The electric activity of the brain and its component can be measured on different scales. The electric field is generally measured on 4 different scales:

1. Single neuron potential: it is possible to measure directly the intracellular voltage of a single neuron through methods such as the patch clamp;
2. Microscale fields: populations of neurons can be measured over a tissue volume of around 10^{-3} to 1 mm^3 range. Those are the Local Field Potentials (LFPs);

3. Mesoscale field: tissue volumes of 1-20 mm³ can be measured. This scale allows measuring mainly over the surface of the cortex through the ElectroCorticoGram (ECoG);
4. Macroscale field: large areas of the brain can be measured through this scale, with tissue volume around the range of 10³ to 10⁴ mm³. The most used technique at this scale is ElectroEncephaloGraphy (EEG), where each electrode catches the spontaneous cooperative activity of the neural structure within the brain. The EEG measures the activity over the scalp.

BCI

Definition and History

The definition of BCI according to Wolpaw [10] is the following:

“A BCI is a system that measures CNS activity and converts it into artificial output that replaces, restores, enhances, supplements, or improves natural CNS output and thereby changes the ongoing interactions between the CNS and its external or internal environment.”

In essence, BCIs are systems that allow communication between the brain and an external machine.

Systems that control external devices through other biosignals which are not brain signals are not to be considered BCI. Examples of those other biosignals are Electromyography (EMG), ElectroOculoGraphy (EOG), Eye-tracking, Motion capture system, and electrocardiogram (ECG). Nevertheless, those systems can be complementary, and they are often coupled with BCI systems [11] [12].

The first studies on the topic began around the 1970s. In 1973, Vidal published one of the first systemic attempts to implement an EEG-dependent BCI [13].

It is not until the last two decades that the interest in the subject significantly grew. An electronic literature search on PubMed with the keyword “Brain-Computer Interface” published by S. Saha in 2021 [14], shows that the number of publications on the subject has grown considerably in the last ten years compared to the previous decade (Figure 6).

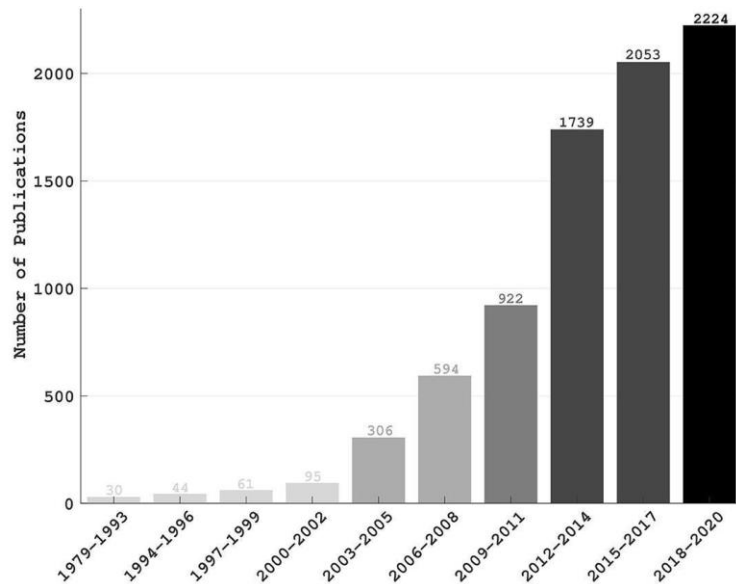


Figure 7: The number of BCI publications over the years. The statistics were based on an electronic literature search on PubMed in which “Brain-Computer Interface” was the search keyword. The articles listed until December 4th have been accounted only. From “Progress in Brain Computer Interface: Challenges and opportunities” by Simanto Saha [14].

This shows a growing scientific community over time interested in the development of this technology. The fields of application are several. BCI can be used in the medical/neuro-rehabilitation field to restore motor output of spinal cord injury patients [15] or as a neuro-rehabilitation tool for post stroke patients. In the gaming sector BCI can be used as a primary means of controlling the game or as an extra channel of communication in games such as Pacman [16] and Tetris [17]. A BCI can also be used in fields such as neuro-marketing, to determine the attitude of a consumer toward a product [18], and security, as a biometric approach for individual identification [19]. Furthermore, it can be used purely for research purposes in closed-loop neuroscience experiments or to do multivariate pattern analysis to learn about brain dynamics [20].

A BCI is of the *active* type when brain activity is directly controlled by the user. In the case where the stimulus arrives from outside, we speak of a *reactive* type of BCI. Conversely, a BCI is said to be *passive* when it uses the extracted information without the goal of voluntary control.

The steps a BCI has to follow to function are the following (Figure 7):

- Signal acquisition;
- Pre-processing;
- Feature extraction;
- Feature translation / Classification;
- Commands / Feedback through a control interface.

The biosignal is acquired during the acquisition phase. The signal is then cleaned and relevant features (useful to the BCI application) are selected. Those extracted features are then classified through the use of machine learning or deep learning algorithms. The outcome or predicted state is then used for the required application [20].

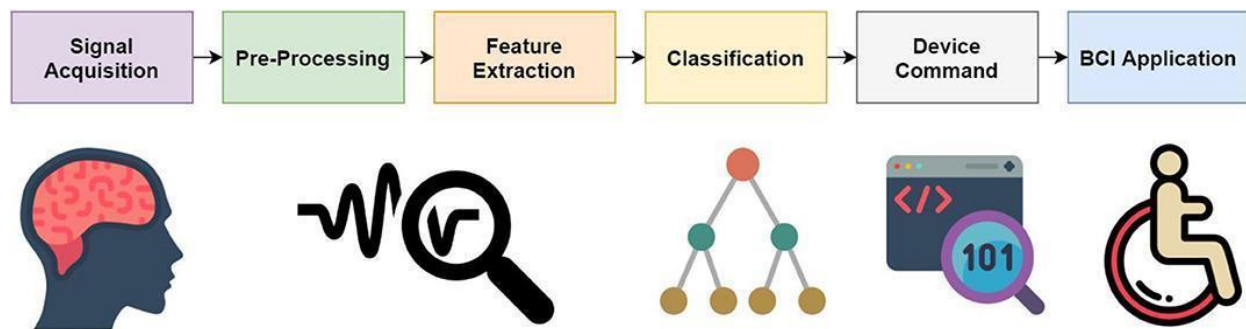


Figure 8: General architecture of a Brain-Computer interface. From M. Rashid (2020) [20].

Applications

It is very important to define the application use of a BCI system. Without a concrete and useful use, a BCI is an interesting research tool but without a practical utility. The most relevant practical use is in the medical field as an assistance tool.

Let's see what important roles it can play in both the medical and non-medical fields:

- Restore the lost natural output. A BCI can be used for the motor rehabilitation of stroke survivors to recover lost or not fully functional movements. It has been shown that treatment by BCI can bring long-term improvements in the upper motor functions of post-stroke patients with mild, moderate, and severe impairment [21];
- Replace the natural output lost due to illness or injury. One of the first uses of a BCI was with patients with locked-in syndrome, who cannot communicate with the outside world and produce any movement, despite their cognitive functions being intact. A BCI system can enable a patient with locked-in syndrome to communicate with the outside world. Another key example is in the case of paraplegic tetraplegic patients, who have therefore lost some motor functions. A BCI system can enable these patients to control an external input and regain their lost mobility by, for example, using a robotic arm or a mouse on a computer. Patients who can no longer communicate either by speaking or writing by hand or using a keyboard can use a BCI system to regain the ability to communicate. There are several more or less advanced speller systems. A state-of-the-art example is a system designed by Francis R. Willett for the 2020 BCI awards. This BCI system is designed for patients with locked-in syndrome to regain fast and accurate communication. It uses MEAs that interpret handwriting movements in people with paralysis [22];

- Enhance and improve the natural brain output. A BCI can help an individual who is performing a task. It can be used to detect the mental state (for example when driving) and provide an output when the attention is going down. It can also be used in neurofeedback, a technique that helps the individual to control the brain waves consciously [23].

Type of brain signal input

The most crucial distinction between different types of BCIs is the origin of the input, the origin of the brain signals.

The 2 kinds of input signals are:

1. Electrophysiological input: the electrical or magnetical activity of the brain is observed through different data acquisition instrumentations. The most popular one is surely Electroencephalography (EEG). Other significant ones are Electrocortycogram (ECoG), Magnetoencephalography (MEG), and Micro-Electrode-Arrays (MEAs). Those techniques are all characterized by a very high temporal resolution while the spatial resolution can vary between instrumentations;
2. Hemodynamic input: the hemodynamic brain response is observed. It is not the neuronal activity that is measured directly but the metabolic response induced by this activity. Cerebral blood flow and neuronal activity are supposed to be coupled. When an area of the brain is activated blood flow in that area increases. The most popular instrumentation for looking at brain hemodynamics are functional Magnetic Resonance (fMRI) and Near-InfraRed Spectroscopy (NIRS).

Another fundamental distinction between the type of data acquisition systems is their invasiveness.

We can divide between:

- Invasive techniques: the sensors are placed directly into the cortex. The invasive approach certainly guarantees very good signal quality, but it brings with it numerous problems, first and foremost the risk of surgery and the formation of scar tissue that deteriorates signal quality over time;
- Semi-invasive techniques: the sensors are placed under the skull, without being implanted directly into the grey matter;
- Non-invasive techniques: they carry minimum to zero risk for the patient as no surgery is required. The sensors are positioned above the scalp, either with or without contact depending on the technique, in a non-invasive manner.

EEG signal

Definition and History

The electroencephalogram (EEG) provides the electrical activity of the neural structure of the cerebral cortex, it measures synchronized patterns of electrical activity involving a large number of neurons. It is the most used BCI non-invasive application thanks to its high portability and low cost.

One of the first recordings of the electrical signal of the brain was made by the English physiologist Richard Caton in 1875 on animals [24]. Only 50 years later, in 1924, the first electrical activity of the human brain was recorded by the German physicist Hans Berger. In his publications, he documented the first spectral variations of the EEG with repetitions of certain oscillations: *alpha* waves and *beta* waves. He was the first to coin the term electroencephalogram, publishing a paper in 1929 entitled “*Über das Elektrenkephalogramm des Menschen*” in the “*Archive für Psychiatrie und Nervenkrankheiten*” [25]. Together with Siemens, he improved the instrumentation, trying to reduce the artifacts. Andrew and Matthews introduced a 3-channel system with differential amplification to simultaneously take multiple signals from different areas.

Properties of EEG signal

EEG only measures the post-synaptic potential. Pyramid cells are the main source currents for EEG signals, thanks to their elongated shape and their perpendicular alignment to the cortical surface. Nonpyramidal neurons, lacking these characteristics, scarcely contribute to the signal.

EEG has its weakness in the low spatial resolution and low spatial-to-noise ratio. The number of sources is enormous compared to the number of electrodes used. EEG signal is a mix of large groups of neurons firing together from different areas of the brain close to the electrodes. Furthermore, the signal has to cross several layers up to the skull (Figure 8) with different electrical conductivities causing a “smearing” phenomenon of the electrical potential which dampens and spreads the signals [26]. Consequently, the spatial accuracy of the signal is also inferior.

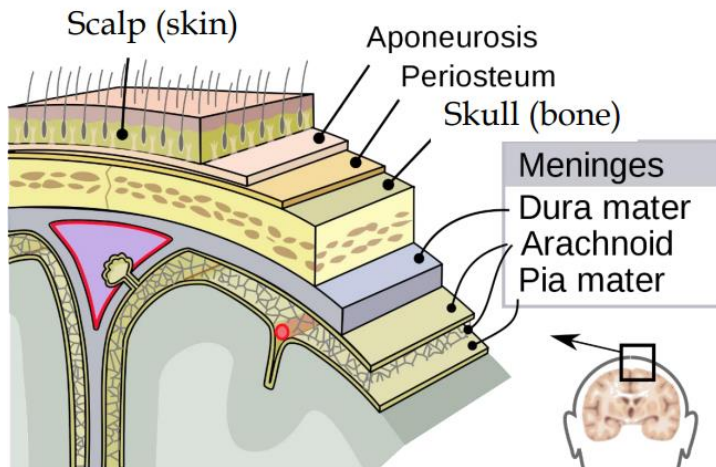


Figure 9: The different layers between the cerebral cortex and the scalp. From "<https://www.hopkinsmedicine.org>".

Invasive techniques such as electrocorticography (ECoG) or micro-electrode arrays (MEAs) [27] can partially overcome these issues, but carry other difficulties such as their invasiveness.

Ultimately, the spatial resolution depends on the number of electrodes and their positioning on the scalp. Increasing the number of electrodes and bringing them closer together increases the spatial resolution.

The temporal resolution, however, is very good. If an electrical variation occurs within the cranial box, it can be read instantly anywhere on the scalp.

The measurement of a very large number of independent sources, as just mentioned, makes EEG a random process.

The voltage amplitude of scalp EEG can vary approximately between 10 μV to 500 μV , although signals are generally around 50 μV to 100 μV and the amplitude decreases attenuated by the distance between the brain source and the electrode. EEG is most sensitive to currents just underneath the electrodes, but in addition to these superficial radial currents, it can also sense tangential and deep currents.

Regarding the spectral component, the EEG signal is divided into precise and contiguous frequency bands. The overall band ranges from approximately 0.5 to 80 Hz, although generally it cannot be observed over 40 Hz. This is mainly due to the fact that as the frequency increases, the value of the amplitude component of the signal decreases. This is mainly due to destructive and constructive signal interference.

The bands are approximately subdivided as it follows (Figure 9):

- Delta (1-4 Hz);
- Theta (4-8 Hz);
- Alfa (8-13 Hz);
- Beta (13-30 Hz);
- Gamma (>30 Hz).

Of particular interest for this thesis are *mu* waves. These waves have a frequency between approximately 7.5 and 12 Hz (the same frequency as the alpha rhythm) and are present in the motor cortex. They are normally present but are suppressed following a movement or intention to move. Consequently, they are widely used in the field of BCI.

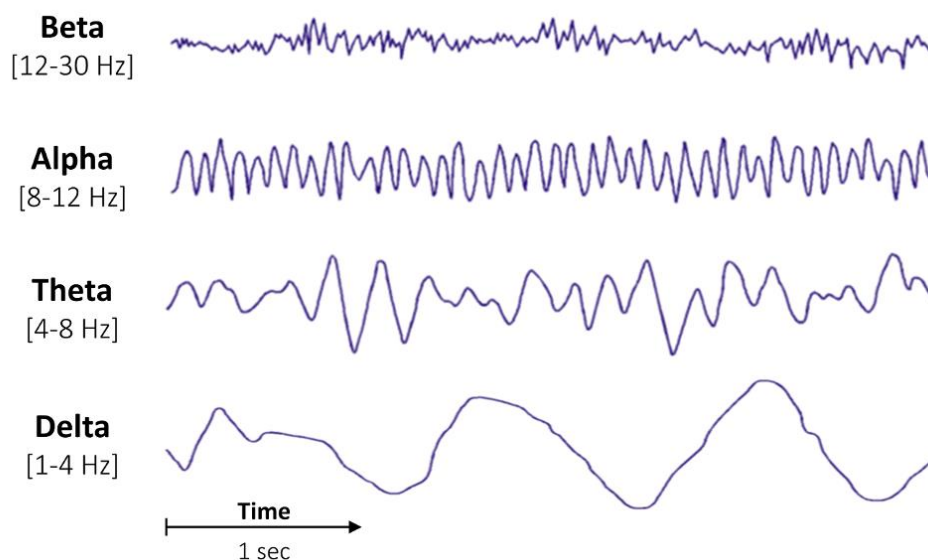


Figure 10: EEG spectrum bandwidths. From “www.raphaelvallat.com”.

Instrumentation

An EEG acquisition system consists of the following parts:

1. an electrode system;
2. an amplifier;
3. an A/D converter;
4. a recording device.

Luis Fernando Nicolas-Alonso in his article [4] defines the EEG acquisitions system as follows: “The electrodes acquire the signal from the scalp, the amplifiers process the analog signal to enlarge the amplitude of the EEG signals so that the A/D converter can digitalize the signal in a more accurate way. Finally, the recording device, which may be a personal computer or similar, stores, and displays the data”.

Electrodes can be placed directly on the subject's scalp or inserted into a helmet. It is common practice to use EEG helmets containing space for the electrode to be inserted. The helmets can be

made of fabric or rigid and can have the electrodes already inserted in them, not allowing repositioning of the electrodes, or leaving the user free to choose where to insert the electrodes.

Electrodes are mainly divided into two categories: wet electrodes and dry electrodes.

Dry electrodes are placed directly on the subject's scalp while wet electrodes require the use of a conductive gel, which is usually inserted into a hole in the center of the electrode. Wet electrodes have a much better contact impedance than dry electrodes. Consequently, the signal extracted by wet electrodes will have a higher quality. However, compared to dry-type electrodes, it will take a longer time to prepare the acquisition, due to the time taken by the operator to insert the gel into each hole. This time can be considerably reduced by the experience of the laboratory operator. Another disadvantage of wet electrodes over dry electrodes is the stability of the signals since the gel dries up during the experiment.

Summing it up, wet electrodes have a better signal quality but lower signal stability over time compared to dry electrodes. It is up to the scientist to choose what is more needed. The signal stability won't be a major problem for short experiments but might be a big issue for longer studies such as sleep studies [28].

While most of the literature focuses on the differences between dry and wet electrodes, when it comes to EEG instrumentation it is interesting to compare not only the type of electrodes used but the amplifier as well. In the present day, thanks to the popularity acquired by non-invasive BCI techniques in different fields of research, a growing number of more affordable BCI instrumentation is gaining ground.

A recent study by Jeremy Frey [29] compared the performance of a consumer-grade EEG amplifier with medical-grade equipment in the field of BCI application reporting the following:

“Overall, the results suggest that the OpenBCI board – or a similar solution also based on the Texas Instrument ADS1299 chip – could indeed be an effective alternative to traditional EEG amplifiers. Even though medical-grade equipment possesses certification and still outperforms the OpenBCI board in terms of classification, the latter gives very close EEG readings. In practice, the obtained classification accuracy may be suitable for reliable BCI, widening the realm of applications and increasing the number of potential users”.

Sampling rate

The EEG signal is an analog continuous signal (in voltage) that must be converted to a discrete digital signal by an analog-to-digital converter. The main characteristic of the A/D converter is the signal *sampling rate*, also called *sampling frequency*.

To know at what frequency to sample the signal, one must rely on the *Nyquist-Shannon Theorem*. This theorem tells us that the minimum sampling frequency that allows a discrete sequence of samples to capture all the useful information of the continuous signal is given by:

$$f_s > 2f_{max}$$

Where f_{max} is the highest informative frequency present in the signal and f_s is the signal sampling frequency. It is then defined as Nyquist frequency f_{Ny} the frequency equivalent to 2 times the f_{max} . Sampling at a lower frequency than the f_{Ny} will cause the phenomenon of aliasing, which appears as a misrepresentation of a high-frequency signal at a lower frequency [10].

Since the band of interest of the EEG signal usually reaches around 40 Hz, it is appropriate to use sampling frequencies above 80 Hz. In practice, it is preferred to stay above 125 Hz anyway, and even up to 500 Hz can be sampled [26].

Electrode positioning

It is necessary to have a standard electrode positioning to make the recording track universal and obtain consistency between different laboratories. The *10-20 International System* is the standard electrode placement recommended by the International Federation of Clinical Neurophysiology (IFCN) [30]. The concept behind this standard positioning is to outline skull landmarks and use them to partition the skull proportionally.

Four skull reference points are taken [31]:

1. Nasion: the fossa above the root of the nose;
2. Inion: located posteriorly along the midline of the skull, before the occipital bone ends. It is the bony lump at the base of the skull;
3. Two preauricular points: located below and in front of the auricle of the ear on both sides of the head.

Measuring the distance between those points an imaginary grid is drawn and the electrodes are placed at 10% and 20% of this distance (Figure 10).

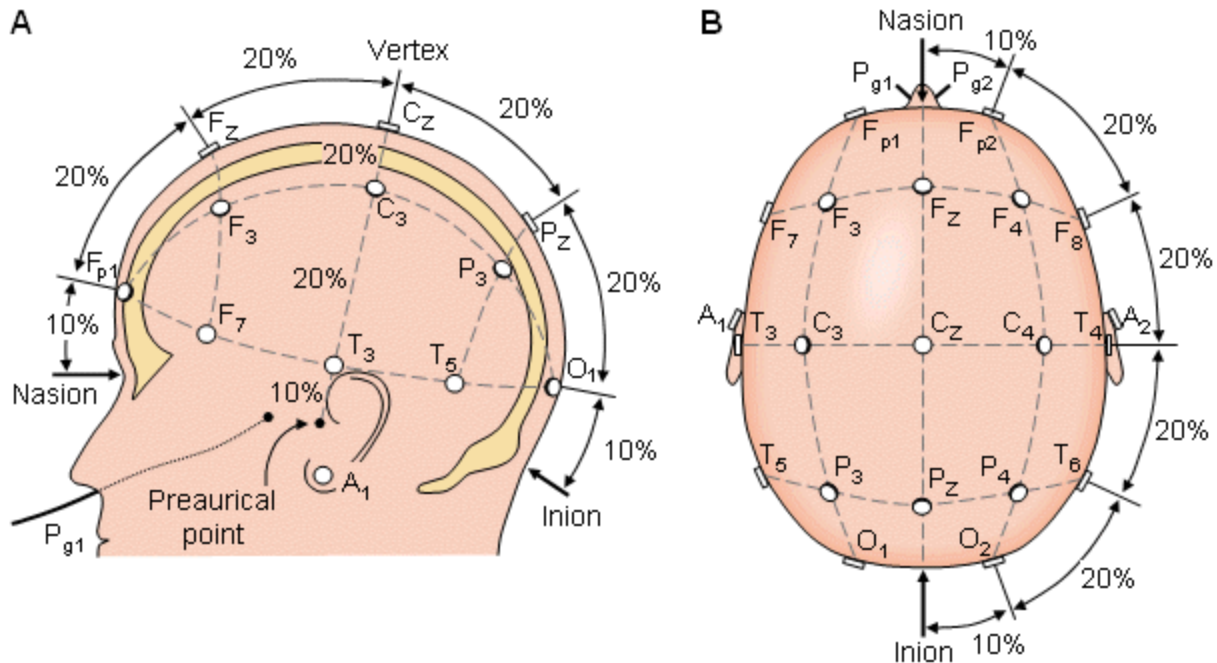


Figure 11: The 10-20 system of the international federation for the standardization of the placements of EEG electrodes. From R. Shriram (2012) [31].

Letters and numbers are used to identify the electrode position. Letters correspond to the cortical location:

- F, frontal lobe;
- T, temporal lobe;
- P, parietal lobe;
- O, occipital lobe;
- C, central area;
- A, ear lobes.

Letters are combined to show intermediate locations. For example, FP indicates the frontal polar electrodes. Following the letters, we have the numbers. On the left hemisphere, we have odd numbers, while on the right side of the head we have even numbers. The “z” indicates the midline.

The 10-20 system does not prescribe the number of electrodes but prescribes the positions. The total number of possible electrodes in the 10-20 system is 21. Using all the positions in the system, we obtain a total of 19 electrodes. The 2 remaining electrodes are placed on the ear lobes as reference.

More electrodes can be used by extending the 10-20 system to obtain a high-density grid. The 10-10 system and 10-5 system use 10% and 5% of the distance between the skull reference point. With

the reference one, and the ground electrode. The ground electrode is connected to the amplifier ground and consequently collects electrical noise that does not reach the scalp electrodes.

Each of the two recording electrodes on the scalp measures the difference: [*scalp electrode - ground electrode*] and carries a common mode potential, common to both electrodes, due mainly to power line field interference and other minor factors such as ECG signal. To eliminate this ground-related noise, EEG activity is always measured with differential amplifiers.

As a result, the EEG signal is measured as the difference between two recording electrodes placed on the scalp instead of the simple difference between a scalp electrode and a ground electrode. This configuration eliminates much of the common activity between the two electrodes, which is not of interest. We can see from the following formula how the common mode rejection occurs:

$$[(E_{S1} - E_G) - (E_{S2} - E_G)]$$

Where E_{S1} is the first scalp electrode, E_{S2} is the second scalp electrode and E_G is the ground electrode.

One of the two electrodes on the scalp is also called the *reference electrode*. It is essential to define the position of the reference electrode because when we observe the EEG signal we are observing the difference in electrical potential between the signal of the chosen electrode and the signal of the reference electrode. There are different criteria for the most correct choice of the reference electrode. It is important to take into account the comparability to other studies, to be able to compare the results of different studies and see what choices have been made on the research topic of interest.

The reference electrode should have a good signal quality and should not pick up excessive noise, which would be added to the signal of interest. At the same time, it should not be located too close to the source of interest to avoid collecting useful signals that would be subtracted during referencing [32].

There is confusion in the literature regarding the concept of bipolar recording vs. monopolar recordings in EEG. Wolpaw [4] writes: “*it is important to recognize that there are no monopolar recordings in EEG. All EEG recordings are bipolar. It is always necessary to use electrode pairs to measure scalp potentials [...] and each electrode in the pair is active. Thus, no EEG recording measures the voltage difference between an active electrode and an inactive, or unchanging, electrode*”. While [33] writes: “*There are two primary types of display montages: bipolar and monopolar/referential*”, defining the use of a common reference channel as a monopolar recording.

If we define a monopolar detection as a difference between an exploring electrode and a stable unchanging electrode, then it is incorrect to define the EEG signal as monopolar, because both electrodes used (recording and reference) are active and measure a changing potential. For example, the g.tec manual for gRecording [34] defines common mode channels: “*when one single*

channel is used as a reference for all of the rests, as a way to set the selected channel as a bipolar channel for all channels of the device”.

Apart from the definition we give to the EEG configuration, in the end, the following referencing possibilities are available for an EEG recording:

1. Common reference: a single electrode is chosen as a reference for all of the recording electrodes. Some of the most popular choices are the *linked ear* and *linked mastoid* reference, and the central electrodes, such as *FCz* or *Cz* [32];
2. Average of the two mastoid electrodes: this reference is particularly used if the signal of interest is in the middle of the head [32];
3. Common Average Reference (CAR): this kind of referencing subtracts, for every time point and every channel, the average of all the non-exclude channels. Note that referencing is equivalent to applying spatial filters. This is why the CAR referencing is often referred to as the CAR filter [35];
4. Chains of electrodes (often referred to as *bipolar montage* in literature). Instead of using a single fixed reference or a fixed average, each electrode is connected to a pair of electrodes. The potential difference between these two electrodes is the measured signal.
 - a. There are several types of “bipolar” configurations possible, a widely used example being the longitudinal one, called double-banana. This type of reference is better for locating sources and measuring the gradient between two brain areas [33];
5. Other kinds of spatial filters can be applied, such as the Laplacian filter [32].

In conclusion, researchers can handle the choice of reference as he or she pleases. However, it is recommended to pay attention to the choice of reference by referring to the criteria set out in this chapter. This choice will influence the analysis of the data and the results. It is important to note that it is possible to choose a reference electrode during recording (online referencing), but during the data processing phase, it is possible to easily change this reference (offline referencing) by performing a subtraction. This process is called *re-referencing* or *offline* referencing and allows the choice of reference made online during data acquisition to be changed.

EEG artifacts

The EEG signal is affected by numerous artifacts. Having a small signal amplitude, around 100 μV , it is more corruptible by artifacts compared to other physiological signals (such as the ECG for example), artifacts that in addition to amplitude also have signal-compatible shapes and frequency content.

We distinguish artifacts into two main categories: physiological type and non-physiological type artifacts. Any signal that does not have a brain-type origin is in essence considered an artifact [36]. Physiological artifacts are those generated by the subject, in particular by the patient's muscle activity. We look at the main ones:

1. Eyeblink: these are movement artifacts due to the fact that the subject opens and closes the eyelids, either voluntarily or involuntarily. This artifact is easily observed on the frontal electrodes and is more pronounced when the movement is voluntary than when it is involuntary. They are artifacts that affect low frequencies and can be removed by a filter that removes delta frequencies. However, this would remove the signal in the useful band. Consequently, more complex filtering methods, such as the ICA filter, are preferred. Note that lateral and vertical eye movements can also cause eye artifacts similar to blinking;
2. Cardiac artifact: this is observed as a slight spike in the signal with frequency of about 1 Hz. It can be easily detected by acquiring EEG and ECG signals simultaneously and comparing the two signals. The ECG artifact does not only involve a few electrodes but the whole skull. Related to the heart, a motion artifact can also be generated due to the pulsation of a blood vessel on the scalp, which slightly displaces the electrode, causing a motion artifact;
3. Muscle artifact: various types of artifacts due to muscle activation can be observed, particularly on facial muscles. An example easily observed by experimenters on the EEG signal is artifacts due to teeth and jaw grinding.

Looking at non-physiological artifacts in more detail, we distinguish the main ones:

1. Network frequency interference: it is caused by the coupling of the electrodes with the alternating current of the power supply. The network frequency can be either 50 or 60 Hz and can be filtered through a notch filter at the network frequency. As the useful signal band is usually below 50 Hz this artifact can generally be eliminated without too much difficulty;
2. Electrode artifacts: very high-frequency artifacts due to a change in voltage referring to a single electrode. They are called electrode pop artifacts.

EEG-dependent BCI

The focus will now be on EEG-dependent BCIs.

In order not to stray from the focus of the thesis, it will be assumed from now on that what is written is related to EEG BCI. This does not detract from the fact that some of these distinctions and features can be applied to non-EEG BCI as well.

First, it is important to distinguish the origin of the BCI signal which can be:

1. Exogenous or evoked: the neuronal activity is elicited by external stimuli, such as auditory, visual, or tactile stimulation;
2. Endogenous: there are no external stimuli. The BCI activity is directly controlled by the BCI user. There is self-regulation of brain activity.

Those two kinds of stimuli usually generate two kinds of EEG phenomena:

1. Event-Related Potentials (ERPs). An ERP (Figure 13) is a scalp-recorded event after stimulus onset (i.e., a manifestation of neural activity that is triggered by a specific event). The ERP is generally quite small compared to the general activity measured by the EEG, it is embedded within the signal. To differentiate it from the general background noise, it can be extracted by averaging multiple trials. This is possible because the ERP is time-locked to the event, while the noise is not. Nonetheless, when averaging trials carefulness is needed because of the jitter problem, there is variation in the latency between the stimulus onset and the brain response. The characteristics of an ERP are:
 - Polarity: the peak can either be Negative (N) or Positive (P). Accordingly, the first letter of an ERP indicates its polarity. It is curious to notice that in literature when an ERP is shown the y-axis is inverted, causing a reversal of the positive and negative peaks in the graphs;
 - Latency: the time between the stimulus onset and the ERP peak. This generally indicates the second part of its name. The latency goes from tens of milliseconds to hundreds of milliseconds.

For example, a “P220” indicates an ERP with a positive peak and 220 ms of latency, a “N500” indicates a negative peaked ERP with a latency of 500 ms. Lastly, the components of an ERP can be endogenous or exogenous. For an ERP to occur there must be an exogenous stimulus that causes it, however some of its components can be generated by information processing in the brain, thus endogenously. The external stimuli generating an ERP can be of different kinds, visual, auditory, and tactile.

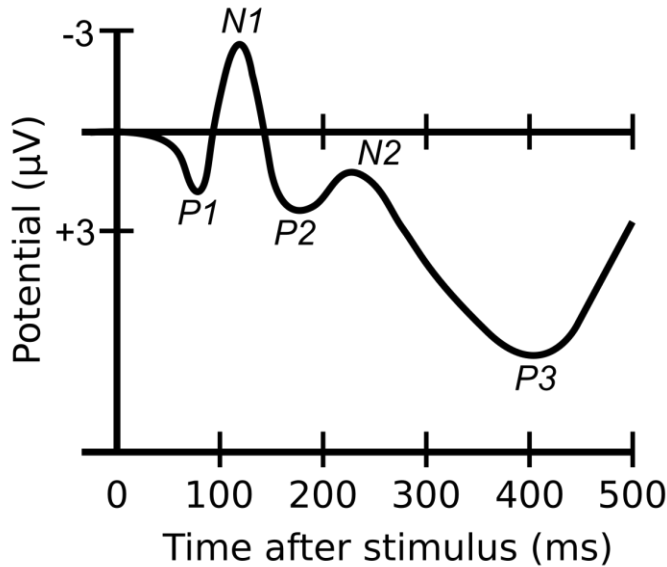


Figure 13: An example of an Event-Related Potential (ERP) with 5 components, 3 positive ones, and 2 negative ones. From “www.wikipedia.org”.

2. Oscillatory Processes, which are connected to the *Event-Related Synchronization/ Event-Related Desynchronization (ERS/ERD)* phenomenon. ERD and ERS are non-phase-locked responses in EEG, related to the increase or decrease in oscillatory activity at a certain frequency following an action [37]. With the ERD an amplitude decrease is observed, while in the case of ERS an amplitude increase can be seen. This phenomenon can occur in different cortical regions at the same time or at different times following events such as the action of a movement, performing an eye blink, thinking, or in response to a sound. For example, we can observe the occurrence of ERS/ERD when opening and closing the eyes. To keep the eyes open, there is a synchronization of alpha waves. When closing the eyes an increase in frequency and a decrease in amplitude occur. Rhythm changes from alpha to beta. This is called alpha block or event-related desynchronization. Different types of actions cause an increase/decrease of different frequency ranges in different cortical areas. For example, it can be seen a change in oscillations in the beta band (19-26 Hz) for foot movement, while we see a change in the same band but at slightly different frequencies (16-20 Hz) for finger movement [38].

Typical BCI experiment

A BCI experiment is usually divided into a hierarchical structure. The base unit of this structure is the *trial*. A group of trials creates a *run* and multiple runs create a *session* (Figure 14).

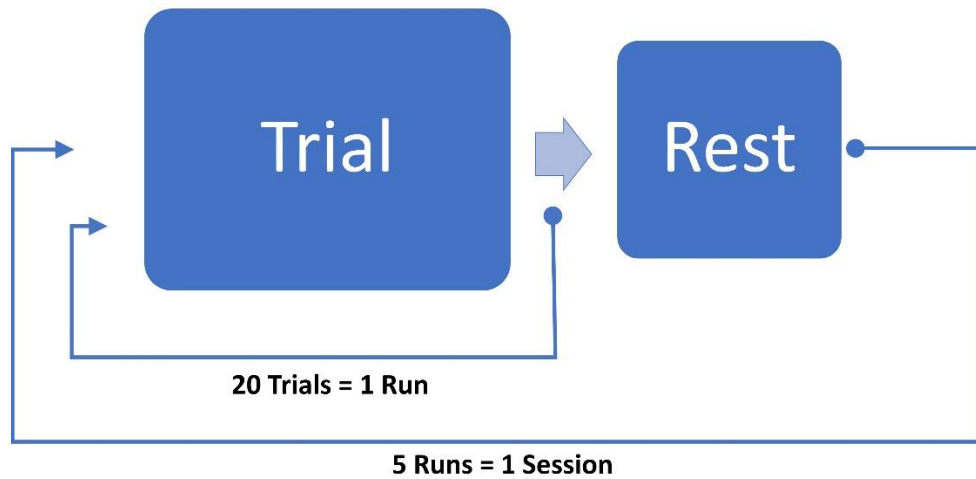


Figure 14: Example of a session structure. In this example each session is composed of 5 runs and each run is composed of 20 trials. Between runs there is a rest phase.

A *trial* usually lasts a few seconds and contains the task of the experiment. A trial paradigm defines what is contained within the trial and the timing of each element within it.

A *run* is a group of trials, usually between 10 to 50 maximum. Between each run, it is good to have a break to let the subject rest.

A *session* is a group of multiple runs and can last several minutes. An experiment may consist of a single session or several sessions in succession. Two consecutive sessions can be spaced apart in time, from a few minutes to a whole day.

The total duration of an experiment varies based on its aim. It usually lasts from a minimum of 10-15 minutes to at most just over an hour.

Some BCIs can decode the signal immediately, while other types of BCI require a *training* period before they can function. When BCIs require training to be able to discriminate between classes it means that to recognize classes correctly, the algorithm must train on a portion of the dataset. Consequently, in these cases, the EEG signals must be divided into two parts: a training dataset and a test dataset. The percentage division between the training and the testing set can vary but the test dataset is generally less numerous than the training one. For example, the dataset can be divided into 80% training set and 20% test set (Figure 16), or 70% training set and 30% test set [39].

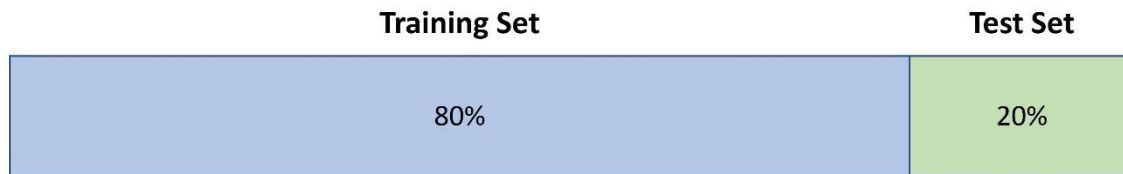


Figure 15: Example of the division of a dataset into 80% training set, and 20 % testing set.

Different BCI systems

There are different kinds of EEG-dependent BCI systems which differ between them for the type of stimuli used, the number of choices a BCI allows the user to make, the type of training required, and the kind of EEG phenomena analyzed.

BCIs that try to restore the motor output are usually based on 2 types of BCI systems [40]:

1. SLOW cortical potentials (SCP) BCI: based on a slow voltage shift that occurs in the cortical activity below the frequency of 1 Hz. It is associated with performed or imagined movement tasks or cognitive tasks. There are two types of SCP, negative SCP, associated with cortical activation and increased neuronal activity, and positive SCP, associated with cortical deactivation and decreased neuronal activity. It is an endogenous type of BCI. When the slow cortical potential is specifically related to a movement it is called Movement Related Cortical Potential (MRCP) [36];
2. Sensory-motor rhythms (SMRs) BCI: based on electric field oscillations recorded near the motor and somatosensory areas of the cortex. These rhythms generally fall in the mu (8-12 Hz), central beta (18-30 Hz), and gamma (30-200 Hz) frequency bands. They are generally linked to sensory and motor events and are based on the ERD/ERS concept expressed in the previous paragraphs [36].

The BCI systems cited above require a training phase before they can function.

There are other BCI systems that do not require this training phase. For example, Visually Evoked Potential (VEP) BCI are systems that function through an external visual stimulus that triggers an evoked potential in the visual cortex and contrary to sensory-motor rhythms and MRCP BCI do not require a training phase [40]. The negative side is that VEP BCI require an external visual stimulus to function and cannot function in the absence of it, whereas a system based on MRCP or sensory-motor rhythms does not necessarily require an external visual stimulus in order to function.

Characteristics of EEG dependent BCI

This chapter will take a closer look at the various characteristics of EEG dependent BCI, with particular focus on those based on MRCP and Motor Rhythms.

Classes

A BCI must allow the user to make different choices. The choice can be binary, such as answering a yes/no question, or it can be more complex, such as choosing a letter of the alphabet. These choices are nothing but the ultimate goal of the system and are referred to in the literature as *classes* or *conditions*. The aim of a BCI is thus to discriminate between a certain number of *classes*.

Movements

There are mainly 3 types of movement a motor rhythm or a MRCP BCI can be based on:

1. *Motor execution (ME)*: the movement is physically performed by the subject. The execution of the movement activates the previously discussed ERD/ERS phenomenon, causing neuronal activation of the motor cortex [41] ;
2. *Motor attempt (MA)*: This occurs when the subject cannot perform the movement correctly or entirely due to a disease or an accident. Similarly to movement execution, motor attempt relies on the ERD/ERS of the involved frequencies. It is often cited in studies involving stroke patients [42] . Stroke patients might lose the ability to perform a full and efficient movement of the arms and even though their disability depends on the single patient, their task is usually classified as motor attempt or motor imagery, but not motor execution. The degree of their disability is generally evaluated by the Functional Independence Measure (FIM) [43]. Other types of patients who fall under this movement category are Spinal Cord Injury (SCI) patients. These types of patients usually have lost the majority of their voluntary motor control functions and BCIs can be of great help and are a promising instrument to restore their motor abilities [15];

Motor Imagery (MI): movement is only imagined by the subject. It is not a performed movement or a motor attempt, as soon as a muscular micro-activation also takes place we no longer speak of motor imagery. Several studies show that motor imagery influences neuronal activity in the motor cortex in a similar way to what is observed with a performed movement [44],[45]. The same principles of ERD/ERS occur in the case of movement attempt and movement execution. Pfurtscheller reports in his article [44]: “*Motor imagery may be seen as mental rehearsal of a motor act without any overt motor output. It is broadly accepted that mental imagination of movements involves similar brain regions/functions which are involved in programming and preparing such movements* [46]”. Consequently,

the major difference between executing and imagining the movement is that in the latter case the signal is blocked at some cortical-spinal level [47]. It is easy to see how, even better than the motor attempt case, motor imagery can be used with stroke and spinal cord injury patients. Furthermore, unlike the motor attempt, it can also be tested on healthy patients. Many studies in the literature use motor imagery for both patients with motor deficits and healthy patients. Imagined movement decoding is used to induce neuronal plasticity, through several training sessions. BCI based on motor imagery can be used to move a virtual limb or be coupled with Functional Electrical Stimulation (FES) [21].

The paragraph has talked about how these motion tasks are analyzed using the sensory-motor rhythms, based on the principle of ERS/ERD. However, several studies also analyze movement tasks through MRCP [43], [42].

Task movement

The movements chosen for the task must be functional for use in daily practice if the aim of the BCI is to be useful for patients with motor disabilities [27], [48]. More movements allow more autonomy to the patient, but, by increasing the number and similarity of movements, the BCI performance decreases [40]. It is more difficult to distinguish between motor tasks performed on the same limb, compared with motor tasks performed on different limbs, particularly because of the low spatial resolution of the EEG signal [48].

Many BCI focus on upper-limb movements with a particular focus on hand movements (Figure 16), but some dataset focus also on other body parts, such as feet and tongue [40].

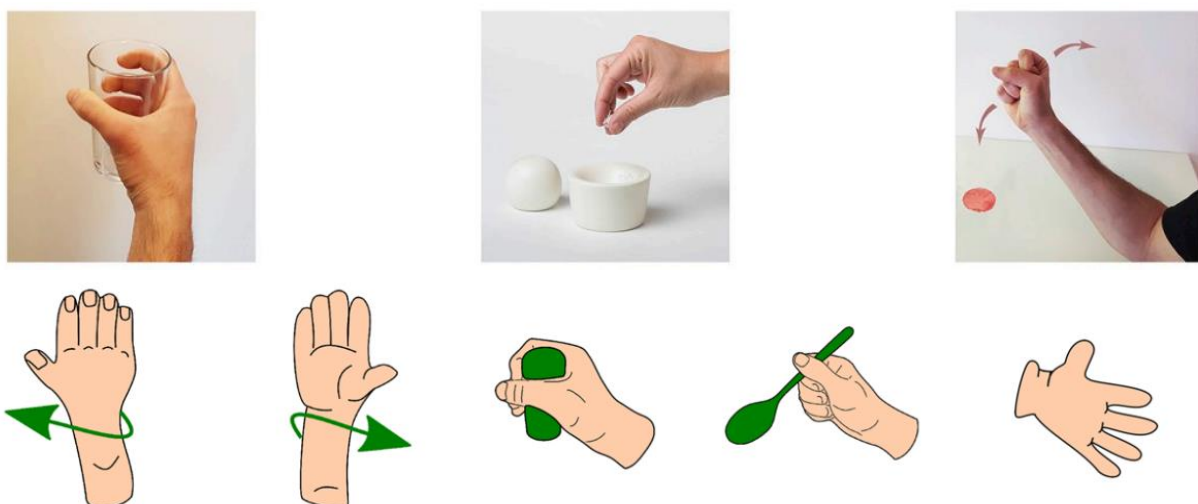


Figure 16: Example of functional movements. Upper row from left to right we have a palmar grasp, pinch, and elbow flexion. From Ana. P. Costa [48]. Bottom row from left to right we have pronation, supination, palmar grasp, lateral grasp, and hand open. From P. Ofner [15].

Number and positioning of the electrodes

The positioning and number of electrodes is another key point. There are studies analyzing the motor imagery signal limited to the use of 3-5 electrodes [49], [11]. Other articles use a much higher number of electrodes, from 60 [50] to 118 electrodes [51]. Increasing the number of electrodes improves the spatial resolution of the signal but also increases the preparation time of the experiment and the analysis of the acquired data.

In addition to the number of electrodes, positioning is important. In order to be able to study sensory-motor rhythms and MRCP, the electrodes must be positioned close to the origin of the signal of interest, the motor cortex (Figure 17). According to the results obtained from studies [48] and [21], 16 electrodes placed over the motor cortex are a good compromise between BCI performance and experiment preparation time. No significant performance improvement is observed in the literature when the number of electrodes increases above 16 [40].

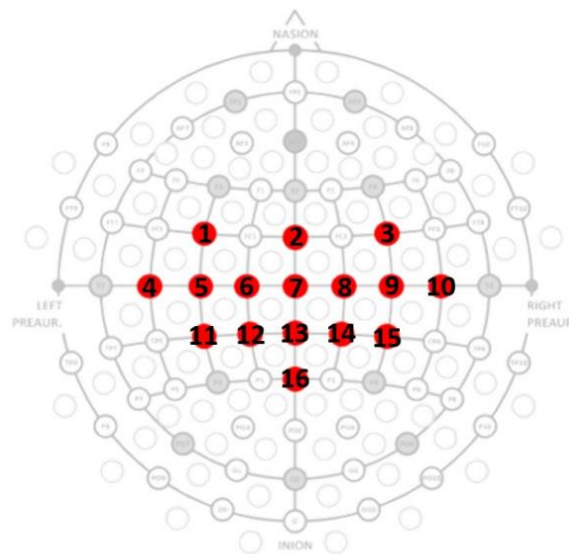


Figure 17: Electrode positioning in the study by S. Romagosa, “Brain Computer Interface Treatment for Motor Rehabilitation of Upper Extremity of Stroke Patients-A Feasibility Study”. From S. Romagosa [21].

There are hybrid-type BCIs, which in addition to using the EEG brain signal also use other bio-signals, such as the EMG signal [52] or the EOG signal [11] [12], which integrated with the EEG signal can help improve the performance and degrees of freedom of the system [12].

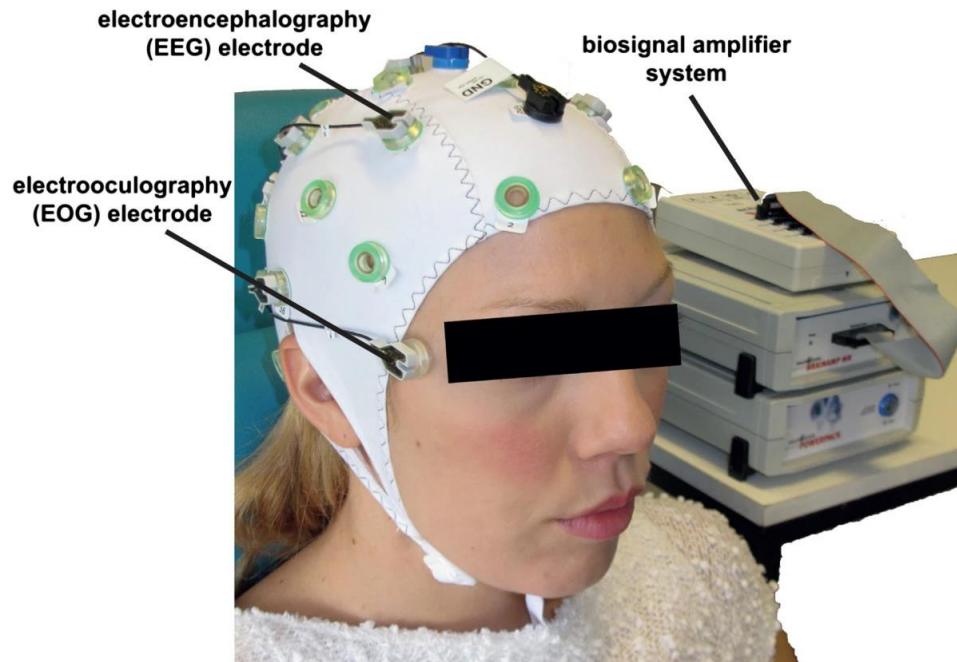


Figure 18: Example of Bio signals recorded through EEG and EOG. EOG follows the standard placement of the left and right outer canthus of the eye (LOC and ROC) [53]. From M. Witkowski (2014) [11].

Calibration and Validation

As it has been said before, a sensory-motor rhythm type of BCI, as well as a MRCP one, doesn't function right away, but it needs training to allow the classification algorithm to function. This is because these types of BCIs are based on supervised machine and deep learning algorithms. This topic will be dealt with in more detail in the materials and methods section. Consequently, a BCI based on these principles cannot start functioning right away but requires the acquisition of a minimum number of trials before it can function online.

A common strategy applied in literature is to acquire the signal in 2 different sessions as it follows:

1. Calibration: the EEG signal is acquired but processed offline. In this phase, the BCI does not work online, so it does not give feedback to the subject but is used to train the classification algorithm;
2. Validation: the BCI can work online right away. The parameters trained during the calibration phase are used to run the BCI right away, there is feedback. This phase aims at giving as much freedom as possible to the subject by canceling waiting times. A self-paced paradigm is therefore usually used, allowing the patient to choose when to perform or imagine movements.

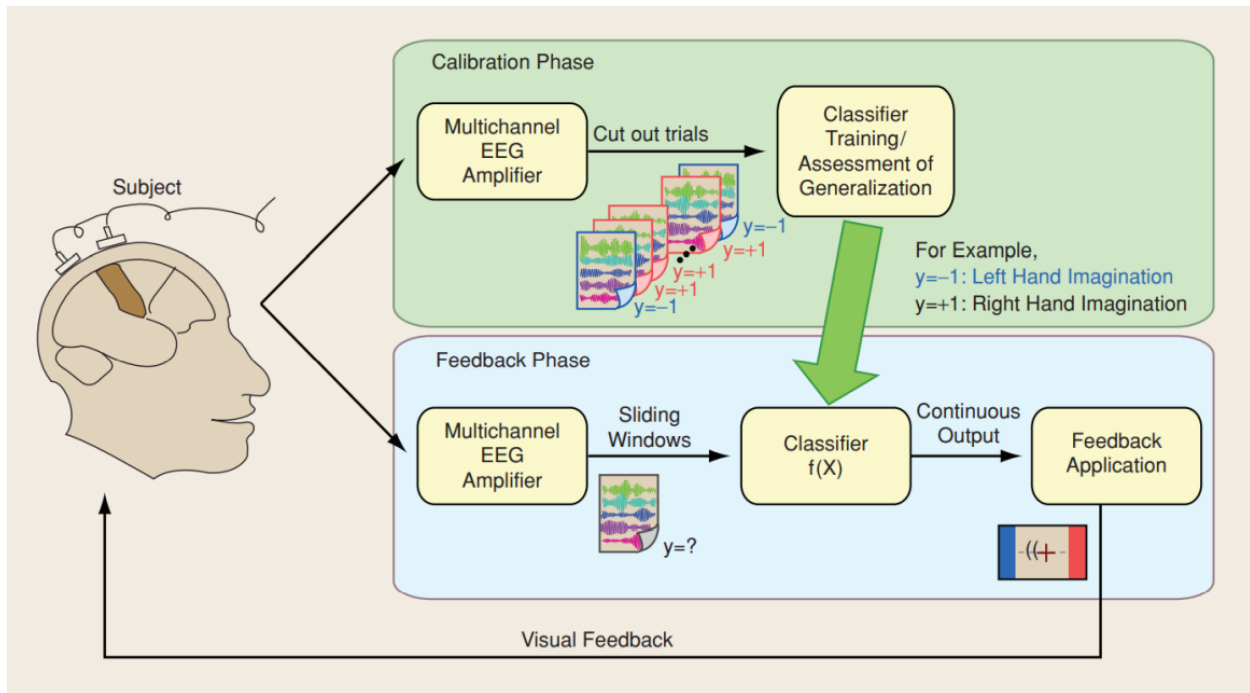


Figure 19: A diagram of how a BCI protocol works based on the two phases of calibration and validation. From Blankertz (2008) [54].

It is important not to confuse the terms *calibration* and *validation* with the terms training and testing. In the calibration part, the dataset will still be divided into training and testing to test the performance of the classification algorithm and efficiently train the parameters of the latter which will then be applied in the validation phase [54],[6].

Subject-dependency

A major obstacle to the use of EEG-dependent BCIs, and in particular to those based on motor rhythms and MRCP, is the great variability of the EEG signal. The latter has a high temporal variability, which can be observed over minutes, hours, and days. The signal changes considerably from one session to the next and can also change considerably within the same acquisition session [55]. In addition to this inter-subject variability, there is also great variability between different subjects [56].

A system that requires a subject-specific training session is said to be *subject-dependent* or *subject-specific*. The limitation of a subject-specific system is the calibration time required for the BCI to work online. A subject-dependent motor imagery system requires approximately 30 minutes of training before it can function effectively. This is an obstacle to the use of BCIs, as it prevents their immediate use. However, a subject-specific system, despite the high variability of the inter-subject signal, guarantees good classification performance.

This obstacle can be overcome by a *subject-independent* system, where the parameters of the classification algorithm can be trained on subjects and applied to different subjects [5]. This allows the BCI to run online right away, eliminating the calibration time of the algorithm. Furthermore, this system is made even more efficient by adaptive BCIs, which modify the parameters of the classification algorithm in progress, adapting them to the subject [57]. The limitation is that numerous subjects are required to train the algorithm before it can be used right away. An initial calibration phase is therefore necessary, but only on the first user subjects.

Furthermore, the high variability of the signal between different subjects does not make this task easy. It is necessary to find an algorithm that can generalize well the significant features responsible for motor imagery between different subjects.

Synchrony

Another distinction is that a BCI can be *synchronous* or *asynchronous*. A *synchronous* BCI is cue-based (i.e., there is an external stimulus that dictates the rhythm of the BCI). The required mental state is generated in response to an external stimulus. Brain activity is therefore activated within predefined time windows. This allows the classifier to focus only on these predefined windows, where the stimulus occurs, and where the cue is present while ignoring the portions of the signal before and after.

An *asynchronous* BCI, instead, does not require an external cue, the subject is free to remain free-thinking or execute/think the experiment task independently. These BCIs are *self-paced*, leave more freedom to the user, and are closer to real-life use of a system outside a laboratory. For this to be possible, the BCI must constantly acquire the signal and classify it, because the task could be thought of or performed by the subject at any time. It is then introduced the distinction between the *No-Control phase (NC)*, in which the subject is not trying to perform any action, and the *Intentional-Control phase (IC)*, in which the subject voluntarily tries to perform the action. This NC phase introduces a further difficulty. In addition to having to classify the signal continuously over time, an additional class is introduced into the problem, the No-Control class.

It is easy to see how BCIs of the synchronous type are therefore easier to realize than those of the asynchronous type.

Paradigm

The paradigm is the basic unity of the experimental protocol. It corresponds to the block commands that are given in the individual trial by defining the extent and duration of each instruction.

The core of the paradigm is the task given to the subject, for example the movement of a hand.

The construction of a paradigm depends on the type of BCI created. In particular, what influences most its form is the synchrony of a BCI.

A synchronous-type BCI is a cue-based BCI, which therefore requires the system to give precise instructions over time to the subject. A synchronous BCI thus needs only one type of paradigm.

Usually, the paradigm of a synchronous BCI is constructed in this way (Figure 19): the total trial duration is about 7-10 seconds [58], and each trial reports one movement instruction. A fixation cross appears before the movement instruction to indicate the imminent arrival of the movement task. The task can vary in duration between 3 and 4 seconds to allow the subject to perform the task long enough for the classification algorithm to decode the signal. Thereafter there is a moment of rest before the next trial arrives. To avoid subject adaptation, the rest period can be variable [58] [6].

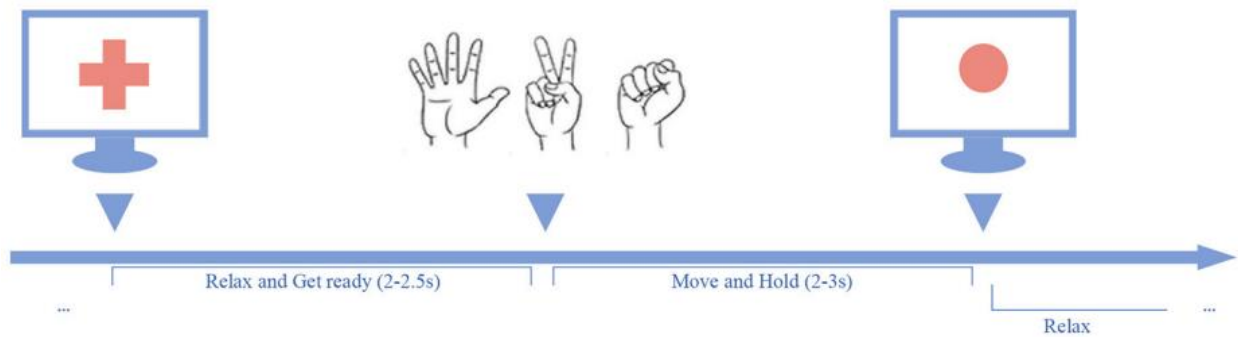


Figure 20: Example of a paradigm for motor execution for a synchronous BCI. From G. Pan (2018) [59].

The paradigm construction is different for an asynchronous BCI. In order to create an asynchronous/self-paced BCI, two phases are needed within the experimental protocol, a calibration phase, and a validation phase. The calibration phase is synchronous, while the validation phase is asynchronous. Therefore, two different paradigms with two different objectives are needed in the two phases. The calibration phase paradigm, as this phase is synchronous/cue-based, follows the same principles explained before. The validation phase paradigm must create a self-paced system, thus allowing the subject to freely choose when to perform the movement.

An example of a paradigm for a self-paced system created by P. Ofner [15] is shown in Figure 21. In this case between fixation cross and pause, a long period is allowed for the subject to freely perform one type of movement. The type of movement is given along with the fixation cross.

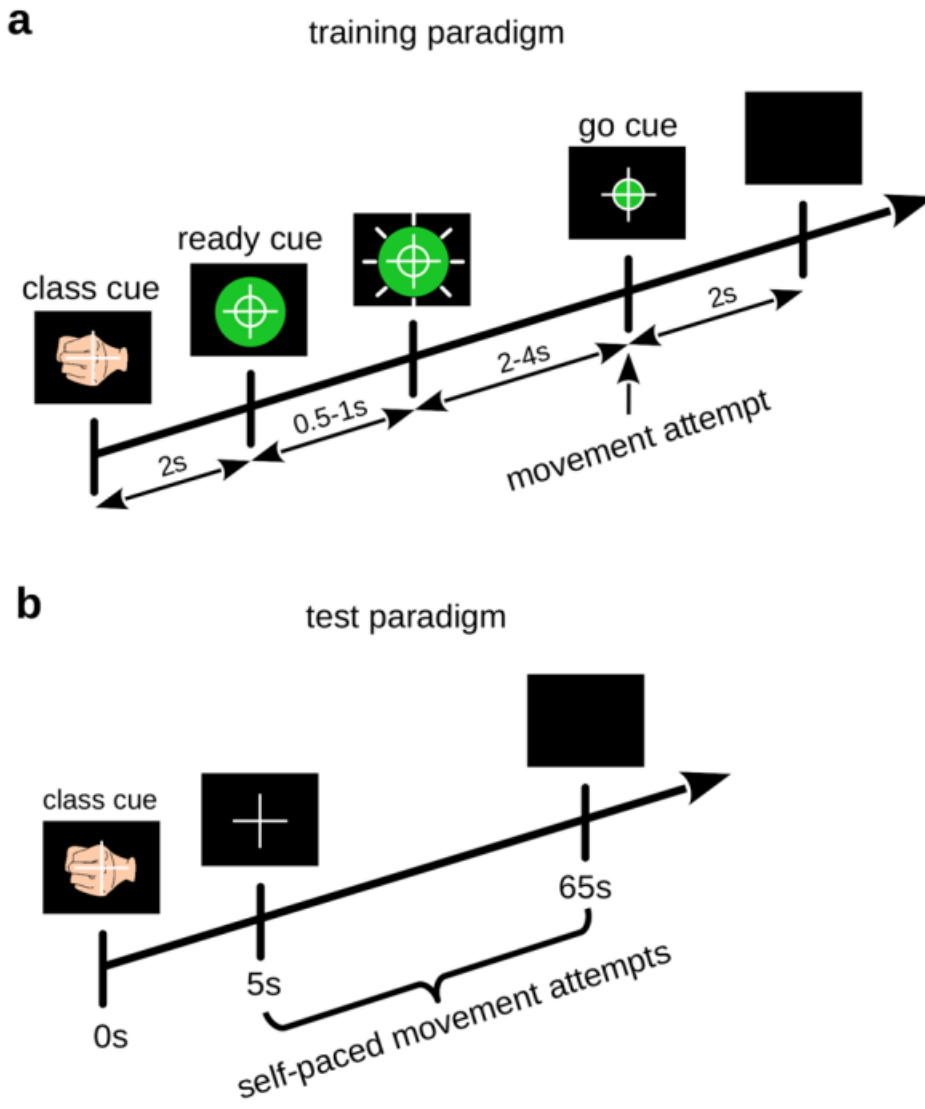


Figure 21: Example of paradigms for motor attempt for a self-paced BCI. A) The paradigm for the calibration phase. B) The paradigm for the validation phase. From P. Ofner (2019) [15].

Literature Analysis

There are many studies with the aim of restoring the functional movements of patients with spinal cord injuries or type of motor impairments [60],[61],[27]. It is clear that invasive techniques (such as ECoG and MEAs) are more effective in restoring motor skills in tetraplegic patients than non-invasive techniques (such as EEG in this case). This is due to the better spatial resolution and signal quality of these techniques compared to EEG.

The present study will focus on EEG, which starts at a disadvantage compared to invasive techniques but has certain advantages, such as versatility and portability.

A literature study has been done with the following keywords: *“Brain-Computer Interface”*, *“EEG”*, *“EEG-based BCI”*, *“Motor Imagery”*, *“Motor Attempt”*, *“Motor execution”*, *“Synchronous”*, *“Asynchronous”*, *“self-paced”*, *“subject-dependent”*, *“subject-independent”*, *“user-specific”*, *“Experimental Protocol”*, *“classification algorithms”*, *“Feature Extraction Methods”*.

The literature study carried out had a twofold purpose. On the one hand to identify the models used in EEG-dependent BCI for movement classification, and on the other hand to analyze the characteristics of experimental protocols for EEG-dependent BCI in order to implement one.

The research of the model (feature extraction + classification technique) has been done analyzing 12 articles and 2 reviews [40] [20] about motor rhythms and movement related cortical potentials BCI. The summary of the different techniques used are reported in table 1.

Simultaneously, 12 datasets of EEG dependent BCIs concerning BCIs based on motor rhythms and MRCP were analyzed. The results are shown in table 2.

Table 1: summary of the literature search over the models used in EEG-dependent BCI for movement classification

EEG Pattern	Synchrony + number of classes	Subject-dependency	Features	Classifier	Reference
Motor Imagery	Asynchronous 2 IC classes + NC	Subject dependent	FBCSP	Non - Linear Regression	[50]
Motor Imagery	Synchronous 2 IC classes	Subject dependent	FBCSP	Naïve Bayes	[49]
Motor Imagery	Synchronous 4 IC classes	Subject dependent	FBCSP	LDA	[49]
Motor Imagery	Synchronous 4 IC classes	Subject dependent	Time Frequency CSP	LDA	[62]
Motor Imagery	Synchronous 2 IC classes	Subject dependent	Band Power + PCA	PNN	[63]
Motor Imagery	Synchronous 4 IC classes	Subject dependent	Adaptive CSP	RDA	[48]
Motor Imagery	Synchronous 3 IC classes	Subject dependent	Adaptive Regularized CSP	RDA	[48]
Motor Imagery	Synchronous 3 IC classes	Subject dependent	CSP	LDA	[64]
Motor Imagery	Synchronous 2 IC classes	Subject dependent	CNN	SVM	[51]
Motor Imagery	Synchronous 4 IC classes	Subject dependent	Band pass Covariance	RMDM	[65]
Motor Imagery	Synchronous 2 IC classes	Subject dependent	Band Power	DBN	[66]
Motor Imagery	Synchronous 3 IC classes	Subject dependent	Band Power	SVM	[67]
Motor Imagery	Synchronous 2 IC classes	Subject independent	CSP/CNN	LDA	[5]
Motor Attempt	Synchronous 5 IC classes	Subject dependent	Low Frequency EEG (MRCP)	sLDA	[15]
Motor Attempt	Asynchronous 2 IC classes + NC	Subject dependent	Low Frequency EEG (MRCP)	sLDA	[15]

FBCSP: Filter Bank Common Spatial Pattern; **LDA**: Linear Discriminant Analysis; **CSP**: Common Spatial Pattern; **PCA**: Principal Component Analysis; **PNN**: Probabilistic Neural Network; **RDA**: Friedman's regularized version of Discriminant Analysis; **CNN**: Convolutional Neural Network; **SVM**: Support Vector Machine; **RMDM**: Riemannian Minimum Distance to the Mean classifiers; **sLDA**: shrinkage Linear Discriminant Analysis; **DBN**: Deep Belief Network.

Table 2: summary of the literature search over the characteristics of experimental protocols for EEG-dependent BCI.

Dataset	Number of Channels	Subjects	Movement type	Synchrony + number of classes	Paradigm	Session's structure
BCI Competition IV - Dataset 1 (2012), by Berlin BCI group: Technische Universität Berlin [68].	59 EEG	4 healthy subjects	Motor Imagery	Asynchronous 2 IC classes + NC	<p><i>Calibration paradigm:</i></p> <ul style="list-style-type: none"> - 2 s fixation cross; - 4 s MI task; - 4 s rest. <p><i>Validation paradigm:</i></p> <p>Alternates between rest and MI task, random variable time between 1.5 to 8 s.</p>	<p><i>Calibration session:</i> 2 runs of 100 trials, 15s rest after every 15 trials, 5-15 minutes rest between trials.</p> <p><i>Validation session:</i> 4 runs of 60 trials, 15 s rest every 30 trials, 5-15 min rest between trials.</p>
BCI Competition IV - Dataset 2a (2012), by Institute for Knowledge Discovery (Laboratory of Brain-Computer Interfaces), Graz University of Technology [68].	22 EEG + 3 EOG	9 healthy subjects	Motor Imagery	Synchronous 4 IC classes	<p>Paradigm:</p> <ul style="list-style-type: none"> - 2 s fixation cross; - 1 s cue; - 3 s MI task; - random variable break (1.5-2.5 s). 	Calibration and Validation session on different days. Each session 288 trials.
BCI Competition IV - Dataset 2b (2012), by Institute for Knowledge Discovery (Laboratory of Brain-Computer Interfaces), Graz University of Technology [68].	3 EEG + 3 EOG	9 healthy subjects	Motor Imagery	Synchronous 2 IC classes	<p>Paradigm:</p> <ul style="list-style-type: none"> - 2 s fixation cross; - 1 s cue; - 3 s MI task; - random variable break (1.5-2.5 s). 	<p>5 sessions: 2 sessions without feedback and 3 sessions with feedback.</p> <p>No Feedback session = 6 runs, 20 trials per run</p> <p>Feedback session = 4 runs, 40 trials per run.</p>

<p>BNCI Horizon - Movement Classification (2020), by Institute of Neural Engineering, Graz University of Technology [69].</p>	<p>61 EEG + 3 EOG</p>	<p>10 spinal cord injury patients</p>	<p>Motor attempt / Motor execution</p>	<p>Synchronous 5 IC classes</p>	<p>Paradigm: - 2 s fixation cross; - 3 s MI task; - random variable break (1-3 s).</p>	<p>1 session: 9 runs with 40 trials per run.</p>
<p>BNCI Horizon - proof of concept online classifier (2020), by Institute of Neural Engineering, Graz University of Technology [69].</p>	<p>61 EEG + 3 EOG</p>	<p>1 spinal cord injury patient</p>	<p>Motor attempt</p>	<p>Asynchronous 2 IC classes + NC</p>	<p>Calibration paradigm: - 2 s fixation cross with class cue; - ready cue (between 0.5 to 1 s); - getting ready for movement attempt (between 2 to 4 s); - 2 s Motor Attempt trial; - random variable break (2-3 s). Validation paradigm: - 5 s fixation cross with class cue; - 60 s of self-paced movement attempts.</p>	<p>Calibration session: 5 movement runs of 30 movement trials and 4 rest runs of 1 rest trial: In total 150 movement trials and 4 rest trials. Validation session: 5 runs, each run comprised 4 movement trials and 1 rest trial.</p>
<p>Dataset from Ana. P. Costa (2018), by Technical University of Denmark [48].</p>	<p>16 EEG</p>	<p>14 healthy subjects</p>	<p>Motor Imagery</p>	<p>Synchronous 3 IC classes</p>	<p>Paradigm: - 2 s fixation cross; - 4 s MI task; - 2 s rest.</p>	<p>2 sessions in 2 different days. 1st day - calibration session: 6 runs, 36 trials for class in total, without feedback. 2nd day - validation session: 54 trials for class total, with feedback.</p>

<p>Dataset G. Pfurtscheller (2009), by Rehabilitation Clinic Tobelbad, Austria [64].</p>	<p>15 EEG</p>	<p>15 complete spinal cord injury patients.</p>	<p>Motor Imagery</p>	<p>Synchronous 3 IC classes</p>	<p>Paradigm: <ul style="list-style-type: none"> - 2 s fixation cross only; - 1 s fixation cross + warning sound; - 1.25 s fixation cross + MI task; - 3.75 s fixation cross endures indicating MI to be performed; - random variable break (0.5 -2.5 s). </p>	<p>6-8 runs (depending on patient physical condition) of 30 trials per run. Short break between each run.</p>
<p>BCI competition III dataset Iva (2006), by the Berlin BCI group, University Medicine Berlin [68].</p>	<p>118 EEG</p>	<p>5 healthy subjects</p>	<p>Motor Imagery</p>	<p>Synchronous 2 IC classes</p>	<p>Paradigm: <ul style="list-style-type: none"> - 3.5 s MI task; - random variable break (1.75 - 2.25 s). </p>	<p>280 trials for each subject, 140 observations for each MI task per subject.</p>
<p>Dataset O-Yeon Kwon et al (2020), approved by the Institutional Review Board of Korea University [5].</p>	<p>62 EEG</p>	<p>54 healthy subjects</p>	<p>Motor Imagery</p>	<p>Synchronous 2 IC classes</p>	<p>Paradigm: <ul style="list-style-type: none"> - 3 s fixation cross; - 4 s MI task; - 6 s rest (± 1.5 s). </p>	<p>The whole experiment is composed of an offline (training) and an online (testing) phase. Number of runs and trial not specified in [5].</p>
<p>Khan Niazi et al (2011), approved by Ethics Committee of Nordjylland, Denmark [43].</p>	<p>10 EEG + 2 EMG</p>	<p>15 healthy subjects</p>	<p>Motor execution</p>	<p>Asynchronous 1 class (NC vs IC)</p>	<p>Fully self-paced paradigm. No external stimuli presented to the subjects. Subjects are free to move and they have feedback on their movement execution task on a computer screen.</p>	<p>5 runs of 5 minutes duration each. 2-3 minutes resting periods between runs. First 2 runs used as calibration and last 3 runs as validation.</p>

<p>Khan Niazi et al (2011), approved by Ethics Committee of Nordjylland, Denmark [43].</p>	<p>10 EEG + 2 EMG</p>	<p>10 healthy subjects</p>	<p>Motor Imagery</p>	<p>Asynchronous 1 class (NC vs IC)</p>	<p>Fully self-paced paradigm. To identify the MI occurrence the subjects were asked to press a button using the hand not used in the MI task 2 s after the imagination of the movement.</p>	<p>4 runs of 5 minutes duration each. First 2 runs the subjects executed the movements. Last 2 runs subject imagined the movement.</p>
<p>Khan Niazi et al (2011), approved by Ethics Committee of Nordjylland, Denmark [43].</p>	<p>10 EEG + 2 EMG</p>	<p>5 stroke patients</p>	<p>Motor attempt</p>	<p>Asynchronous 1 class (NC vs IC)</p>	<p>Fully self-paced paradigm. No external stimuli presented to the subjects.</p>	<p>5 runs of 5 minutes duration each. 2-3 minutes resting periods between runs. First 2 runs used as calibration and last 3 runs as validation.</p>

The study's objective

The application footprint of this research is medical. The aim is to think of a system that is useful for patients with spinal trauma or genetic disorders who have partially or totally lost the use of their upper limbs.

The study will focus on an EEG-dependent BCI. To be able to work with tetraplegic patients, who might have totally lost the ability to move the upper limbs, the type of movements chosen is Motor Imagery.

The final objectives of the study are to attempt to overcome two of the limitations of today's BCI systems.

The first is to create a self-paced, non-cue-based BCI system that allows the patient the freedom to choose when to do the available movements. Most existing BCI systems are based on synchronous paradigms and therefore are far from being applied in a real-life situation [40] [20]. The second is to try to create a subject-independent BCI.

It is important to consider that achieving simultaneously a self-paced and a subject-independent BCI is very complex. Therefore, the 2 objectives of this study can be viewed as single objectives.

Materials and Methods

Two different datasets have been used during this thesis:

1. *Dataset 1 from BCI competition IV*. It's an online available dataset [68] provided by B. Blankertz, C. Vidaurre and K.-R. Müller from the Berlin BCI group [70]. The dataset characteristics can be found in Table 2 of the previous chapter.
2. The second dataset has been acquired during this thesis within the PoliToBIOMed Lab of Politecnico di Torino. The characteristics of this dataset will be set out during this “Materials and Methods” chapter.

Sample population tested

Dataset 1 BCI competition IV: Four healthy participants have been used as experimental subjects. Motor imagery movements have been performed by the subjects during the whole session. No feedback has been provided to the subjects. Each subject performed two classes of Motor Imagery among the following: *left hand movement*, *right hand movement*, *foot movement* (side chosen by the subject, optionally both feet). The dataset description does not specify in detail what exactly is meant by right hand movement or foot movement [68] [6].

Table 3 shows which motor imagery classes were performed by each subject. Subjects are indicated with a letter of the alphabet. The reason for jumping from letter B to letter F is that the other letters belong to artificial datasets not analyzed in this thesis.

Table 3: Motor imagery classes performed by each subject in dataset 1 from BCI competition IV.

Subjects	Motor Imagery classes
Subject A	Left hand, foot
Subject B	Left hand, right hand
Subject F	Left hand, foot
Subject G	Left hand, right hand

PoliTo^{BIO}Med Lab dataset: Four healthy participants have been used as experimental subjects.

The subjects were volunteers. The data acquisition has been conducted within the PoliTo^{BIO}Med Lab of Politecnico di Torino.

Three helmets of different sizes were tried on the subjects before each experiment to choose the most appropriate helmet size. The size of the helmet corresponds to the circumference of the skull

of the subject. The three different sizes are the following: Small (50-54 cm), Medium (54-58 cm), Large (58-62). It is important that the helmet used is snug on the head but does not squeeze too tightly to the point of discomforting the subject [26].

Table 4 shows the helmet size and the ages of the four experimental subjects.

Table 4: Helmet size and age of each experimental subject of the dataset acquired within the PoliTo^{BIO}Med Lab of Politecnico di Torino.

Subjects	Helmet size	Age
Subject A	Medium	25
Subject B	Medium	26
Subject C	Medium	26
Subject D	Medium	20

Both datasets have a numerosity of 4 subjects. The number of subjects in both datasets does not fully allow to reach the goal of a subject independent BCI, as more patients are needed to create a subject-independent BCI [71], but it will allow the implementation of a pilot study for further future analysis.

Description Dataset 1 BCI competition IV

The description of Dataset 1 from BCI competition IV can be found in Table 2 of this thesis in the chapter of “Literature Analysis”. Further details regarding the experimental protocol and the protocol used are reported in this paragraph as described in [6].

The acquisition system consists of a BrainAmp MR plus amplifiers (Brain Products GmbH, Munich, Germany) and a Ag/AgCl electrode cap (EASYCAP GmbH). The signal was filtered in real time, during acquisition, with a bandwidth between 0.05 and 200 Hz. The sampling frequency is 1000 Hz. The signal was then sub sampled at 100 Hz. The data used are from the sub sampled signal.

The paradigm as described in Table 2 can be seen visually in Figure 22.

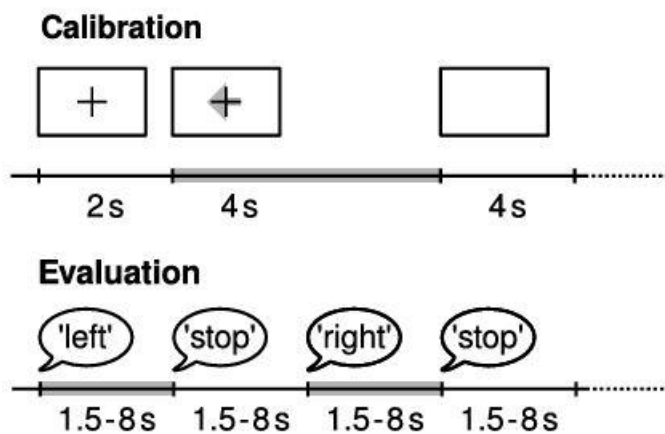


Figure 22: Paradigm structure of Dataset 1 BCI competition IV. The upper paradigm is related to the calibration part of the experiment while the lower paradigm is related to the validation part of the experiment. From M. Tangermann [6].

Acquisition system

This chapter will look in more detail at the software and hardware used to acquire the EEG data belonging to our dataset acquired during this thesis within the PoliTo^{BIO}Med Lab of Politecnico di Torino.

Instrumentation and hardware from “g.tec - medical engineering GmbH” were used.

In addition to the collection of EEG data by means of the g.tec software and hardware described in the following chapter, the creation of a visual stimulus to instruct the subject is necessary for the experiment to function.

It is therefore necessary to have a trigger stimulus that is temporally synchronized with the acquired EEG data.

It is practical to use two computers, one for data acquisition and one for stimulus presentation. The EEG data acquisition amplifier is connected to the computer containing the data acquisition software. A second computer is then used to present the visual stimulus through appropriate software.

Hardware

The following recording devices are used:

1. Biosignal amplifier: we use *g.Hiamp*. It is the data acquisition amplifier;
2. Electrode cap: We use a second-generation *g.GAMMA* cap with high-density electrode placement, 74 labeled standard position (10-10 / extended 10-20 system). The cap comes in 3 sizes: Small (50-54 cm), Medium (54-58 cm), and Large (58-62 cm), allowing the experimenter to choose the most fitting cap for the subject;
3. Electrode system: We use a *g.Scarabeo* active electrode system, compatible with *g.Hiamp* and *g.GAMMA* cap. The system uses active sintered Ag/AgCl ring electrodes;
4. A Recording computer: used to record EEG data. It is directly connected to the biosignal amplifier *g.Hiamp*;
5. A Visual stimulus computer: containing the stimulus created with the visual stimulus software.

Recording Software

The software used to acquire EEG data is *gRecorder*.

It is a software package for the recording of biosignal data such as EEG, ECoG, ECG, EOG, EMG and sensor data, and it allows to capture trigger information [34]. It can acquire data from *g.tec*'s biosignal amplifiers, such as *g.Hiamp*. The recorded data in *gRecorder* are saved in the '.hdf5' format file. In the case of EEG data acquisition, the output contained in the '.hdf5' file only contains a matrix of dimensions [number of channels \times time points].

The graphical user interface of the software appears as in Figure 23 and allows the user several choices. It gives the experimenter the ability to do a raw data inspection, to select the number of observable channels and the length of the observation window. It also allows the user to implement preprocessing on the signal. The preprocessing steps applied on the *gRecorder* software are in turn applied to the saved data in the '.hdf5' format.

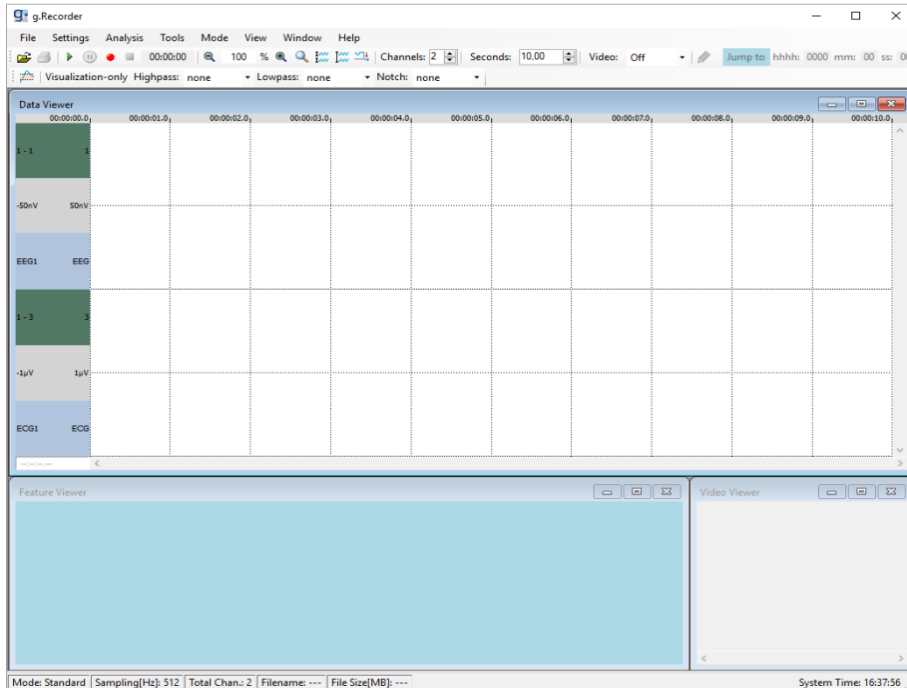


Figure 23: *gRecorder* software graphical user interface.

Visual stimulus software

The stimulus presentation software chosen for this study is *Psychopy* [72].

The *g.tec* acquisition environment, consisting of *g.Hiamp* and *gRecorder*, allows the visual stimulus, from the stimulus computer, to be connected via a parallel port to the amplifier, which transmits the stimulus times directly to the acquisition software *gRecorder* (Figure 24).



Figure 24: The g.tec parallel port used to connect the g.Hiamp amplifier to the stimulus computer.

The limitation of this system is that if the stimulus computer does not contain the appropriate port for the parallel port, a special Trigger Interface Box is required. A virtual COM port (8-bit TTL output) to LPT/parallel port adapter is needed.

Due to the costs of this interface system, it was decided to link the trigger stimulus and the data in a different way, as it will be further explained in the experimental protocol chapter.

Psychopy: It is a stimulus presentation control package for neuroscientists used worldwide. It is a free, open-source package for running experiments in Python.

Psychopy has a dual interface, a *builder interface* (Figure 25) that allows the creation of the experiment with minimal coding, and a *coder interface* (Figure 26) that allows everything to be created by coding.

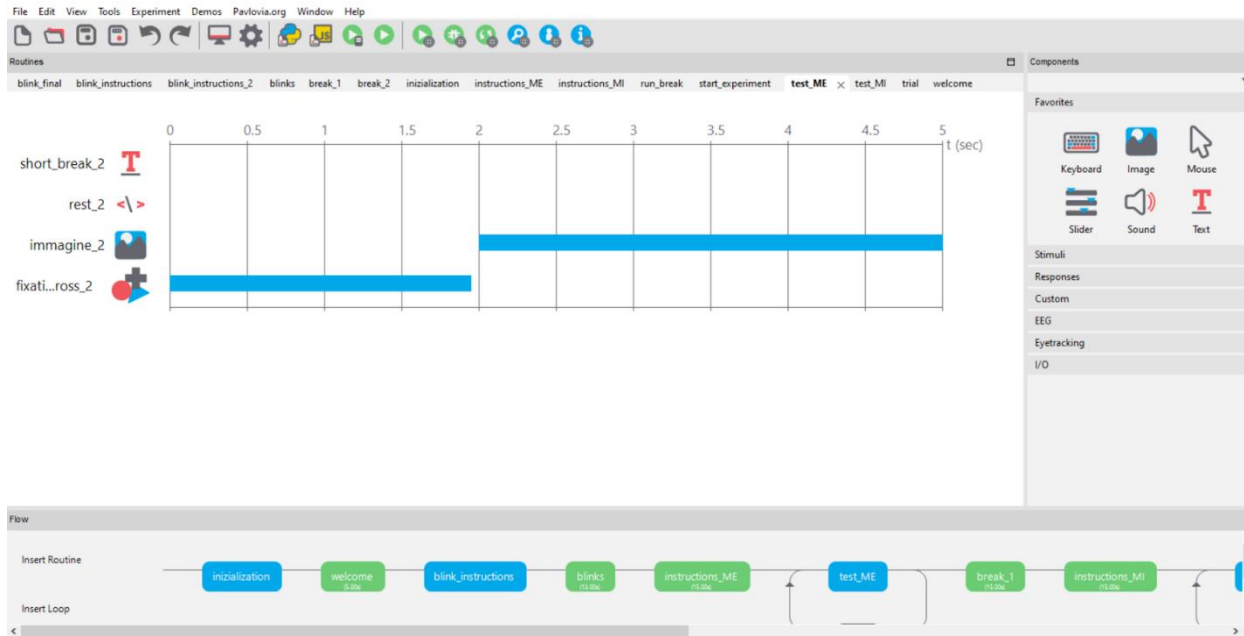


Figure 25: Psychopy Builder Interface.

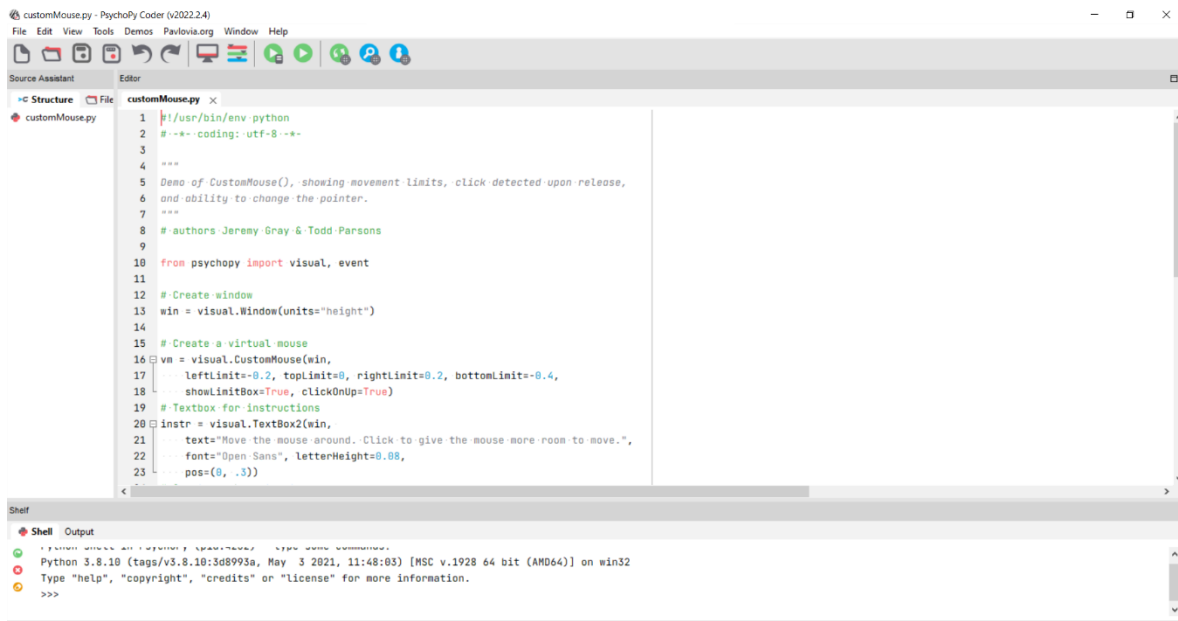


Figure 26: Psychopy Code Editor Interface.

Analysis Software

Two different programming languages have been used to do the data analysis part of this thesis:

1. Matlab: It is a high-level programming language and a numeric computing environments developed by MathWorks [73]. It is designed for scientists and engineers to work with matrix manipulations, data-plotting, develop algorithms and create models.
2. Python: It is a high-level programming language, object oriented, with dynamic semantics. It was first designed by Guido van Rossum and it is developed by the Python Software Foundation [74].

Experimental protocol

This experimental protocol is designed for the acquisition of our own dataset within the PoliTo^{BIO}Med Lab of Politecnico di Torino.

The movement task within this experimental protocol will be the opening and closing of the right hand (Figure 27). It will be a Motor Imagery task so the movement will only be imagined by the subjects and will not be executed or attempted.

The *hand open task* requires the subjects to imagine to fully open the right hand with a full extension of the fingers of the hand (Figure 27a).

The *hand closed task* requires the subjects to imagine to fully close the right hand in a fist position (Figure 27b).

During the experiment when there is no task/hand movement to be done the participants have to keep a neutral hand position, with the hand relaxed and without activating any muscles.

The choice to limit the research to these 2 movements has several explanations. The first is related to a simplification of the system. Having only 2 classes makes it more possible to increase degrees of complexity in other aspects of the system, such as user-specificity and system synchrony [40]. Secondly, two movements such as opening and closing the hand are everyday movements that would allow a user to regain an important motor skill, enabling them to grasp and release objects. Although there are only 2 classes, the use of 2 movements of the same hand complicates its classification compared to movements of two different body parts (for example in comparison to hand and foot, or the same movement but of the right hand and left hand) [48].

Furthermore, the BCI competition IV dataset 1 also uses two movements. Although the movements used in this dataset are different, the use of 2 IC classes, as in dataset 1 of BCI competition IV, allows the same classification models to be applied with appropriate modifications.

a) Hand open



b) Hand closed



Figure 27: Experimental protocol tasks: a) Hand open; b) Hand closed.

The following definitions are defined within the protocol:

6. **Task:** the exercise of imagining a flexion/extension movement of the fingers of the hand, which is initiated and terminated by appropriate on-screen signals;
7. **Trial:** a sequence of a rest period and an execution period of the task;
8. **Run:** a set of n consecutive trials;
9. **Session:** a set of n consecutive runs. The experiment can be paused between 2 sessions by letting the subject rest and by interrupting the recording of the signal.

The experimental protocol is divided into 2 phases: a calibration phase and a validation phase. The 2 phases have different paradigms.

The Calibration phase has two uses. The first is to be used as training for the validation phase. The second is to test a subject independent BCI that can work by training and testing the algorithm on different subjects.

The Validation phase tests a self-paced (and possibly also subject-independent) BCI.

Calibration phase

The calibration is divided into a first subject practice phase in which the signal is not recorded, and the patient is allowed to get used to the task, and a second phase in which the signal is recorded.

Practice: The practice phase consists of 2 short runs with a total duration of 10 trials each. Between each run there is a 30-second rest period. During the first run, the subject performs the task by executing the movement (ME). In the second run, the subject performs the task by imaging the movement (MI). At the end of the second run, there is a one-minute break before the recording phase begins.

Recording: During the recording phase, 4 runs of 315 seconds each (5 minutes) are performed. Between each run, there is a 1-minute break in which the volunteer can relax. Each run consists of 40 trials lasting between 7 and 8 seconds.

Each trial, both in the practice phase and in the recording phase, consists of the following. During the first 2 seconds, a fixation cross appears on the screen indicating to the subject the imminent start of the task. In the end, the type of MI task (open/close right hand) to be performed is shown on the screen. The task execution phase has a constant duration of 3 seconds in each trial, while the rest phase varies randomly between 2 and 3 seconds (Figure 28). The random variation of the rest phase is introduced to avoid adaptation of the subject [15] [6].

Furthermore, within the single run, after the execution of the first 20 trials, there is a 15-second pause to allow the volunteer to relax.

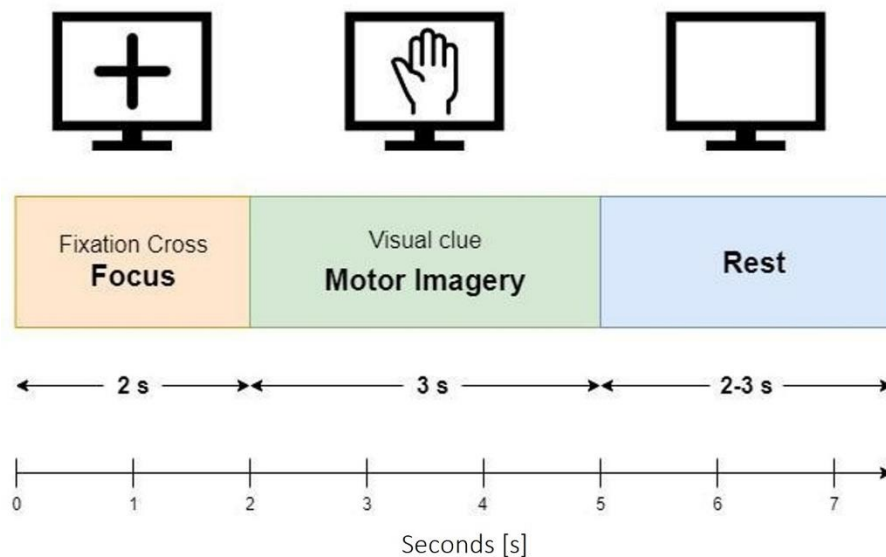


Figure 28: Calibration Phase Trial.

This results in a total of 160 trials per subject, respectively 80 trials per task, in the recording phase. The total duration of the calibration phase, including practice and recording, is around 28 minutes (Table 5).

Table 5: Sequence of the runs in the calibration phase.

		Calibration	Duration (s)
Practice	1	Motor execution test	75
	2	rest	30
	3	Motor Imagery test	75
	4	rest	60
Recording	5	run 1	315
	6	rest	60
	7	run 2	315
	8	rest	60
	9	run 3	315
	10	rest	60
	11	run 4	315

Validation phase

The validation phase consists of 4 runs. Each run consists of 5 trials, respectively 4 of Motor Imagery and 1 of Rest ().

Table 6: Single-run organization in the validation phase.

RUN	
1	Movement trial
2	Movement trial
3	Movement trial
4	Movement trial
5	Rest trial

The trial structure is presented in Figure 29.

The class cue (open hand, closed hand, and rest), a fixation cross, and an acoustic signal are presented at the start of the trial. The class cue is removed at second 5 and only the fixation cross remains on the screen. In the following 60 seconds, the subject may freely perform the movement related to the class just shown. In the case of a rest class cue, the participant must avoid any movement. In the case of a movement-related class signal, the participant may attempt more than one self-performed movement of the required movement class during the 60-second period. In

addition, the subject must signal any MI task after 2 seconds by whispering. The experimenter promptly presses a button on the computer to mark the successful imagining of the movement. Between each run, there is a 25-second break to allow the volunteer to relax. The subject is asked to wait at least 3 seconds between one movement and the next.

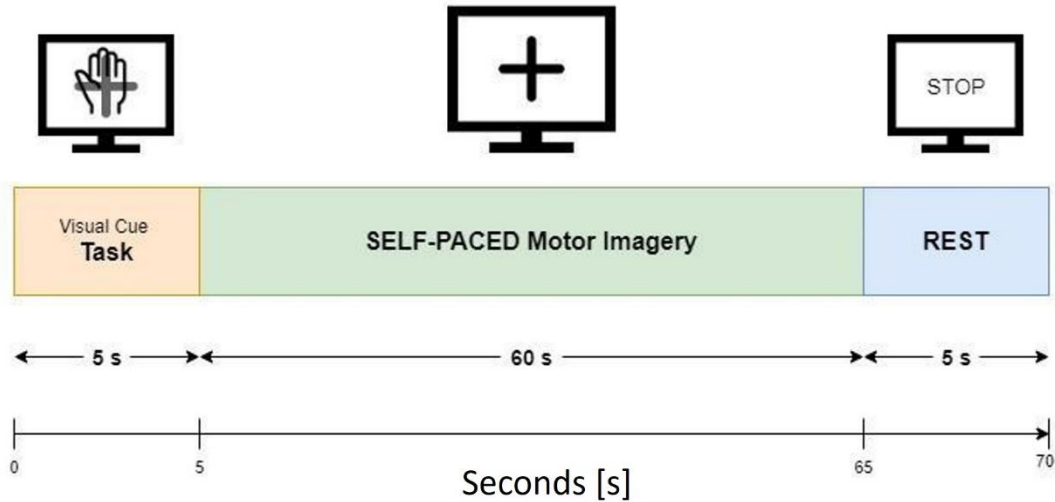


Figure 29: Validation phase trial.

The total duration of the validation phase is around 24 minutes (Table 7).

Table 7: Sequence of the runs in the validation phase.

Validation		Duration (s)
1	run 1	350
2	run 2	350
3	run 3	350
4	run 4	350

Synchronization of stimuli and data

To synchronize the EEG signal recording through the *gRecorder* software with the trigger stimuli obtained through the *Psychopy* software a manual way is used since it isn't possible to connect them through the hardware. The idea is to use the eye-blinking artifact to locate the signal in time.

Eye Blinking: The following sequence is done both at the beginning of the experiment and at the end of it (Figure 30).

visual stimulus	1..	2..	3..	4..	5..	6..
sound stimulus						
eye blink						
blink artifact						

Figure 30: Schematic representation of the synchronization process.

The subject is asked to blink 3 times at a certain rhythm. A visual stimulus counting from 1 to 6 appears on the screen. There is 1 second between each consecutive number. The first 3 seconds are accompanied by a sound stimulus. Those first 3 seconds have the purpose of giving rhythm to the subject. The last 3 seconds have only the visual stimulus, but not the sound one. Based on the rhythm of the previous 3 (1.. 2.. 3..) the subject blinks 3 times during the last 3 seconds (4.. 5.. 6..).

The Psychopy software output contains the time information of when the eye blink is reported on the stimulus presentation computer. On the other hand the gRecorder software output only returns a matrix of dimensions [number of channels x time points]. To synchronize the two outputs the beginning of the eye blinking must be detected in the EEG signal. Once the time point of the beginning of the eye-blink is detected the difference in time points between the two outputs is calculated. The two outputs can now be synchronized by subtracting to the longer output a portion of the dataset corresponding to the difference between these two outputs.

The beginning of the eye blinking is identified manually. When plotting the EEG signal of one of the frontal electrodes the three spikes of the three voluntary eye blinks can be clearly seen with our naked eye at the beginning and at the end of the experiment.

They appear as three consecutive spikes with a distance of about 1 second and an amplitude of approximately 10 times the resting EEG signal. Once the three spikes have been found the beginning of the first three eye blink is manually selected to mark the corresponding time point (Figure 31).

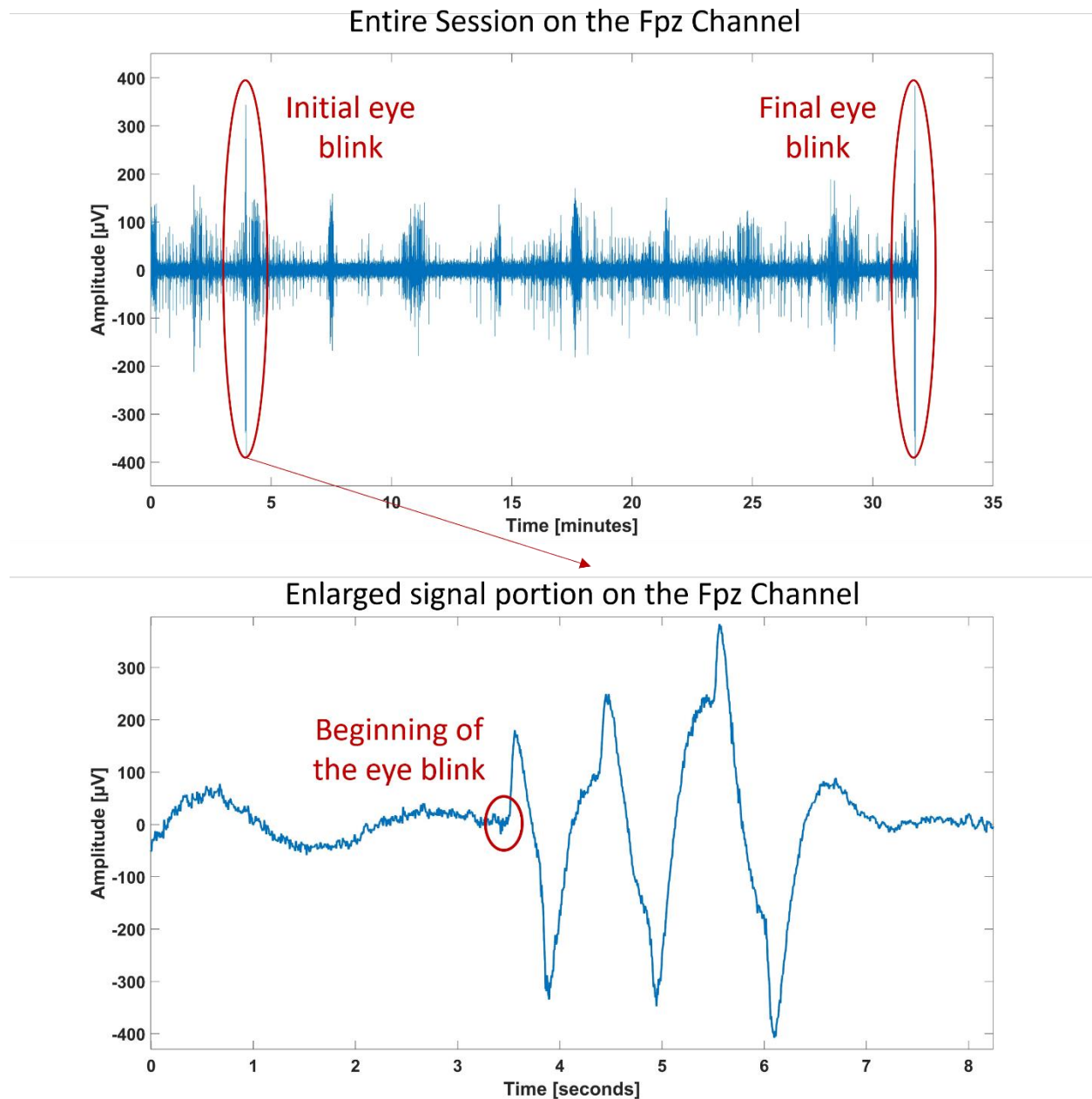


Figure 31: The voluntary eye-blinks recorded on the Fpz channel of subject A from the PoliTo^{BIO}Med Lab dataset. Upper Figure: a picture of the whole length of the signal shows the three eye-blinking spikes at the beginning and at the end of the experiment. Bottom Figure: an enlarged portion of the signal showing the three eye-blinking spikes at the beginning of the experiment.

Electrode positioning

The EEG signal has been recorded using 21 electrodes placed as in Figure 32.

The following electrode positions are used: *FP1, FP2, FPz, FC3, FC1, FCz, FC2, FC4, C3, C1, Cz, C2, C4, CP3, CP1, CPz, CP2, CP4, Pz*.

16 electrodes are placed over the motor cortex. 3 Electrodes are placed in the frontal position. The ground electrode is placed in the AFz positions. The reference electrode pinches the right ear.

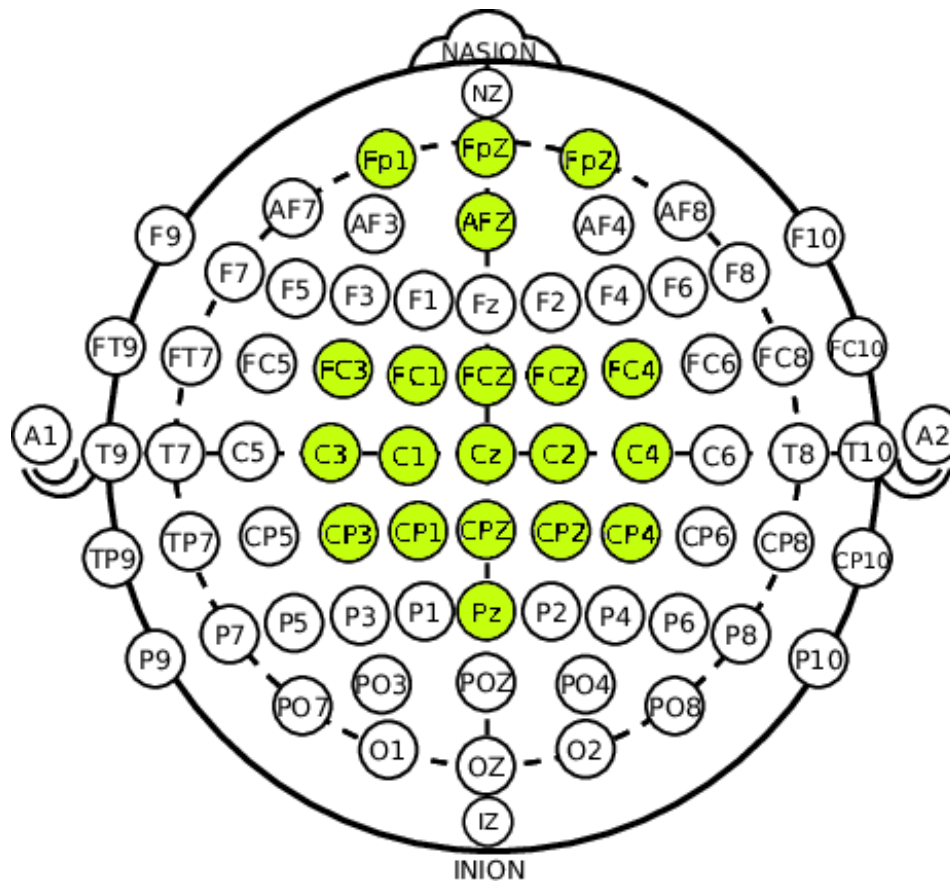


Figure 32: Electrode positioning within the extended 10-20 system/10-10 system. The electrodes colored in green have been used for the data acquisition related to this thesis. Modified from Zhang et al. [75].

The electrodes cover the motor cortex area since the aim of the data acquisition is to study the motor rhythms, which can be found over the motor cortex [8]. The positioning of the electrodes was inspired by the following datasets: *BCI Competition IV - Dataset 1* [68], *BCI Competition IV - Dataset 2a* [68], *Dataset from Ana. P. Costa* [48], *S. Romagosa et al.* [21]. All the datasets just mentioned deal with Motor Imagery and use electrode placement on the motor cortex similar to that of Figure 32.

Sixteen electrodes were chosen to cover the motor cortex. The choice of numerosity has a twofold reason. On the one hand, the performance of the BCI, on the other hand the experiment preparation time. It has been seen that datasets using fewer electrodes classify worse. For example, *BCI Competition IV - Dataset 2b* [68] that uses only 3 electrodes has lower classification performance compared to dataset with higher numerosity such as the dataset from *S. Romagosa et al.* [21] and *Dataset from Ana. P. Costa* [48], which have both 16 electrodes. On the other hand, datasets with a larger number of electrodes, such as *BCI Competition IV - Dataset 1* [68], which has 59

electrodes, and Dataset O-Yeon Kwon et al [5], which has 62 electrodes, do not perform better in classification than the previous cited dataset with only 16 electrodes.

This is probably due to the limits of the EEG spatial resolution. When there are too few electrodes, a choice must be made between a high electrode spacing, which limits the spatial resolution of the signal, and a closer spacing of the electrodes, which, however, limits the useful area covered on the scalp. Increasing the number of electrodes and the proximity between electrodes improves the signal spatial resolution and increases the area of the scalp covered by the electrodes. Continuing to increase the number of electrodes, however, would not seem to improve the performance of the classifier [40]. This could be due to a limitation of the EEG signal, which has a low spatial accuracy due to the “smearing” phenomenon of the electrical potential which dampens and spreads the signals [26].

Furthermore, increasing the number of electrodes increases the experimenter's preparation time for the experiment. Using 16 electrodes allows for obtaining a good classification performance without requiring too much preparation time for the experimenter. It is important to note that the preparation time for electrode placement can also vary depending on the experimenter's experience.

Recording setting

The following settings have been chosen on the *gRecorder* software for the data acquisition:

10. The signal sampling frequency has been set at 512 Hz, high enough not to incur in the aliasing phenomena.
11. Each channel has selected a bipolar reference, using channel 1 as a reference electrode.

Subject's Questionnaire

At the end of each experiment, we verbally conduct a survey asking the subject to answer the following question:

1. Did you find the duration excessive?
2. Were you able to maintain your concentration for the entire duration of the experiment? Did you have moments of distraction? If so, can you quantify them?
3. Did the electrode cap bother you?
4. Did it seem to you as if you were able to imagine the required movement well?
5. During the individual trials, did you get the imagery and rest times right?
6. Did you feel like you were able to meet the demand in all tasks? How many times did you approximately make mistakes? Could you quantify?
7. Do you have any further comments about the experiment just conducted?

The results of the questionnaire are reported in the Results chapter of this thesis.

Experimental protocol aim

The aim of the experimental protocol is to satisfy the two goals contained in the study's objective, and, therefore, to create a protocol that allows us to work on an asynchronous, self-paced and subject-independent BCI.

The structure of the experimental protocol allows us to achieve both goals, and, at the same time, to concentrate only on one in case the other is too complex. The use of a calibration phase and a validation phase is intended to study a self-paced BCI, but this self-paced system is unlikely to be subject-independent. While for the application of a subject-independent system one can be satisfied with the calibration paradigm that is synchronous, thus creating a subject-independent but synchronous system.

PoliTo^{BIO}Med Lab Data Visualization

Before starting to process the data acquired during the experiment at the PoliTo^{BIO}Med Lab, a pre-analysis was performed to check the raw data to see how the acquired EEG data appeared compared to the given external stimulus. Data for subject A were observed during the calibration phase of the experiment.

The stimulus vector or trigger vector of the subject appears as in Figure 33. When the ordinate value is at 0, it means that no type of stimulus is presented to the subject. This is class 0 which corresponds to the No Control phase. When the value rises to 1 or 2 it means that a stimulus is presented to the subject, corresponding to the Intentional Control phase. When the trigger value is at 1 the Hand open stimulus (class 1) is presented to the subject, when the trigger value is at 2 the Hand closed stimulus (class 2) is presented to the subject.

It can be clearly seen the division between the 4 runs of the experiment and the minute break within the runs. It can be seen how within the runs the presentation of the hand open, hand closed stimuli appear randomized.

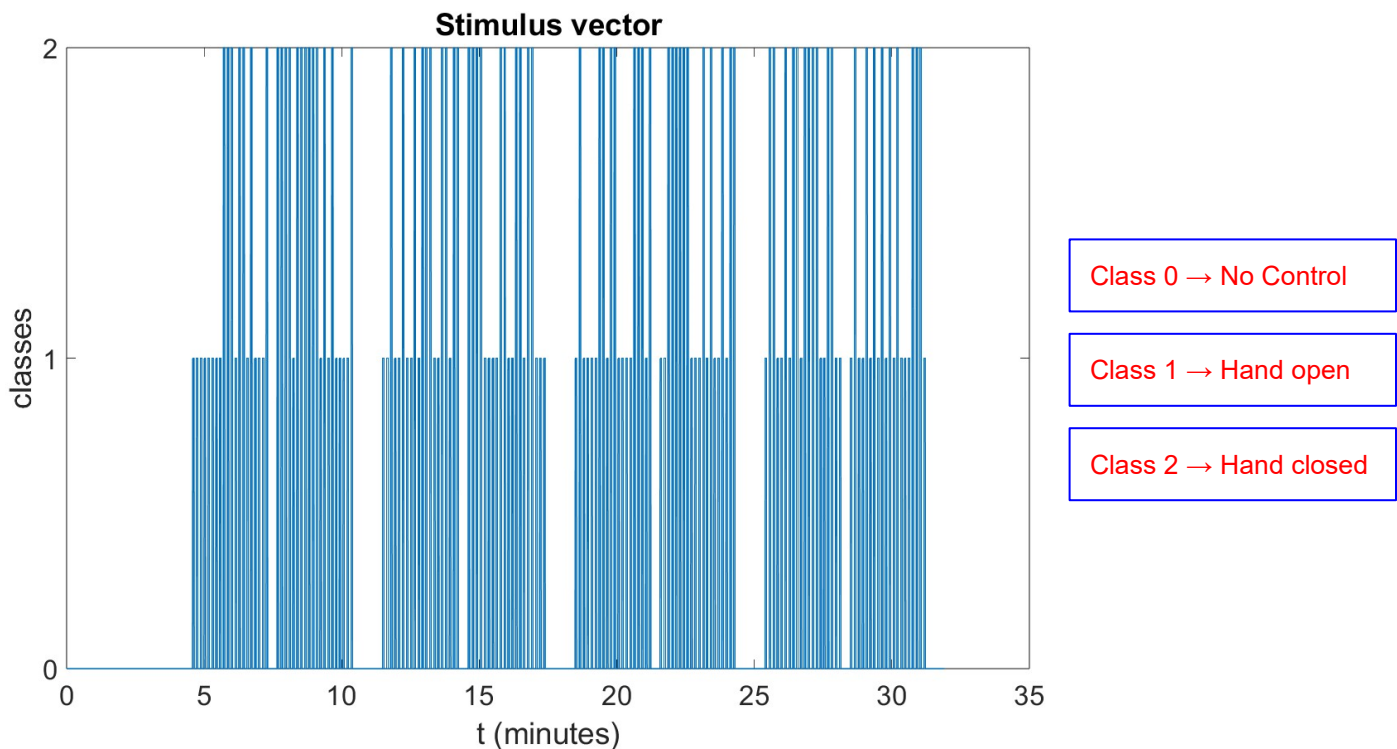


Figure 33: Stimulus Vector for subject A of the PoliTo^{BIO}Med Lab dataset during the calibration phase of the experiment. The x-axis shows the time axis in minutes. On the y-axis the value corresponding to the class: class 0 (no stimulus), class 1 (open hand), class 2 (closed hand).

Figure 34 shows the EEG signal of electrode CP1 throughout the experiment. The stimulus vector is superimposed on the raw EEG signal. This allows us to distinguish at what times in the recording

the desired stimulus is delivered. The blue signal corresponds to the NC phase, the green and red signal correspond to the IC phase.

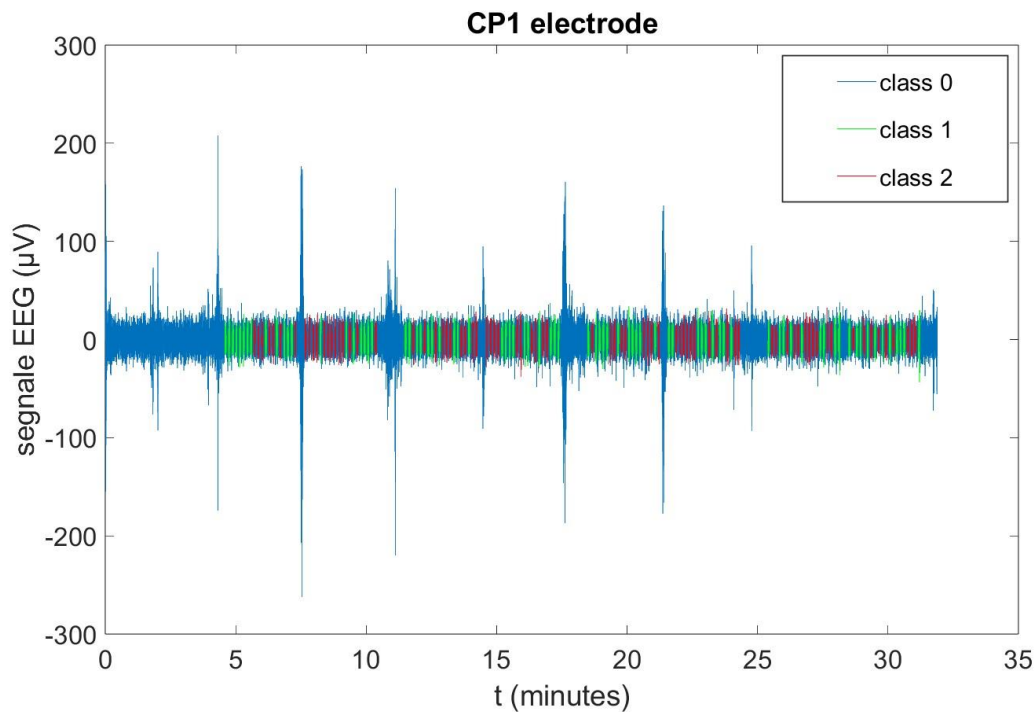


Figure 34: EEG signal on the CP1 electrode for subject A of the PoliTo^{BIO}Med Lab dataset during the calibration phase of the experiment. The signal is colored in blue during the NC phase (class 0), in green and red during the IC phase. When the signal is green the hand open stimulus is presented (class 1). When the signal is red the hand closed stimulus is presented (class 2).

Zooming in on a portion of the signal about one minute long (Figure 35), it can be seen that it is impossible to distinguish with the naked eye on the raw EEG signal to which class each portion of the signal belongs.

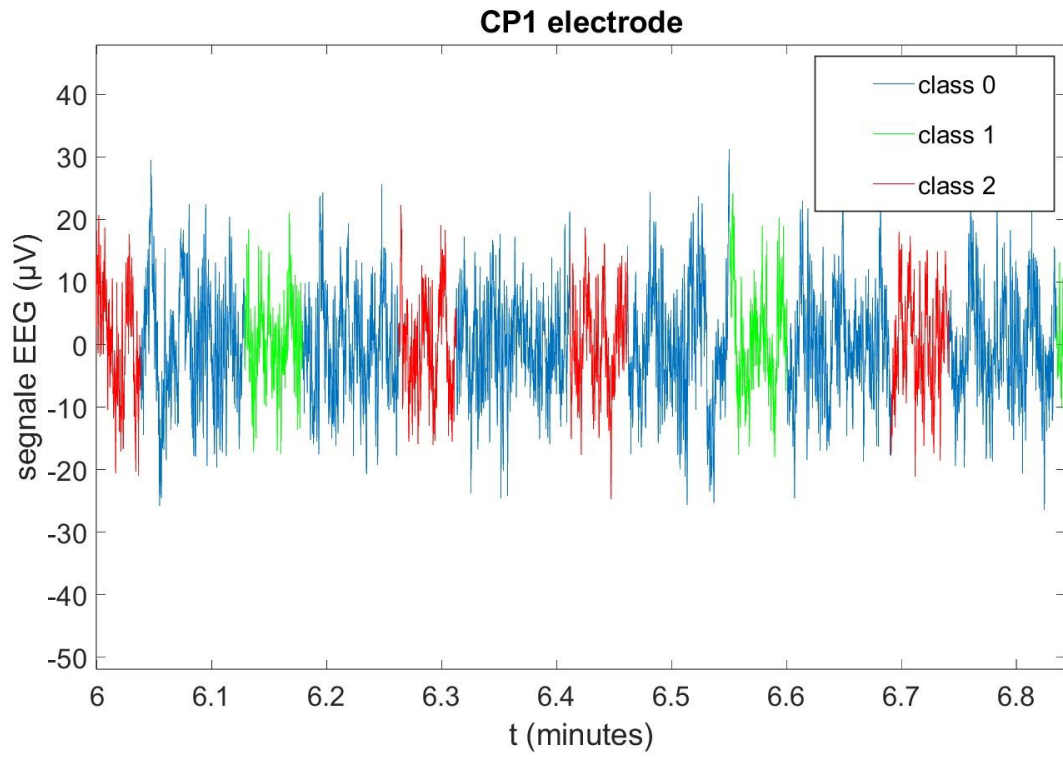


Figure 35: Zoom in of Figure 34. The zoom is applied to a portion of the signal about one minute long between minute 6 and minute 7 of the experiment.

Processing steps

This chapter will analyze all the processing steps that, starting from the raw signal, allow to reach the output of the experiment.

Processing steps can be divided into three categories:

1. Pre-processing, here the raw signals are processed through various steps that clean the data, trying to remove noise and artifacts, preserving only the part of the data useful for later analysis [36].
2. Feature extraction, the aim here is to describe the signals using few relevant values which can be named “features” [20].
3. Classification, from the extracted features the data are classified into the classes using machine learning or deep learning algorithms [20]. The algorithms used in this thesis are machine learning algorithms.

The pipeline with all the processing steps can be seen in Figure 36. The same pipeline is used to analyze both datasets, the Dataset 1 from BCI competition IV, and the PoliTo^{BIO}Med Lab dataset. The pre-processing steps used are the same in both the calibration and validation phases. What differentiates the two phases are the feature extraction and classification steps.

In this thesis, all analyses, both for data related to the calibration phase and data related to the validation phase are performed offline.

However, the ultimate purpose of the validation phase would be to act online, classifying classes in real-time. Consequently, the processing steps of the validation phase are designed to be able to implement in a later study a BCI that classifies online in real time.

The calibration phase involves dividing the signal into epochs. Each signal epoch will subsequently be classified into a class.

Following the division into epochs, a k -fold cross validation is carried out to train and test different classifier models and choose the best one. The k -fold cross validation works as follows:

1. Once all epochs of the signal have been extracted, these epochs are randomly reordered, losing the information related to the temporal position of the epoch with respect to the signal. The epochs are then divided into k subgroups with the same number of epochs called folds.
2. $k-1$ folds are used for training the classifier model. The remaining fold is used for testing. This process is repeated k times so that each fold is used once as a testing fold.
3. After each iteration, the performance of the testing fold is looked at and the average performance over all k folds returns the calibration performance.
4. The model parameters related to the testing fold that obtained the best performance are saved for use in the validation phase.

Two models are trained during the calibration phase:

1. A model which distinguishes the two *IC* classes.
2. A model which distinguishes between the class of *NC* and the class of *IC*.

In the validation phase, because it is designed for an online analysis, the signal is no longer divided into randomized epochs. A window of length t that runs along the signal is used, and each x samples performs the feature extraction and classification steps by classifying the epoch on which the window is located. The window length used in the validation phase for Dataset 1 from BCI competition IV is $t = 2s$ and the classification is done each 10 samples. This means that the BCI returns a classification output every 0.1s being $fs = 100$ Hz.

The best parameters for each classifier, saved in the calibration step, are used for classification of the signal window. Thus, there is no longer a training and testing phase of the models here, which were precisely trained in the calibration phase.

As the window slides over the signal, a classification is made to distinguish between the *NC* class and the *IC* class, using the model trained in the calibration phase for the distinction between *IC* and *NC* classes. If the window is classified as *NC*, no further steps are taken. If the window is classified as *IC* then a further step is taken to distinguish between the two *IC* classes.

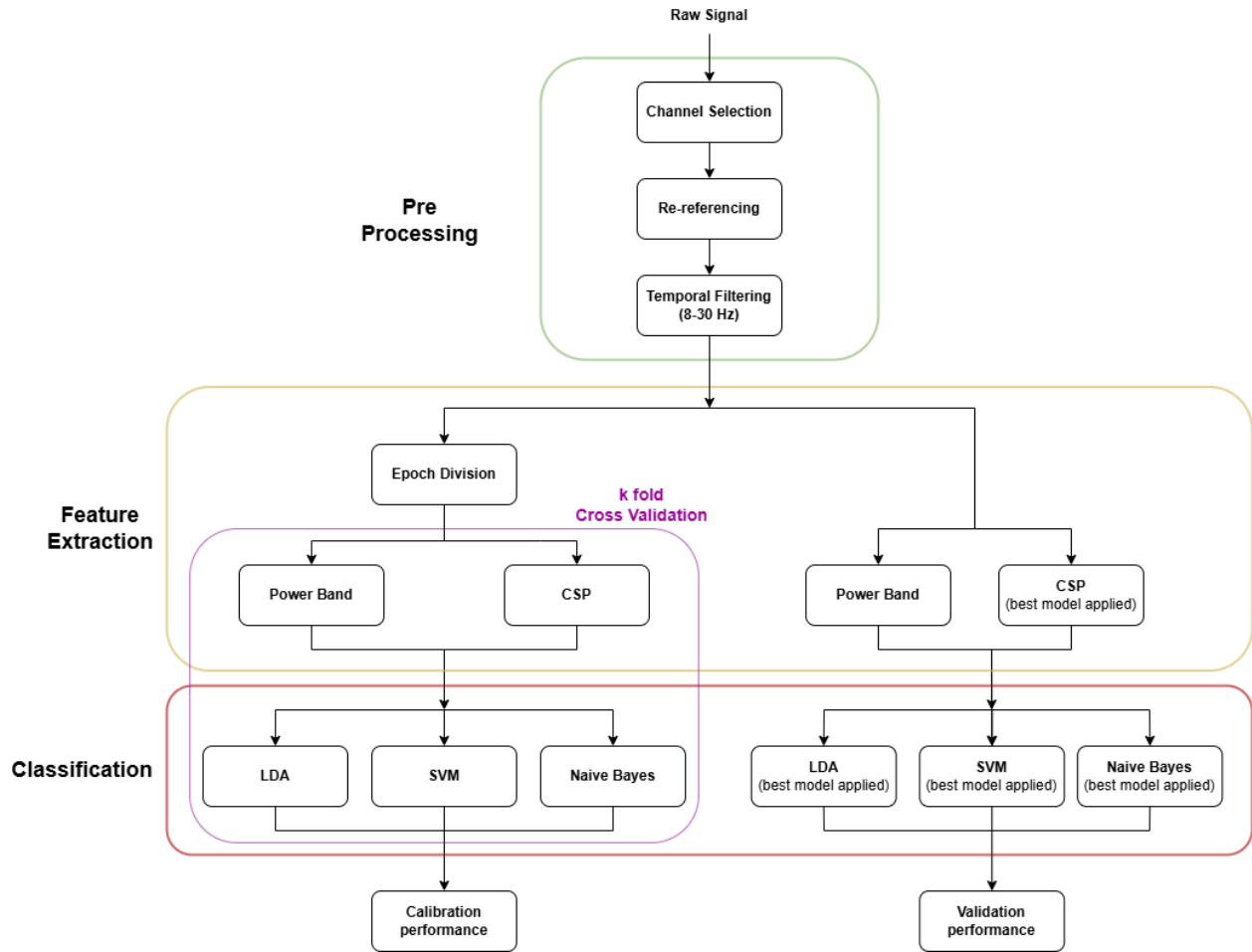


Figure 36: Pipeline of the processing steps used in the analysis of the data.

All of the processing steps are analyzed into further details in the next paragraphs.

Subject Independent BCI steps

To create a subject independent BCI the model is trained on the total of the 4 subjects minus one and tested on the remaining subject. Four combinations are created as it can be seen in Table 8 for Dataset 1 from BCI competition IV and in Table 9 for the PoliTo^{BIO}Med Lab dataset.

Data from the 4 subject calibration phase are used, while data from the validation phase, which were structured for a user-specific BCI, are not used.

Two stages are used for the construction of an independent subject BCI within this thesis:

1. A *calibration phase* for the subject independent BCI: within this phase, the epochs of the three training subjects are grouped, randomized, and a 5-fold cross-validation is done on these epochs. The average performance over the k folds returns the calibration

performance. The model parameters related to the testing fold that obtained the best performance are saved for use in the validation phase.

2. A *validation phase* for the subject independent BCI: the model trained in the calibration phase is used to test the performance on the test subject.

Table 8: Combination of training and testing subjects for the subject independent BCI of Dataset 1 from BCI competition IV.

	Train on subjects	Test on subject
Combination 1	A, F, G	B
Combination 2	A, B, G	F
Combination 3	F, B, G	A
Combination 4	A, B, F	G

Table 9: Combination of training and testing subjects for the subject independent BCI of the PoliTo^{BIO}Med Lab dataset.

	Train on subjects	Test on subject
Combination 1	A, C, D	B
Combination 2	A, B, D	C
Combination 3	C, B, D	A
Combination 4	A, B, C	D

Pre-processing

Channel selection

Dataset 1 BCI competition IV: Of the 59 available channels, the 16 channels closest to the motor cortex were selected by using as a reference [48] and [21]. The selected channels are as follows: Fc3, Fcz, Fc4, C5, C3, C1, Cz, C2, C4, C6, CP3, Cp1, Cpz, Cp2, Cp4, Pz, O1, Oz, O2, POz, Fpz. Using channels far from the motor cortex could worsen BCI performance by introducing non-significant features [76], as the aim of the data acquisition is to study the motor rhythms, which can be found over the motor cortex [8].

PoliTo^{BIO}Med Lab dataset: Since channel selection was already done within the experimental protocol, there was no need to make a subsequent selection during analysis. No channel exclusion analysis was carried out to eliminate any possible noisy channels.

Re-Referencing

The re-referencing has been done using a CAR filter in the analysis of both datasets. Both datasets have been studied with and without the CAR filter applied.

Temporal filters

There are two main types of digital filters used in signal processing [36]:

1. FIR (Finite Impulse Response) filters produce an output that depends only on a finite number of past and present input values. They are called finite because the impulse response, that is, the output of the filter, eventually settles to zero. They are generally stable filters, meaning that rounding errors or overflow issues are minimized. They are not filters that can be used for real-time analysis.
2. IIR (Infinite Impulse Response) filters use a recursive algorithm that considers both past input values and past output values, thus allowing the signal to be processed in real time. They are less stable than FIR filters.

Both datasets have been pre-filtered during the acquisition of the data and then have been filtered offline during the data analysis.

Dataset 1 BCI competition IV: The data have been pre-filtered during acquisition as described previously in this thesis in the chapter of Materials and Methods in the paragraph “Description Dataset 1 BCI competition IV”. During the data analysis a bandpass Butterworth filter of 4th order is applied between 8 and 30 Hz. The Butterworth filter is an IIR filter, which makes it suitable for future online/real-time analysis.

PoliTo^{BIO}Med Lab dataset: The signal has been filtered online during data acquisition using the gRecorder software. The following online filters have been applied:

1. A 0.5-100 Hz Band-pass filter.
2. A 48-52 Hz Notch filter.

The order and type of filters applied is not specified in the software or in the instruction manual of the software used [34]. As the filters are applied in real-time it can be said that these are IIR filters. During the data analysis a bandpass Butterworth filter of 4th order is applied between 8 and 30 Hz.

To see the effect of the filters applied using the gRecorder software, an estimation of the power spectral density (PSD) of the signal has been made (Figure 37), which shows how the signal power is distributed among different frequencies. The PSD is done on the data of subject A during the calibration phase of the experiment. electrode FCz is selected. The PSD has been done throughout the whole duration of the signal. Since the signal before filtering is not available, it is not possible

to make a comparison between before and after. However, something can be observed by magnifying the signal in the frequencies of interest:

- Figure 38 shows the application of the Notch filter. The signal power is indeed clearly lowered around 50 Hz.

- By magnifying the signal between the frequencies of 0 and 5 Hz (Figure 39), it can be seen that the signal power has been lowered below the frequency of 0.5 Hz.

- Looking at the signal in the frequencies above 70 Hz (Figure 40), one can see how the signal power has been knocked down above the frequency of 100 Hz.

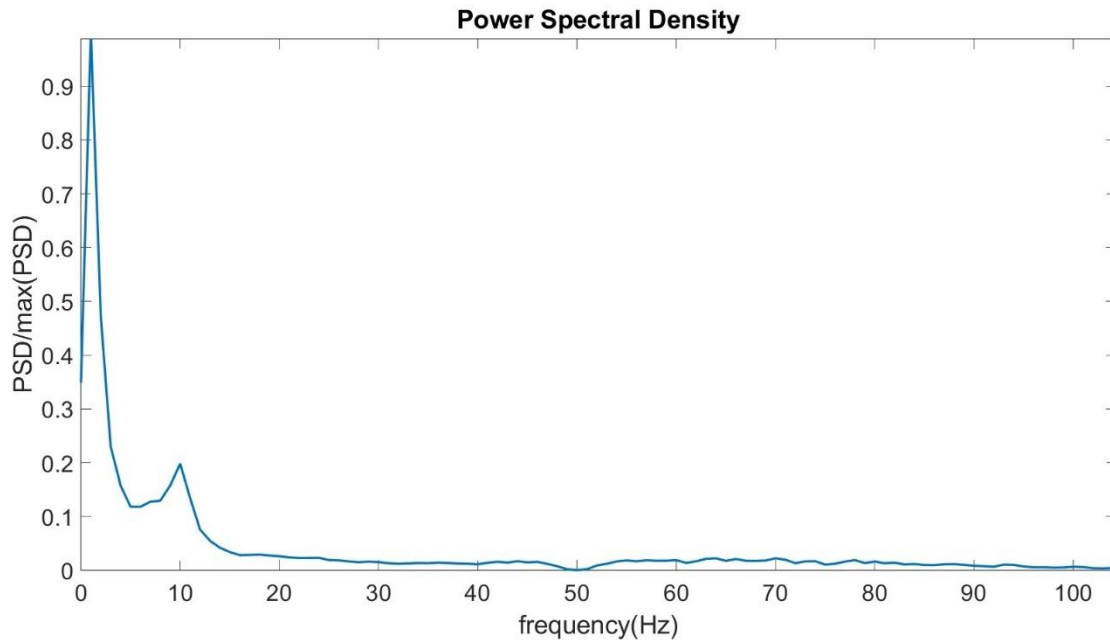


Figure 37: PSD of the signal of the FCz electrode of subject A during the calibration phase of the experiment.

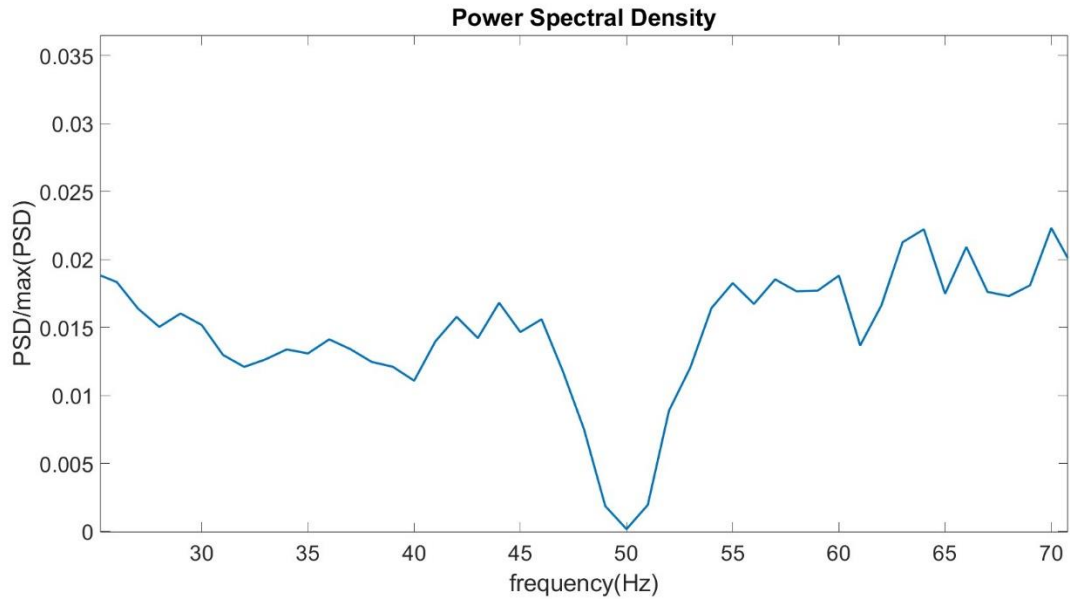


Figure 38: Zoom in of Figure 37. The zoom is done on the x-axis in order to see the reduction of the signal's power around 50 Hz.

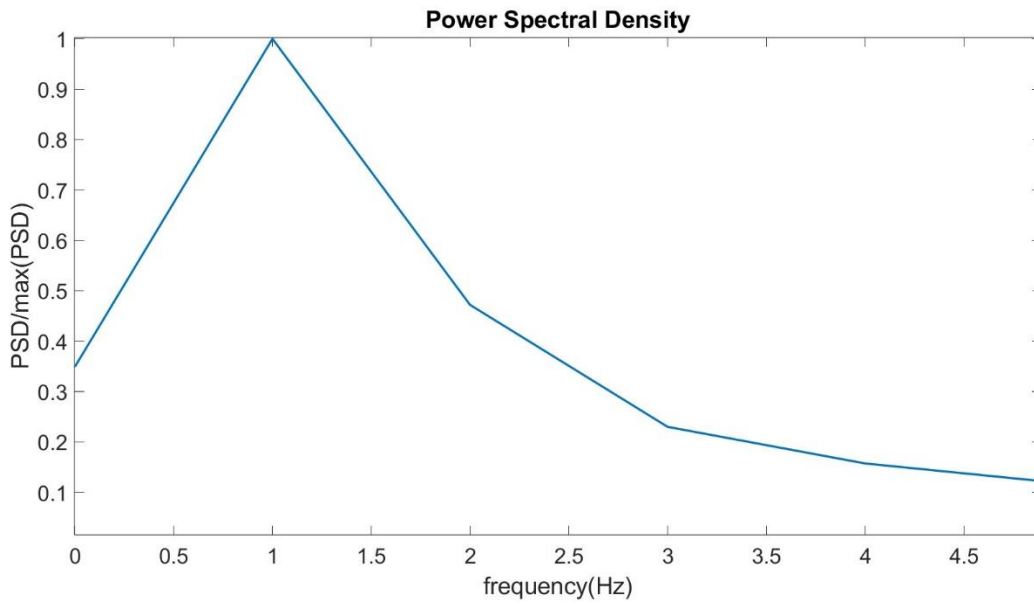


Figure 39: Zoom in of Figure 37. The zoom is done on the x-axis in order to see the reduction of the signal's power below 0.5 Hz.

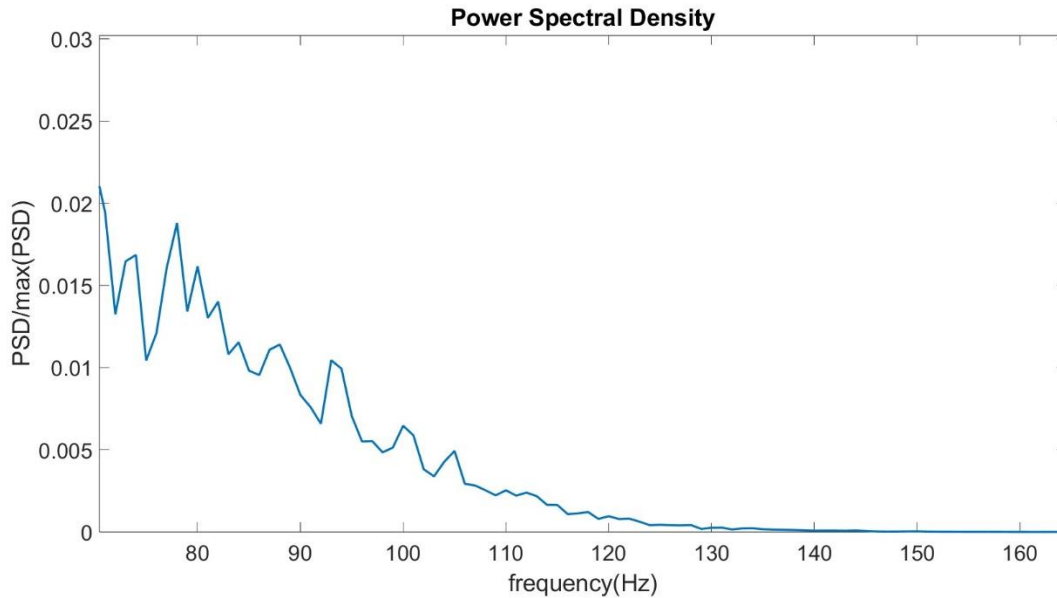


Figure 40: : Zoom in of Figure 37. The zoom is done on the x-axis in order to see the reduction of the signal's power above 100 Hz.

Epoch Division

In order to do feature extraction, the signal must be previously divided into epochs [36]. The signal is a matrix $C \times S$, where C is the number of EEG channels and S are the signal samples. The total number of signal samples S is given by the sampling rate multiplied by the total duration of the signal in seconds. An epoch is a portion of the signal of size $C \times E$, where $E = fs \times \text{epoch duration (seconds)}$.

Epochs can vary according to the following characteristics:

1. Duration of the epoch in seconds (L).
2. Beginning of the epoch, the starting time in seconds from the start of the cue (I).

If the purpose of epoch division is to classify a portion of the signal within a class, the epoch duration is related to the duration of the stimulus corresponding to that class. The epoch may therefore have a duration equal to the duration of the stimulus or less. An epoch is unlikely to have a duration longer than the duration of the stimulus, since it would go on to incorporate within it a part of the signal that is not significant for the classification of the epoch. For the same reason, the epoch may begin with the onset of the stimulus, or later, if the signal within it is contained within the portion of the signal related to the stimulus to be classified.

Feature extraction techniques make it possible to extract from each epoch $C \times E$, a vector F , where F is the number of features contained in a signal epoch.

Feature extraction

Feature extraction techniques used in the BCI world can be of two types [40]:

1. Supervised feature extraction: They make use of labeled data to extract features, meaning that they use the class information of the data to extract features. An examples are Mutual information Feature Selection techniques [77].
2. Unsupervised feature extraction: rely only on input data and do not use any class labels. An example of this are Principal Component Analysis (PCA) and Independent Component Analysis (ICA) techniques [40]. These techniques are often referred to as part of the pre-processing steps, rather than the feature extraction steps [78].

Two Feature Extraction techniques are used within this thesis: the Power band technique, which is an unsupervised technique, and the Common Spatial Pattern (CSP) technique, which is a supervised technique.

Power Band

As has been stated in in the introduction of this thesis the EEG signal is characterized by oscillatory activities in different frequency bands. In particular, the alfa and the beta band can be particularly interesting to discriminate between different mental states during MI by extracting the power contained in those bands [44].

In fact, Power Band features are widely used as a feature extraction method in Motor Imagery detection [40].

To estimate the Power band features 3 signal processing steps are followed (Figure 41) [79]:

1. The EEG signal is band-pass filtered in the frequencies of interest (mainly alfa and beta band as stated before). This way only informative frequencies are kept, while unnecessary ones are dampened out.
Different literature sources use a Butterworth IIR filter of order 4 [80] [81], but in general different kind of filters can be used and adapted to the problem at hand [35].
2. The filtered signals are then segmented into epochs, each one corresponding to the MI trial of interest. Thereafter each channel is squared and averaged over the epoch to estimate the power.
3. In the end the features are logarithmically squared.

The total number of features extracted for each trial of interest corresponds to the number of EEG channels.

The approach explained above is one of the most popular approaches to extract power band features and it is the one adopted in this thesis. Other approaches are possible, for example: power spectral density estimation using an auto-regressive model, The Wigner-Ville distribution, the periodogram, the spectrogram and the Morlet wavelet scalogram [82].

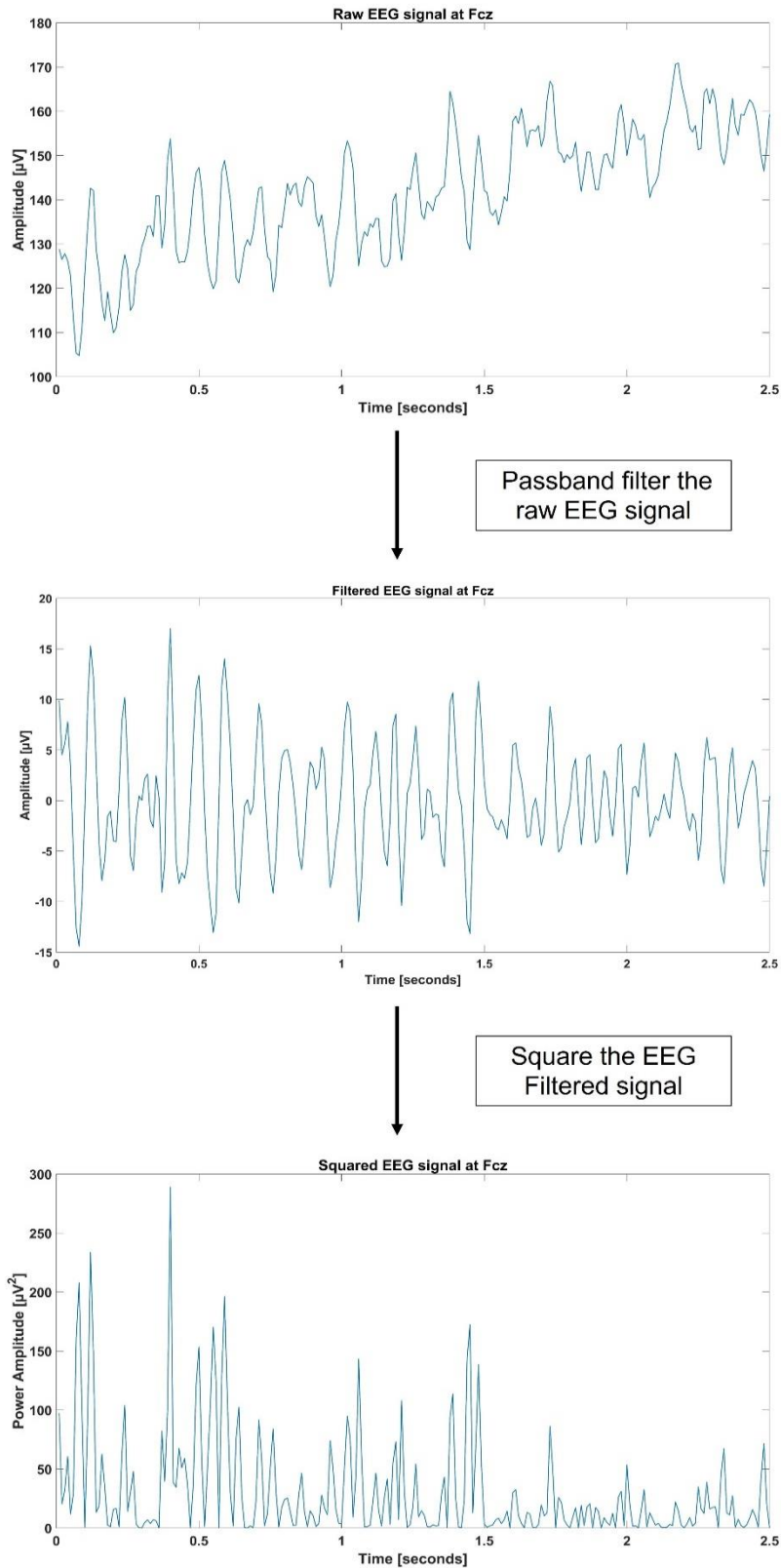


Figure 41: Application of the three steps of Power band feature extraction over a signal epoch of subject A of dataset 1 of BCI competition IV. The channel in the figure is the Fcz channel.

Common Spatial Pattern

Spatial filters are commonly used as a method to separate between classes in MI task experiment. The Common Spatial Pattern (CSP) is one of the most popular spatial filters used in literature [21] [40] [48] [49] [54] [62]. Originally it was conceived and designed for a two-class classification, although it can be adapted to a larger number of classes [62]. In this work it will be used to discriminate between 2 classes.

The assumptions behind this method are as follows:

12. The time windows and frequency band are known.
13. The band-passed signal is jointly Gaussian between this time-frequency window.
14. There is a difference between how activity is expressed between two conditions, i.e. there is some information that is informative about our classes.

CSP is a data-driven supervised method to decompose the epochs of the signal and transfer a high dimensional EEG signal into a lower dimension spatial subspace through a transformation matrix W . This transformation allows to discriminate between the 2 classes by maximizing the filtered signal variance for one class while minimizing it for the other [54] (Figure 42).



Figure 42: Application of CSP filter on a signal epoch of subject A of dataset I of BCI competition IV. On the left: the scatter plot of the first and last row of the unfiltered EEG signal for the 2 classes of Intentional Control. The distribution of sampling before the CSP filtering is shown. On the right: the scatter plot of the first and last row of the CSP filtered signal for the 2 classes of Intentional Control. The ellipses show the estimated covariance and the direction of the CSP projections. This figure shows how the variance of class 1 is maximum in X_{csp} row n.16 but minimum in X_{csp} row n.1 while the variance of class 2 is opposite to class 1. It is observed that the application of CSP significantly increases the separability of epochs of different classes.

In particular, the spatial filtering is applied to the EEG signal $X \in R^{CxT}$ in the original sensor space by the matrix $W \in R^{CxC}$, where C is the number of channels and T is the number of samples, to

linearly transform the signal and obtain $X_{CSP} \in R^{CxT}$, which belongs to a surrogate spatial subspace.

$$X_{CSP} = W^T X$$

The column vectors of W , $w_i \in R^C$ (with $i = 1, \dots, C$), are the spatial filters.

The matrix W allows the simultaneous diagonalization of the two covariance matrices S_1 and S_2 , belonging to the two classes respectively, by solving the eigenvalue decomposition problem [4].

$$S_1 W = (S_1 + S_2) W D$$

Where D is the diagonal matrix containing the eigenvalues of S_1 . W can be easily calculated in Matlab with the command $W = eig(S_1, S_1 + S_2)$.

To recapitulate, the variance for class 1 trials is greatest in the first row of X_{CSP} and decreases with the following rows, and the opposite happens for class 2 trials. One can exploit this property to extract features from the CSP based on the variance. Features are extracted by isolating the first three components and the last 3 components of the X_{CSP} matrix. Then the variance VAR_p of each of these time series is calculated over a time window of the epoch of interest. Following normalization and logarithmic transformation, 6 features f_p are extracted, 1 for each time series taken from the X_{CSP} vector.

$$f_p = \log \left(\frac{\text{Var}_p}{\sum_{p=1}^6 \text{Var}_p} \right)$$

Classification

Three different types of classifiers have been used during the data analysis, the Linear Discriminant Analysis (LDA), the Support Vector Machine (SVM) and the Naïve Bayes. They all use a supervised learning approach to solve the classification problem. This means that these types of classifiers need labeled training data. After they have been trained on labeled data the classifiers can then be used to distinguish between classes on the testing or validation set.

They all receive as input a matrix $F \times N$, where F is the number of parameters and N is the number of epochs to be classified. Together with the input matrix they also receive a vector of the length of N with the label of the classes of each epoch. Thanks to the matrix $F \times N$ and the labeled vector they realize the prediction model which can then be used on the testing/validation set to assign to each unknown epoch the corresponding predicted class.

Performance evaluation

This section will focus on describing the metrics used to evaluate the performance of a BCI.

It is essential to have a common performance metric within the literature to be able to effectively compare research from different laboratories. However, there is no single metric to describe the performance of a BCI, but there are several parameters that can be applied to different types of BCIs. For example, a 6-class synchronous BCI will use different parameters from a 2-class asynchronous BCI, as the objectives are different, and therefore the performance metric must also be different. In the same way, a BCI designed to work in real-time will have different objectives and a different evaluation metric from an offline BCI.

For an M-class classification problem, the tool used to describe the classification performance of a BCI is the *confusion matrix* [83]. A confusion matrix is a table layout in which each row represents the actual condition of each class, its actual classification, and each column represents the predicted class. Therefore, the predicted output is related to the actual condition.

Table 10: Example of a confusion matrix for a 3-class classification problem with a balanced dataset.

		predicted output			
	Class	1	2	3	Total
actual condition	1	80	10	10	100
	2	15	65	20	100
	3	12	18	70	100
Total		107	93	100	300

In Table 10 we can see an example of a confusion matrix of a 3-class classification problem. The individual elements of the confusion matrix n_{ij} indicate how many class i trials were classified as class j . The elements on the diagonal n_{ii} , the blue elements, indicate the correctly classified trials. Elements outside the diagonal indicate incorrect classifications. N represents the total number of samples, and it can be calculated as the sum of all the elements of the confusion matrix.

If the confusion matrix is asymmetrical, it means that there is a biased classification toward certain classes.

The confusion matrix gives a clear idea of classification performance by eye. However, it is inconvenient for comparing different studies containing a different number of classes and total trials. In order to make an effective comparison, a single parameter defining the performance of a

BCI is needed. There are mainly 2 parameters used in the literature, one applies to balanced datasets and the other applies to unbalanced datasets.

A dataset is defined as balanced when all classes appear an equal number of times throughout the session. When this does not happen, the dataset is defined as unbalanced. Different performance metrics are used in the two cases:

1. **Balanced:** If the aim is to measure the overall performance of a BCI as the number of correctly classified trials, the metric to be used is *accuracy*, or its mirror version, i.e. *classification error*. This parameter, the accuracy, measures the number of correctly classified trials compared to the number of total trials (correct + incorrect) [39].

$$Accuracy = P = \left(\sum_{i=1}^M n_{ii} \right) / N$$

M represents the number of classes. N represents the total number of trials.

It is important to compare the accuracy performance of a BCI with its baseline, i.e. the performance that the BCI would achieve by randomly classifying. This percentage is obtained by doing $100\%/M$, where M is the number of classes.

For example, a perfectly balanced two-class BCI is completely random when it has an accuracy of 50% ($100\%/2$). whereas a perfectly balanced four-class BCI is completely random when it has an accuracy of 25% ($100\%/4$).

This is true when the dataset is balanced.

2. **Unbalanced:** if the dataset is unbalanced accuracy no longer makes sense, as accuracy gives more weight to the most frequent classes and less weight to the least frequent classes. Consequently, the accuracy value is no longer an indication of the true performance of a BCI in an unbalanced dataset, regardless of the number of classes. Cohen's Kappa coefficient, κ , should be applied in this case [83]. the κ takes into account both the classification accuracy P and the chance agreement Pe .

$$chanceagreement = Pe = \left(\sum_{i=1}^M n_{ic} * n_{ir} \right) / N^2$$

where n_{ic} is the sum of the i th column, while n_{ir} is the sum of the i th row. They are respectively the a posteriori and a priori probability. The κ coefficient is then calculated as follows:

$$\kappa = (P - Pe) / (1 - Pe)$$

Although not to be taken as a rule, a study of the literature shows that unbalanced datasets are typical of self-paced BCI systems.

The metrics seen so far measure the average classification rate of each trial. They do not take into account the duration of the trial or the classification time due to the algorithm.

In the case where the BCI is seen as a communication channel and the objective becomes to understand the “speed” of the interface in terms of providing information another metric is used, the *Information Transfer Rate* (ITR).

The ITR measures system performance based on bit/rate. This metric takes into account the number of classes in the system, the correct classification of these classes, and the time taken to perform this classification.

Two methods were proposed to measure the ITR. The first was proposed by Wolpaw [84], where B is the bit rate or bits/trial:

$$B = \log_2(M) + P \log_2 P (1 - p) \log_2 + [\log_2(1 - P)/(M - 1)]$$

M represents the number of classes and P is the probability that each class is correctly classified, i.e. the accuracy. The limitation of this formulation is the assumption that each class has the same accuracy and that the distribution of the individual classes is the same.

These conditions are not met in several applications. Consequently, an alternative approach was proposed by Nykopp [85] based on the distribution and accuracy of the individual classes.

A $10 \times k$ fold cross validation is used to obtain performance results in the calibration phase. A $10 \times k$ fold cross validation is used to obtain a robust estimate of the performance of a machine learning model. In this case robust means that the performance of the model is stable and little affected by small variations in the performance data [86].

The $10 \times k$ fold cross validation works by repeating 10 times the k fold cross validation process explained in the “processing” section of this thesis. The performance obtained is then the average performance of the 10 iterations, where in turn the performance of each iteration is the average performance of the k folds.

The performance score is accompanied by its standard error SE .

The SE is the measure of variation in the mean of scores for k folds. it is calculated as follow [87]:

$$SE = \frac{s}{\sqrt{n}}$$

where: s is the standard deviation of the score of k folds, n is the number of k folds.

Using a $10 \times k$ fold cross validation in the calibration step, the value of SE will be the average of the SE values for the 10 iterations.

Statistical testing

Once the BCI performance results are obtained, statistical tests are used. These tests allow us to understand whether there are significant differences in the final performance of the BCI using different processing parameters, e.g. different feature extraction and classification techniques. This gives us the possibility to choose which techniques are more effective than others. Statistical analyses can also be used to find out whether there is a significant difference in the results obtained between different subjects or whether the performance values obtained are significant compared to a null classification.

These analyses are possible by comparing two or more sets of results, which means that two single values cannot be statistically compared. Since all analyses are done using a $10 \times k$ cross-fold validation, the BCI performance result is never a single value, but a group of values which allow us to perform the statistical test. The following tests are used [87]:

1. The *t*-test: it is used to test whether there is a significant difference between the mean of two groups. There are different types of *t*-tests. In this thesis, the *t*-test for independent samples is used, which compares the mean between two different groups. The *t*-test returns the *p*-value, a parameter measuring the probability that the observed results are due to chance rather than a significant difference. The *p*-value is calculated from the data. The significance level α plays an important role in the result's interpretation. If the *p*-value is less than the predefined α , the null hypothesis is rejected, meaning that the difference between the averages is significant. If, on the other hand, the value of *p* is greater than the predefined α , the null hypothesis is not rejected and therefore the difference between averages cannot be considered significant. In this thesis $\alpha = 0.05$ (5%) is chosen, which means that we accept a 5% probability of committing a type I error.
2. Analysis of Variance (ANOVA): this is used to test whether there are significant differences between the averages of several groups at the same time. In this thesis, the one-way ANOVA will be used to compare the averages of several groups with respect to a single independent variable. The results of an ANOVA test report:
 - The *F*-value, which represents the ratio of between-group variability to within-group variability;
 - The degrees of freedom;
 - The *p*-value which has the same function as the *p*-value in the *t*-test.

If the *p*-value is smaller than the significance level α it means that at least one of the groups has a significantly different average from the others. To identify which groups differ from others a *post-hoc* test is used.

3. Tukey's HSD (Honest Significance Difference) is one of the most common tests for a multiple comparison between groups. It also uses the *p*-value to identify which groups have a statistically significant average.

Results

Questionnaire answers

The following are the responses of the subjects of the PoliTo^{BIO}Med Lab dataset in relation to the questionnaire conducted after data acquisition as reported in the Materials and Methods section of this thesis.

Subject A:

1. The subject found the duration slightly long.
2. The subject reports slight bouts of sleepiness probably due to the proximity of the experiment to the meal.
3. The helmet over the eyes slightly bothered the subject.
4. Movement visualization was well present according to the subject. He struggled to imagine at first. The perception of correct imagining of the movement improved during the experiment. He felt well the imagination of the stretching of the fingers opening and the pressure of the fingers on the hand.
5. The subject reports that he found the rest interval too long, while he reports that he found the task execution interval to be of a more correct and comfortable length. The gray screen time during the trial (rest phase) is slightly too long according to the subject. He found the 15-second rest in the middle of the run useful.
6. The subject reports that in his opinion he performed almost all the tasks correctly, missing a maximum of 2-3 tasks during the experiment.
7. None.

Subject B

1. The subject expressed neither positive nor negative opinion about the overall duration of the experiment.
2. The subject reports that he maintained good concentration during the calibration phase of the experiment, but struggled to stay focused for the validation phase
3. The helmet did not bother the subject.
4. The subject reports that he correctly perceived imagining the movement during the calibration phase but became confused in distinguishing between imagining and rest during the validation phase.
5. The subject was comfortable with the duration of Motor Imagery and rest during the calibration phase. In contrast, he found the self-paced motor imagery phase during the validation phase too long.
6. The subject cannot precisely establish whether the tasks were met. Generally, he accomplished the given task well, but he reports getting it wrong occasionally.

7. The subject found the gray screen with white lettering difficult to understand; the combination of gray and white colors fatigued his eyesight, according to the subject, causing him to “cross his eyes”. The subject is completely nearsighted in his right eye.

Subject C

1. The subject found the total duration of the experiment a little long.
2. The subject reported difficulty in maintaining concentration for a long time. He had moments of distraction during the experiment.
3. The subject reported no discomfort related to the helmet.
4. The subject found the concept of imagining movement complex. He seemed to focus more on the image than on the task of imagining the movement.
5. The subject found the rest and motor imagery times comfortable.
6. The subject reports that he generally perceived that he accomplished the given task well, with some errors toward the last trials.
7. The subject thinks it would have been easier for him to use an auditory stimulus rather than a visual one.

Subject D

1. The subject reports finding the duration of the experiment tiring, but reports having a particularly tiring day before performing the experiment.
2. The subject reports having minimal moments of distraction, for most of the time of the experiment he was able to stay focused.
3. The helmet did not bother the subject.
4. The subject attempted to imagine the opening and closing of the hand both physically, imagining physically opening and closing the hand, and visually. He reports that he perceived as if the hand wanted to close or open without actually doing so. Sometimes he visually imagined opening and closing the hand. He tried both ways, what the subject defined as physical mode or visual mode.
5. The subject reports finding the focus time slightly short in preparation for the motor imagery task. The few times he felt distracted was because the focus time was too short for the subject.
6. The subject reports being wrong less than 5 percent of the time. It seemed to him that he gave micro muscle inputs in a couple of motor imagery tasks.
7. The brightness of the screen caused the eye to fatigue somewhat leading the subject to perform more eye blinks than normal.

Experimental Notes

The following notes were taken during the data acquisition at the PoliTo^{BIO}Med Lab regarding the subjects and the conduction of the experiment:

1. Subject A did not perform the validation part of the experiment, due to an error during the setting of the experiment.
2. Subject B is completely nearsighted from the right eye. This might influence the results of the experiment.

Data Results

Dataset 1 BCI competition IV

Calibration data - User specific

Several parameters influence the performance of the BCI during the calibration phase. A multilevel analysis is therefore done to understand which parameters are the best within the pipeline, so that choices could be made later and not repeat the analysis for each different parameter every time.

Analysis Intentional Control

First, we look at the classification between the two classes of Intentional Control. A total of 200 epochs of *IC* is looked at. A 10×5 cross fold validation is made.

A first-level analysis is conducted on the preprocessing and feature extraction steps to see how they go about influencing the final classification.

The steps of the pipeline that are analyzed during this first-level analysis are: the application or non-application of the CAR filter and the two feature extraction techniques applied in this study, the Power Band and Common Spatial Pattern features.

Therefore, 4 possible combinations are analyzed within the 4 subjects:

1. The CAR filter is applied during pre-processing and the features are extracted through the Power Band technique.
2. The CAR filter is not applied during pre-processing and the features are extracted through the Power Band technique.
3. The CAR filter is applied during pre-processing and the features are extracted through the CSP technique.
4. The CAR filter is not applied during pre-processing and the features are extracted through the CSP technique.

The training and testing window length is fixed at $L = 2.5s$ and the beginning of the training window and of the testing window is $I = 1.5s$. An LDA classifier is applied.

Figure 43 shows the performances' results in the 4 possible combinations for each subject. The performance score used is accuracy together with its standard error.

Table 11 reports the same results of the bar graph of Figure 43 in a numerical form.

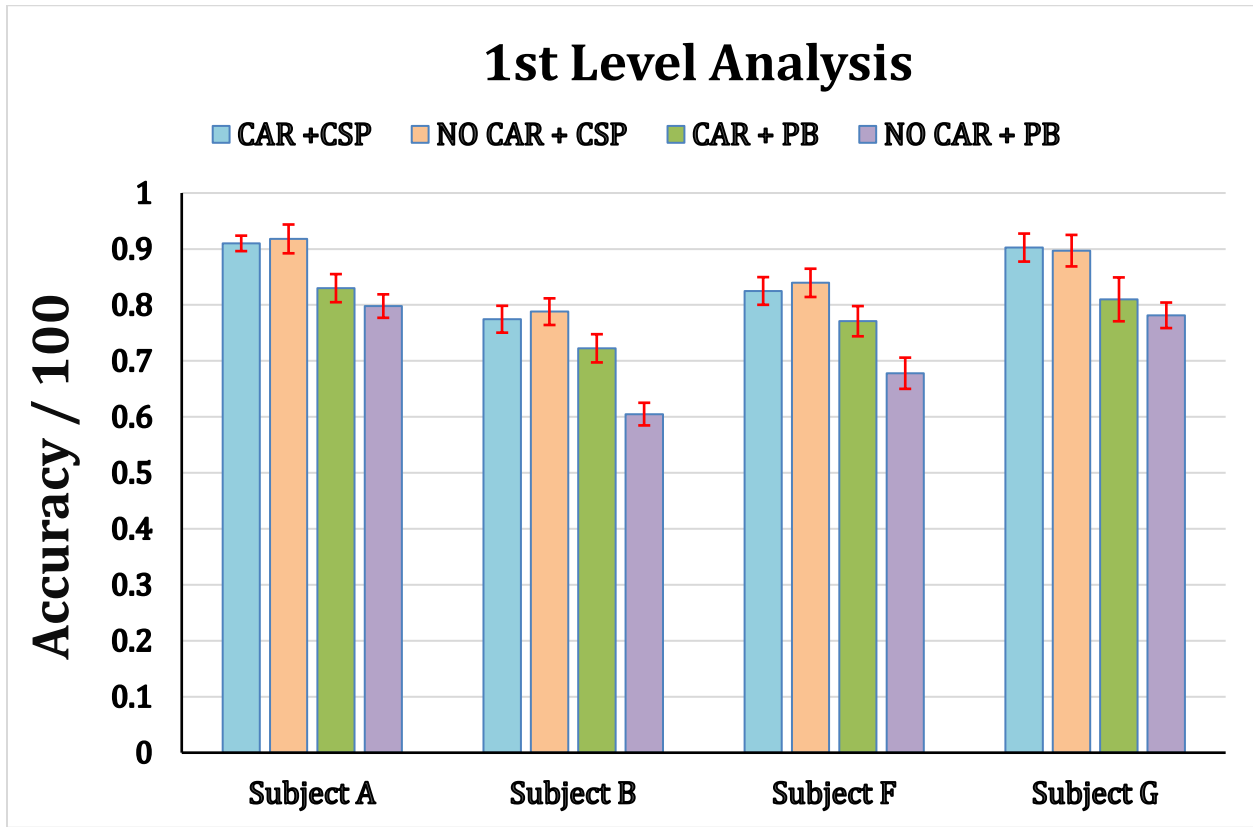


Figure 43: Bar graph showing the results of performance for a 10×5 cross fold validation during the calibration phase of Dataset 1 BCI competition IV. The graph shows the ability of the algorithm to classify between the two classes of Intentional Control. 4 different cases are looked at: CAR + CSP, NO CAR + CSP, CAR + PB, NO CAR + PB. The graph shows the performance results for all subjects of the experiment.

Table 11: Table showing the results of performance for a 10×5 cross fold validation during the calibration phase of Dataset 1 BCI competition IV. Combinations of different pre-processing and feature extraction techniques are looked at.

Accuracy + Standard Error				
	Subject A	Subject B	Subject F	Subject G
CAR + CSP	0.91 ± 0.01	0.78 ± 0.03	0.83 ± 0.03	0.90 ± 0.02
NO CAR + CSP	0.92 ± 0.02	0.79 ± 0.02	0.84 ± 0.03	0.90 ± 0.02
CAR + PB	0.83 ± 0.03	0.72 ± 0.03	0.77 ± 0.03	0.81 ± 0.03
NO CAR + PB	0.80 ± 0.03	0.61 ± 0.03	0.68 ± 0.04	0.78 ± 0.02

Statistical analyses are carried out to assess which parameters are more appropriate. The subject that is classified best and the subject that is classified worst are taken for the analysis, in order to obtain statistical results that are as generalized as possible. Table 11 shows that subject A is ranked best in all 4 cases taken into consideration, while subject B is ranked worst in all 4 cases. These two subjects are therefore chosen.

First you look at whether there are significant differences between the average performance results using the CAR filter. One looks at whether for the same feature extraction technique the CAR filter generates a significant difference. A series of *t*-tests is used. To make a comparison between groups, the performance results of the 10×5 cross fold validation are used as groups. It means that each group will contain 10 values, corresponding to the average performance of the *k*-fold cross validation. The significance value α is set at 0.05. Independent sample *t*-tests are performed in the following cases:

1. Comparing the CAR + PB and NO CAR + PB case in subject A it is obtained $p = 1.3 \times 10^{-4}$ ($p < \alpha$). The difference between the means is statistically significant.
2. Comparing the CAR + PB e NO CAR + PB case in subject B it is obtained $p = 1.84 \times 10^{-11}$ ($p < \alpha$). The difference between the means is statistically significant.
3. Comparing the CAR + CSP e NO CAR + CSP case in subject A it is obtained $p = 0.15$ ($p > \alpha$). The difference between the means is not statistically significant.
4. Comparing the CAR + CSP e NO CAR + CSP case in subject B it is obtained $p = 0.18$ ($p > \alpha$). The difference between the means is not statistically significant.

When the CAR filter is coupled with the Power Band feature extraction technique, the use or non-use of the filter generates a statistically significant difference in the results for both subjects. In contrast, when the CAR filter is coupled with the CSP filter, no statistically significant mean is generated in either of the two subjects under analysis.

Next, it is observed whether any significant differences exist between the averages of the performance results using the two different feature extraction techniques: CSP and Power Band. For this statistical analysis the case where the CAR filter is applied is chosen. The *t*-test with independent samples is performed. The significance value α is set at 0.05:

1. Comparing the CAR + CSP e CAR + PB case in subject A it is obtained $p = 3.2 \times 10^{-11}$ ($p < \alpha$). The difference between the means is statistically significant.
2. Comparing the CAR + CSP e CAR + PB case in subject B it is obtained $p = 2.4 \times 10^{-6}$ ($p < \alpha$). The difference between the means is statistically significant.

There is a statistically significant difference between the results obtained with the CSP technique compared to the Power Band technique.

By looking at the upper results, CSP will be used as the feature extraction technique for the subsequent analyses. As no statistically significant differences were found in the use of the CAR

filter in combination with CSP, the choice of filter use does not influence subsequent investigations. It is arbitrarily chosen to continue using the CAR filter.

A second-level analysis is then carried out to see which classifier works best. There are 3 classifiers used in the analysis: the LDA, the SVM and the Naïve Bayes.

Figure 44 shows the performances' results in the 3 possible combinations for each subject. The performance score used is accuracy together with its standard error.

Table 12 reports the same results of the bar graph of Figure 44 in a numerical form.

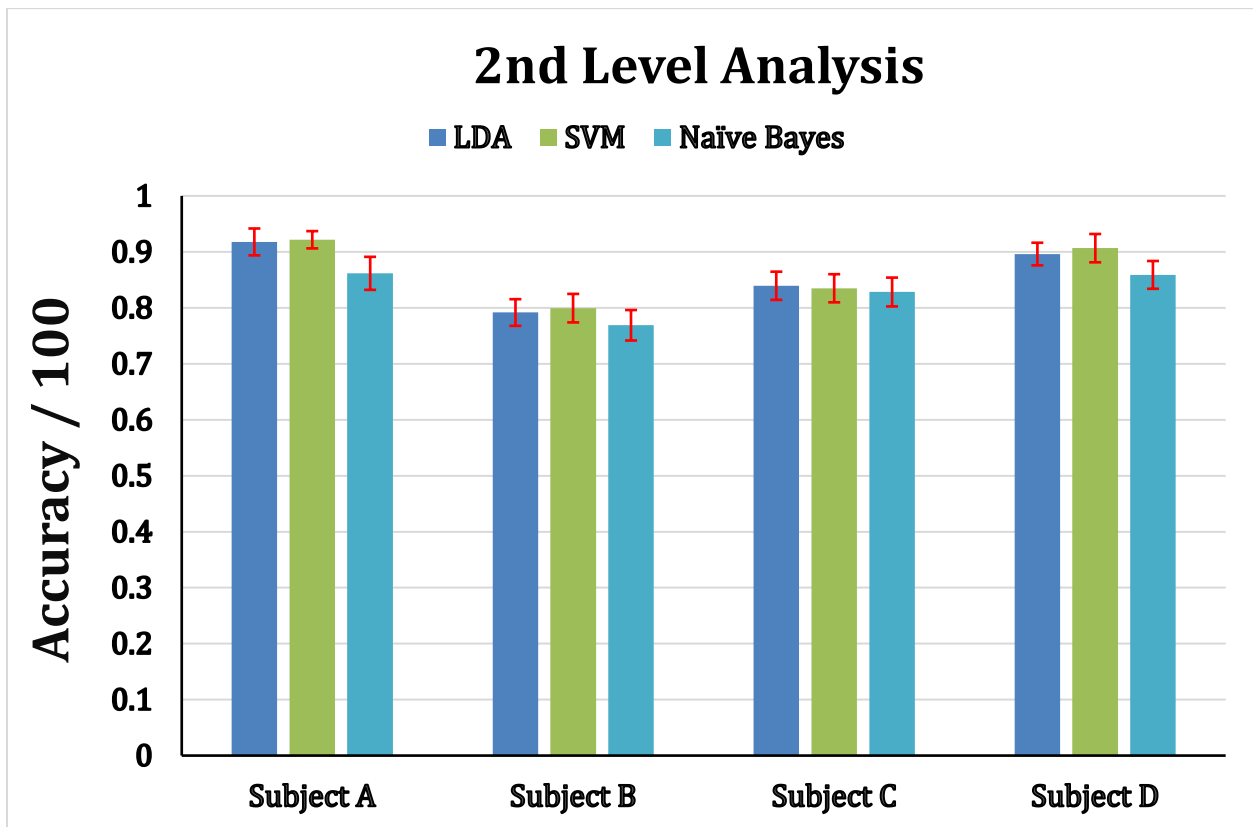


Figure 44: Bar graph showing the results of performance for a 10x5 cross fold validation during the calibration phase of Dataset 1 BCI competition IV. The graph shows the ability of the algorithm to classify between the two classes of Intentional Control. 3 different classifiers are looked at: LDA, SVM and Naïve Bayes. The graph shows the performance results for all subjects of the experiment.

Table 12: Table showing the results of performance for a 10x5 cross fold validation during the calibration phase of Dataset 1 BCI competition IV. Combinations of different pre-processing and feature extraction techniques are looked at.

Accuracy + Standard Error				
	Subject A	Subject B	Subject F	Subject G
LDA	0.92 ± 0.02	0.79 ± 0.02	0.84 ± 0.03	0.90 ± 0.02
SVM	0.92 ± 0.02	0.80 ± 0.03	0.84 ± 0.03	0.91 ± 0.03
Naïve Bayes	0.86 ± 0.03	0.77 ± 0.03	0.83 ± 0.03	0.86 ± 0.03

Statistical analyses are carried out to assess which classifier is best to use. Statistical analysis is carried on subject A and subject B, as in the first level analysis. The significance value α is set at 0.05. To determine whether there are significant differences between the results of the 3 classifiers, a one-way ANOVA is conducted on the 3 groups:

1. For subject A, the ANOVA showed a significant difference between the groups, $F(2,27) = 83.03, p = 2.93 \times 10^{-12} (p < \alpha)$. This shows that at least one of the groups differs significantly from the others. Subsequently, a Tukey HSD post hoc test was conducted to determine which groups differed from each other. The test reports that the LDA group differs significantly from the Naive Bayes group ($p = 8.6 \times 10^{-11}$), the SVM group differs significantly from the Naive Bayes group ($p = 1.85 \times 10^{-11}$), while no significant differences were found between the LDA group and the SVM group ($p = 0.73$).
2. For subject B, the ANOVA showed a significant difference between the groups, $F((2,27) = 4.98, p = 0.014 (p < \alpha)$. This shows that at least one of the groups differs significantly from the others. Tukey HSD test shows that the SVM group differs significantly from the Naive Bayes group ($p = 0.011$), while no significant differences were found between the LDA group and the Naive Bayes group ($p = 0.16$), and between the LDA group and the SVM Group ($p = 0.45$).

The statistical results suggest that the two classifiers LDA and SVM perform better than the Naive Bayes classifier. The Naive Bayes classifier is therefore excluded from further analysis. As there is no statistically significant difference between using the SVM versus the LDA, one of the two is arbitrarily chosen. The SVM is chosen.

Once the most effective pre-processing, feature extraction and classification techniques have been chosen, the last parameters to be checked are the length L and starting point I of the testing and training windows.

At first, the training window is studied by keeping the length of the testing window fixed at $L = 2.5s$ and the onset at $I = 1.5s$. The performance results for subject A are analyzed for the following parameters of the training windows: L varies over 3 values, 1.5s, 2s and 2.5s and I is varied between 0s, 0.75s and 1.5s. The accuracy results with the corresponding SE are shown in Table 13.

Table 13: Table showing the results of performance for a 10×5 cross fold validation during the calibration phase of Dataset 1 BCI competition IV for subject A. Combinations of different epoch divisions are looked at.

Accuracy + Standard Error			
	L = 1.5s	L = 2s	L = 2.5s
I = 0 s	0.89 ± 0.03	0.9 ± 0.02	0.92 ± 0.02
I = 0.75 s	0.91 ± 0.02	0.91 ± 0.02	0.9 ± 0.02
I = 1.5 s	0.91 ± 0.01	0.91 ± 0.02	0.92 ± 0.02

A one-way ANOVA test is used to determine whether there are statistically significant differences between the results. The ANOVA shows a significant difference between the groups, $F(8,81) = 7.56, p = 1.7 \times 10^{-7} (p < \alpha)$. This shows that at least one of the groups differs significantly from the others.

Subsequently, a Tukey HSD post hoc test was conducted to determine which groups differed from each other. Since there are 9 different groups to be compared, a total of 36 group comparisons with corresponding p -values will be obtained. Only comparisons with significant p -values ($p < \alpha$) are extracted and shown in Table 14.

Table 14: Results of the Tukey HSD post hoc test on Table 13 data. Only results with $p < \alpha$ are reported.

Compared groups		p-value
I = 0s, L = 1.5s	I = 0.75s, L = 1.5s	0.0011
I = 0s, L = 1.5s	I = 1.5s, L = 1.5s	7.9×10^{-4}
I = 0s, L = 1.5s	I = 0.75s, L = 2s	0.0016
I = 0s, L = 1.5s	I = 1.5s, L = 2s	0.0119
I = 0s, L = 1.5s	I = 0s, L = 2.5s	1.12×10^{-5}
I = 0s, L = 1.5s	I = 1.5 s, L = 2.5s	5.96×10^{-7}
I = 0s, L = 2s	I = 0s, L = 2.5s	0.0045
I = 0s, L = 2s	I = 1.5 s, L = 2.5s	3.8×10^{-4}
I = 0.75s, L = 2.5s	I = 1.5 s, L = 2.5s	0.0292

The two training windows that classify best are:

1. The window $I = 1.5s, L = 2.5s$ with an accuracy of 0.92 ± 0.018 . The results of this window are statistically significantly better than 3 other windows (see Table 14).
2. The window $I = 0s, L = 2.5s$ with an accuracy of 0.92 ± 0.02 . The results of this window are statistically significantly better than 2 other windows. (see Table 14).

The training window $I = 1.5 s, L = 2.5s$ is chosen as the best window.

Once the length L and the beginning I of the training window are chosen, an analysis is done using different beginnings I of the testing window. The pre-processing, feature extraction and classification techniques used are the ones chosen above. The testing window length L is fixed at 2.5s.

Figure 45 shows how classification accuracy, on subject A, varies as the beginning I of the testing window changes. Since the dataset is balanced between the two IC classes the random classification happens when the accuracy is 50%. The cue of the IC class starts at $t = 0s$ and ends at $t = 4s$.

Figure 45 shows that the classification is random when the testing window is outside of the stimulus window. The classification improves as the testing window enters the cue window and it gets worse as the it goes out, going back towards the random classification.

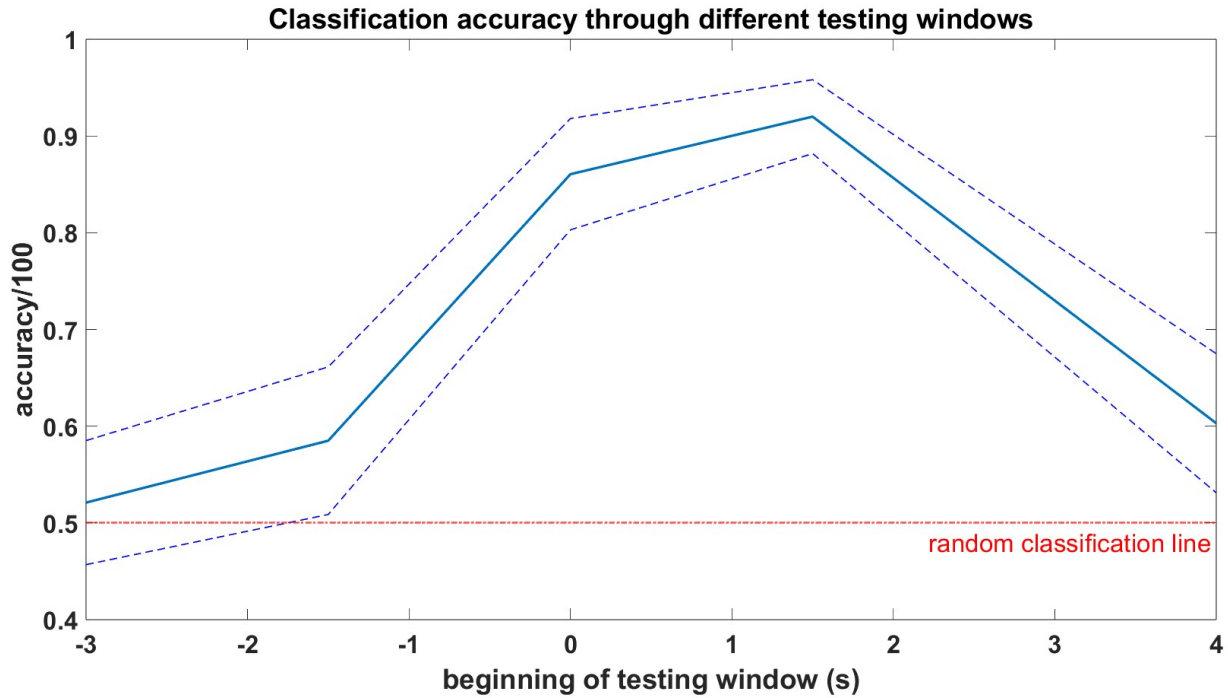


Figure 45: Classification accuracy + SE between the two IC classes. Subject A during the calibration phase of Dataset I BCI competition IV. The blue continuous line is the accuracy. The two dotted line represent the accuracy \pm its SE. The red dotted line represents the random classification line.

Analysis No control vs Intentional Control

The subsequent analysis aims to observe the algorithm's performance in distinguishing between the class of *NC* and the class of *IC* within the calibration phase. The two classes of *IC* are considered as a single class. The previously selected pre-processing, feature extraction and classification parameters are retained. The division of epochs changes. The signals is divided into *NC* epoch and *IC* epochs. The *NC* epochs have a length of $L = 2s$ and correspond to the 2 seconds before the class cue. The *IC* epochs have a length of $L = 2s$ and they start 2s after the stimulus presentation. A total of 400 epochs are extracted from the signal, 200 epochs for the *NC* class and 200 epochs for the *IC* class. The dataset is therefore balanced. A 10×5 cross fold validation is done to determine the classification accuracy between the 4 subjects.

The results are reported in Figure 46 and Table 15.

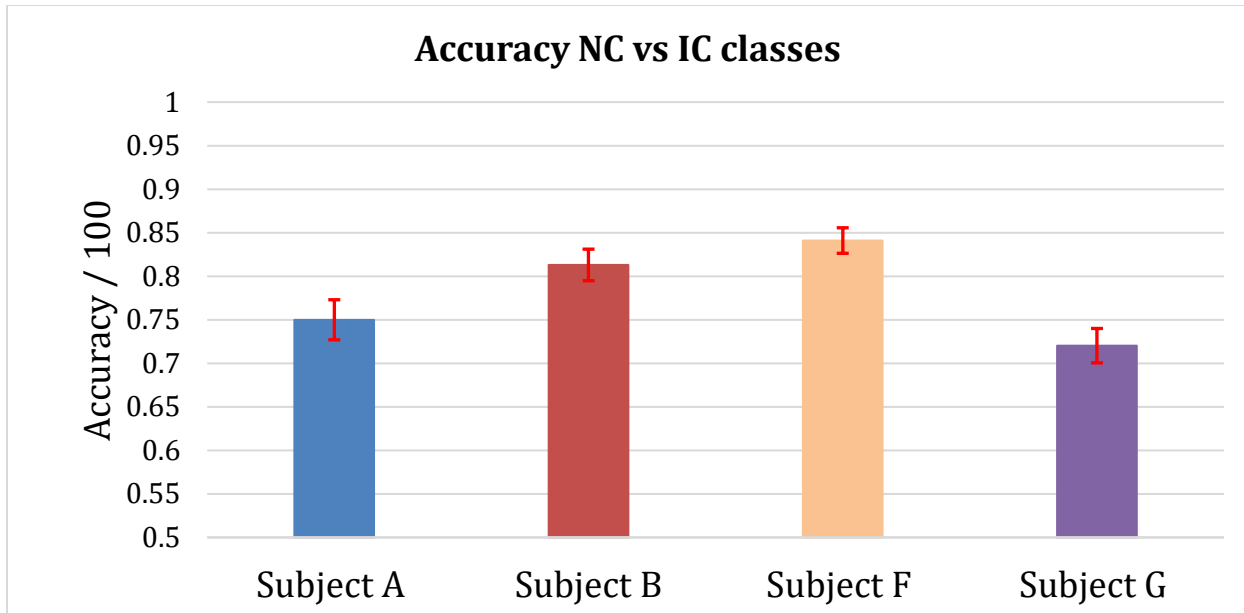


Figure 46: Bar graph showing the results of performance for a 10×5 cross fold validation during the calibration phase of Dataset 1 BCI competition IV. The graph shows the ability of the algorithm to classify between the class of NC and the class of IC. All 4 subjects are looked at.

Table 15: Table showing the results of performance for a 10×5 cross fold validation during the calibration phase of Dataset 1 BCI competition IV between the IC and NC classes.

	Subject A	Subject B	Subject F	Subject G
Accuracy + SE	0.75 ± 0.02	0.81 ± 0.02	0.84 ± 0.01	0.72 ± 0.02

An ANOVA test is done to determine whether there are statistically significant differences in accuracy results between the four subjects analyzed.

The ANOVA test reports a p -value of 7.2×10^{-23} ($p < \alpha$). This means that at least one of the groups differs significantly from the others. Therefore at least one of the 4 subjects' accuracy has a statistically significant difference from the other subjects' accuracies.

Validation data – user specific

Initially, the model is used to distinguish between the class of *NC* and the class of *IC*.

Classification is performed every 10 samples. Classification is carried out throughout the signal, excluding the 0.5 seconds before and after the *IC* cue from the analysis to reduce the samples where the classification window lies between the two classes. The pre-processing, feature extraction and classification techniques selected earlier are used.

As the dataset is unbalanced between the two classes, accuracy is not used as performance metric but Cohen's Kappa coefficient κ is used. The analysis is carried out on all 4 subjects and the results are reported in Table 16.

Subject A is the only subject whose κ differs from zero. The confusion matrix for subject A is reported in Table 17. No other confusion matrix is reported as the models of subject B, F and G classify all classes as NC. The model struggles to distinguish the class of IC from the class of NC.

Table 16: Cohen's Kappa coefficient κ results for the validation phase of Dataset 1 BCI competition IV between the IC and NC classes.

	Subject A	Subject B	Subject F	Subject G
κ	0.1170	0	0	0

Table 17: Confusion matrix of subject A during the validation phase of Dataset 1 BCI competition IV between the IC and NC classes. It is highlighted in green when the predicted class and the real class coincide. It is highlighted in red otherwise.

		Predicted class		
		Class NC	Class IC	Total number of classes
Real class	Class NC	7523	880	8403
	Class IC	6587	1879	8466
Total number of classes		14110	2759	16869

Since it has not been built a model able to distinguish between the classes of IC and NC, no further analysis are made on the validation dataset.

Subject Independent classification

The pre-processing, feature-extraction and classification models selected in the user-specific BCI (CAR, CSP, SVM) are used.

Analysis No control vs Intentional Control

The first step is to distinguish NC classes from IC classes. For the NC epochs the 2 seconds before the MI cue are extracted. The IC epochs are extracted between 2 and 4 seconds after the beginning of the MI cue. A total of 1200 epochs are extracted for the calibration phase, 800 NC epochs and 800 IC epochs. The validation phase is tested on a total of 400 epochs, 200 NC epochs and 200 IC epochs. The dataset is balanced both in the calibration phase and in the validation phase. The accuracy results are reported in Figure 47 and Table 18. Accuracy results during the validation phase do not carry a SE since no cross-fold validation is done.

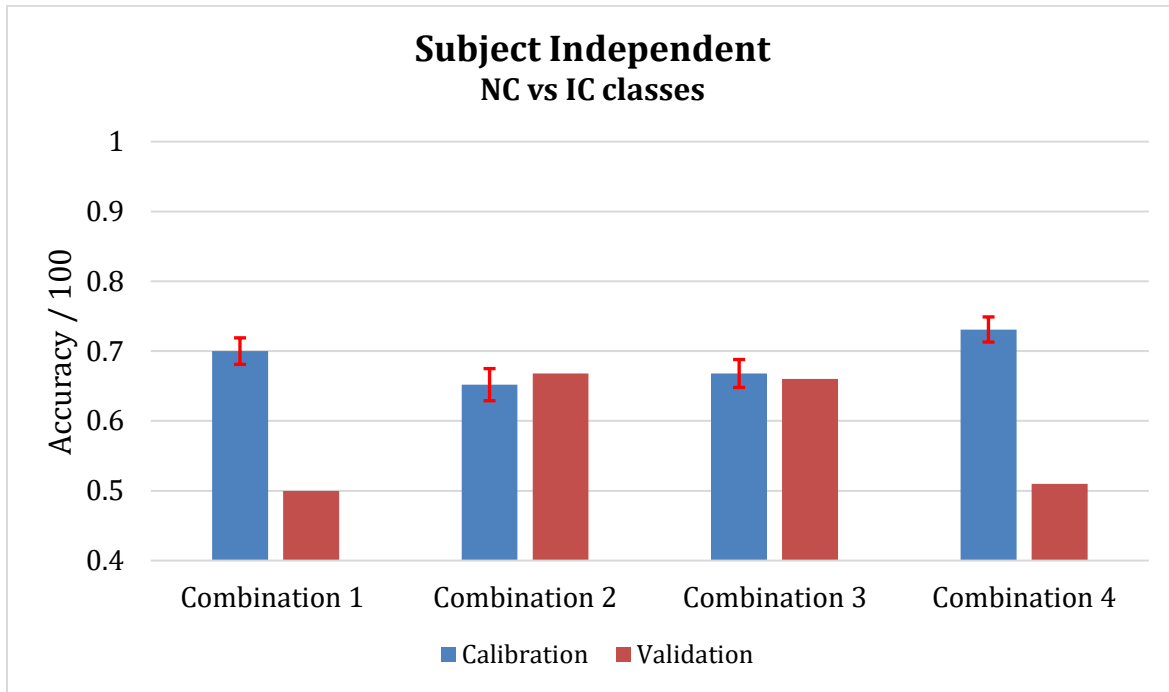


Figure 47: Classification performance of the subject-independent BCI for Dataset 1 BCI competition IV between the IC and NC classes.

Table 18: Classification performance of the subject-independent BCI for Dataset 1 BCI competition IV between the IC and NC classes.

Accuracy + Standard Error				
	Combination 1	Combination 2	Combination 3	Combination 4
Calibration	0.70 ± 0.02	0.65 ± 0.02	0.67 ± 0.02	0.73 ± 0.02
Validation	0.5	0.67	0.66	0.51

Analysis Intentional Control

The second step is to distinguish between IC classes. The epochs both for the testing window and the training window have a length of $L = 2.5s$ and they start at $I = 1.5s$. A total of 600 IC epochs are extracted for the calibration phase. The validation phase is tested on a total of 200 epochs. The dataset is balanced both in the calibration phase and in the validation phase.

The accuracy results are reported in Figure 48 and Table 19. Accuracy results during the validation phase do not carry a SE since no cross-fold validation is done.

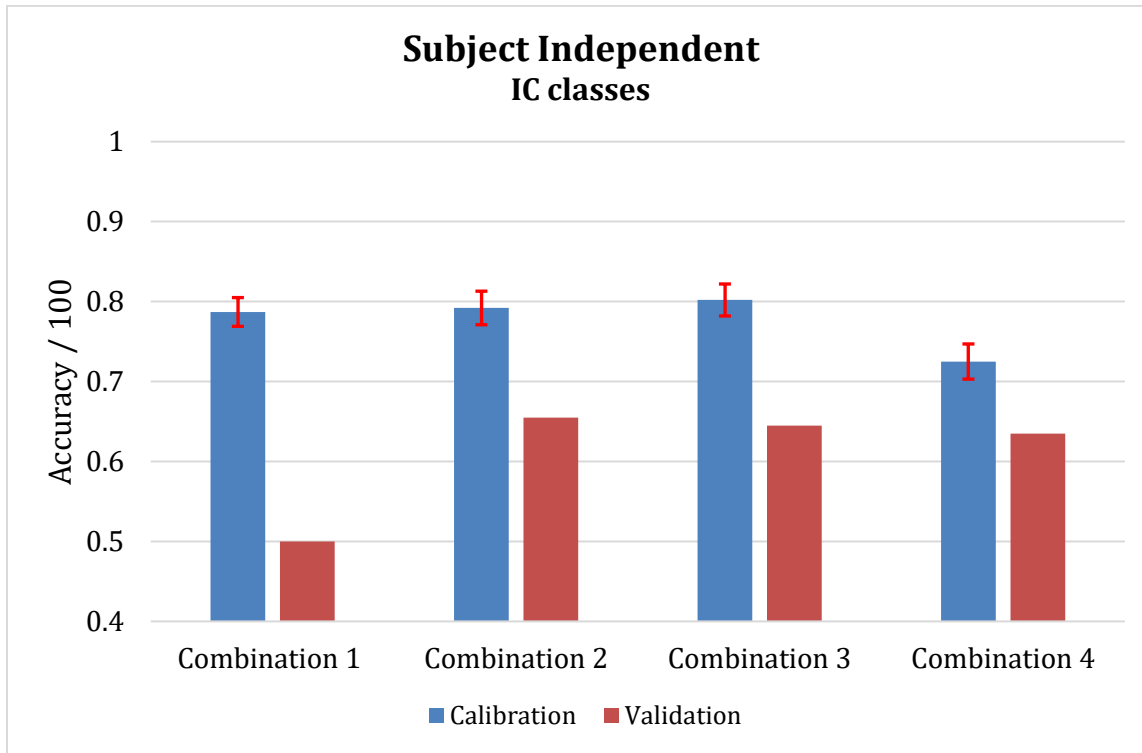


Figure 48: Classification performance of the subject-independent BCI for Dataset 1 BCI competition IV between the IC classes.

Table 19: Classification performance of the subject-independent BCI for Dataset 1 BCI competition IV between the IC classes.

Accuracy + Standard Error				
	Combination 1	Combination 2	Combination 3	Combination 1
Calibration	0.79 ± 0.02	0.79 ± 0.02	0.80 ± 0.02	0.72 ± 0.02
Validation	0.5	0.66	0.65	0.64

PoliTo^{BIO}Med Lab data results

To analyze the results of the PoliTo^{BIO}Med Lab dataset, all the multi-level analyses performed in the case of Dataset 1 from BCI competition IV were not repeated. The pre-processing, feature extraction and classification steps selected with Dataset 1 from BCI competition IV are chosen. Therefore, the following techniques are used:

1. the CAR filter during pre-processing.
2. the CSP during feature extraction.
3. the SVM as classifier.

No analysis has been done on the validation phase of the dataset as no satisfactory results were obtained on Dataset 1 from BCI competition IV.

Calibration data – user specific

Analysis Intentional Control

A total of 160 *IC* epochs are compared. A 10×4 cross fold validation takes place in this case. The length of the training and testing window L is set at 2.5s, as for the analyses performed on Dataset 1 from BCI competition IV.

In the analysis on the previous dataset, it is seen that the most efficient training window is the one located in the last 2.5 seconds of the cue window. The length of the cue window in Dataset 1 from BCI competition IV is 4 seconds, so the start of the training window is $I = 1.5s$.

For the analysis on the PoliTo^{BIO}Med Lab dataset, it is chosen to keep the last 2.5 seconds of the cue window for the training window. The cue window of the PoliTo^{BIO}Med Lab dataset has a duration of 3 seconds, so the start of the training window is set at $I = 0.5s$.

Figure 49 and Table 20 report the performance results on the 4 subjects. Only subject A, with an accuracy of 63% is not performing a random classification. The classification in the other 3 subjects is random.

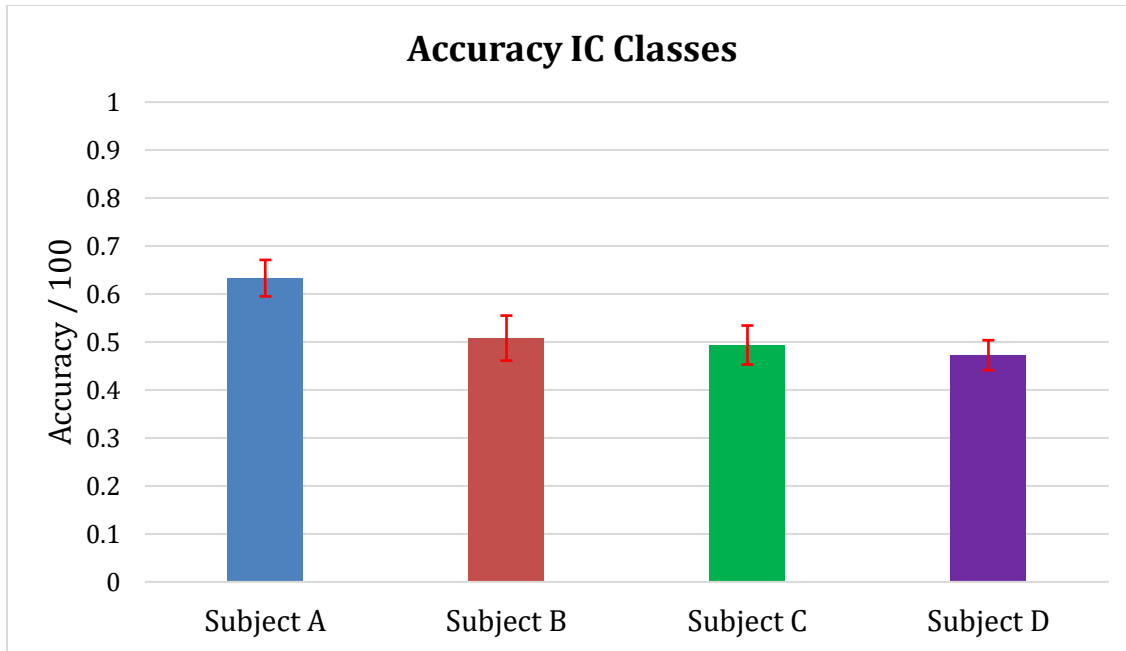


Figure 49: Bar graph showing the results of performance for a 10×4 cross fold validation during the calibration phase of the PoliTo^{BIO}Med Lab dataset. The graph shows the ability of the algorithm to classify between the two classes of Intentional Control.

Table 20: Table showing the results of performance for a 10×4 cross fold validation during the calibration phase of the PoliTo^{BIO}Med Lab dataset. The table shows the ability of the algorithm to classify between the two classes of Intentional Control.

	Subject A	Subject B	Subject F	Subject G
Accuracy + SE	0.63 ± 0.04	0.51 ± 0.05	0.5 ± 0.04	0.47 ± 0.03

An ANOVA test is done between the performance results of the 4 subjects. The ANOVA reports a p -value of 1.06×10^{-12} ($p < \alpha$). This means that at least one of the groups differs significantly from the others.

A Tukey HSD test is performed to determine which groups have a statistically significant difference. The results are reported in Table 21. The observed difference between the performance results of subject A is statistically significant compared to all other subjects. The p -value in the comparisons between subject A and the other subjects is always less than α . In contrast, there are no significant differences between the performance results of subjects B, C and D, as p -value $> \alpha$. Another way of seeing this is through Figure 50, that shows the confidence intervals for the differences in mean between subjects. Looking at the confidence intervals, we can see that the differences between subject A and subjects B, C and D are statistically significant. In contrast, the differences between subjects B and C, between B and D, and between C and D are not significant.

Table 21: Table showing the results of the Tukey HSD test on the 4 subjects of the PoliTo^{BIO}Med Lab dataset during the calibration phase of the experiment.

Compared groups		<i>p</i> -value
Subject A	Subject B	2.4×10^{-9}
Subject A	Subject C	1.6×10^{-10}
Subject A	Subject D	3.4×10^{-12}
Subject B	Subject C	0.76
Subject B	Subject D	0.09
Subject C	Subject D	0.48

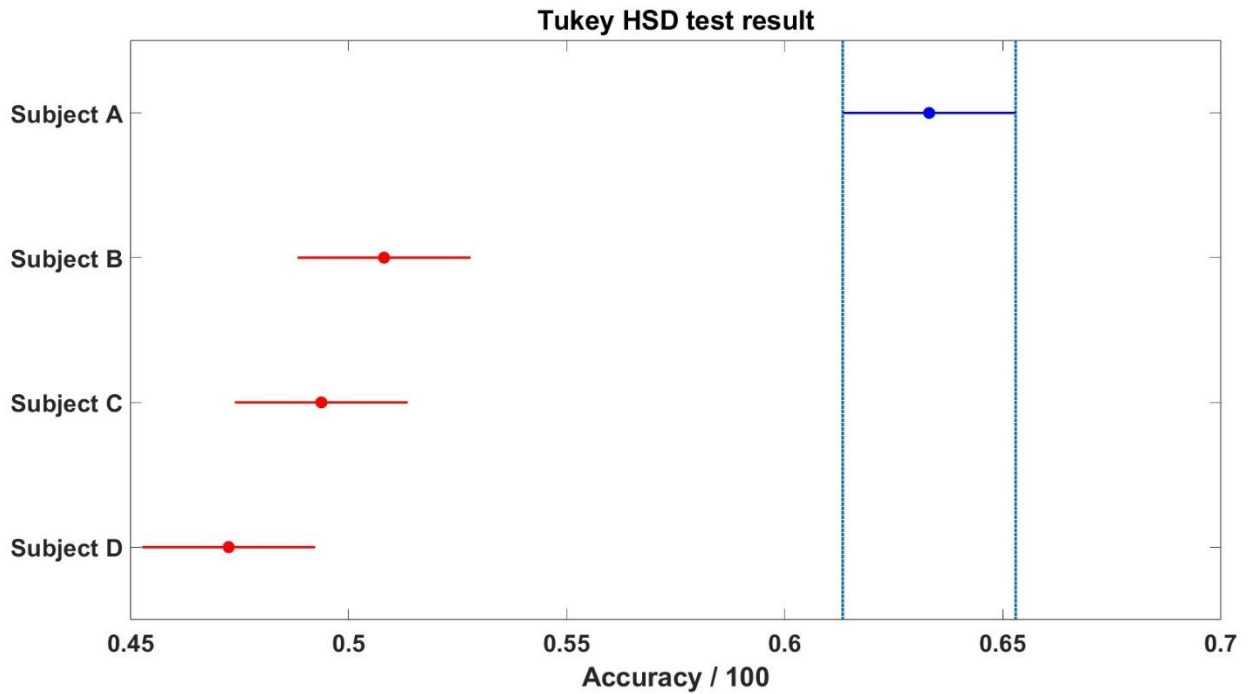


Figure 50: Tukey HSD test to compare the means of the accuracies between the subjects of the PoliTo^{BIO}Med Lab dataset. The data correspond to the calibration phase of the experiment. The horizontal lines represent the means and confidence intervals.

Figure 51 shows how the classification accuracy, on subject A, varies as the beginning I of the testing window changes. Since the dataset is balanced between the two IC classes the random

classification happens when the accuracy is 50%. The cue of the IC class starts at $t = 0$ s and ends at $t = 3$ s.

Figure 49 shows that the classification is random when the testing window is outside of the stimulus window. The classification improves as the testing window enters the cue window and it gets worse as the it goes out, going back towards the random classification.

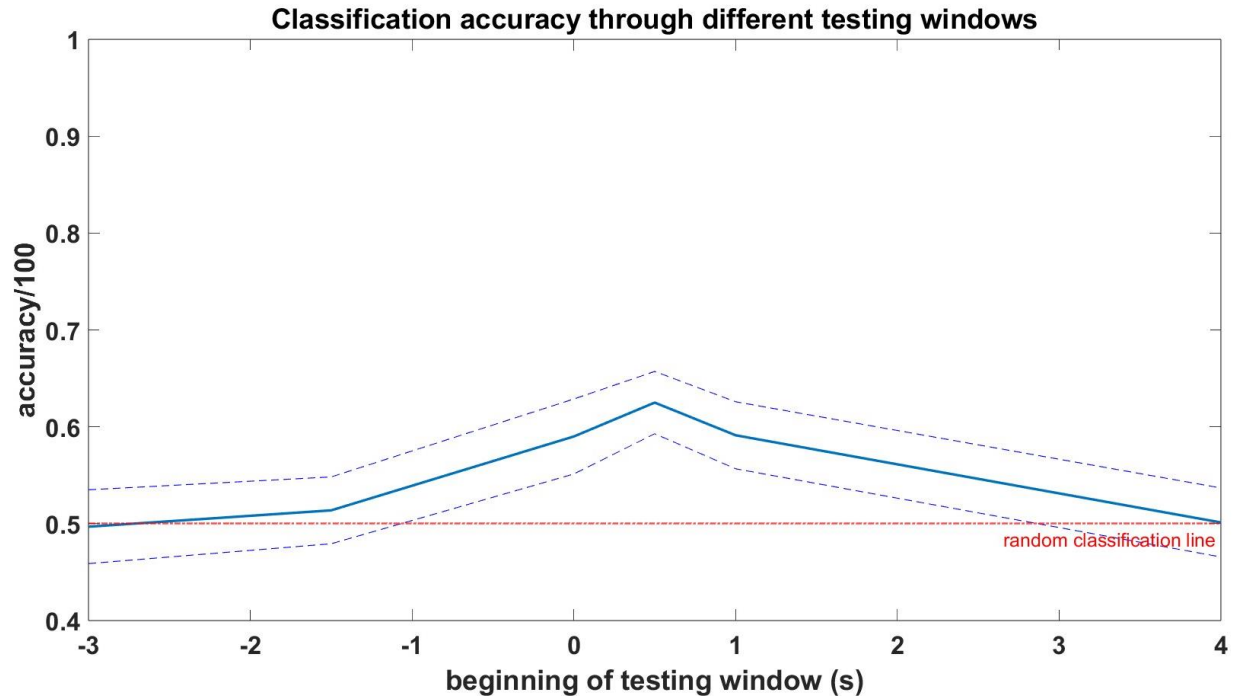


Figure 51: Classification accuracy + SE between the two IC classes. Subject A during the calibration phase of the PoliTo^{BIO}Med Lab dataset. The blue continuous line is the accuracy. The two dotted line represent the accuracy \pm its SE. The red dotted line represents the random classification line.

Analysis No control vs. Intentional Control

The subsequent analysis aims to observe the algorithm performance in distinguishing between the class of *NC* and the class of *IC*. The *NC* epochs have a length of $L = 2$ s and correspond to the 2 seconds before the class cue. The *IC* epochs have a length of $L = 2$ s and they start 0.5s after the stimulus presentation. A total of 320 epochs are extracted from the signal, 160 epochs for the *NC* class and 160 epochs for the *IC* class. The dataset is therefore balanced. A 10×5 cross fold validation is done to determine the classification accuracy between the 4 subjects.

The results are reported in Figure 52 and Table 22.

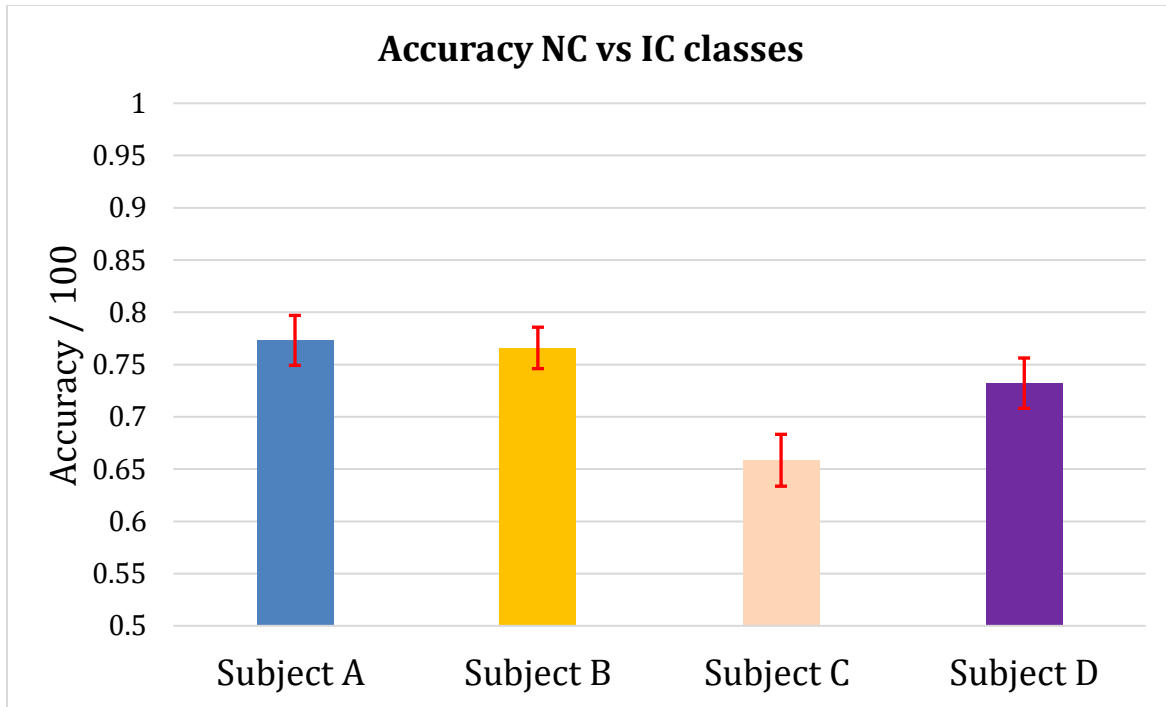


Figure 52: Bar graph showing the results of performance for a 10×5 cross fold validation during the calibration phase of PoliTo^{BIO}Med Lab dataset. The graph shows the ability of the algorithm to classify between the class of NC and the class of IC.

Table 22: Table showing the results of performance for a 10×5 cross fold validation during the calibration phase of the PoliTo^{BIO}Med Lab dataset between the IC and NC classes.

	Subject A	Subject B	Subject C	Subject D
Accuracy + SE	0.77 ± 0.02	0.77 ± 0.02	0.66 ± 0.03	0.73 ± 0.02

An ANOVA test is done to determine whether there are statistically significant differences in accuracy results between the four subjects analyzed.

The ANOVA test reports a p-value of 1.08×10^{-16} ($p < \alpha$). This means that at least one of the groups differs significantly from the others. Therefore at least one of the 4 subjects' accuracy has a statistically significant difference from the other subjects' accuracies.

Subject Independent classification

Analysis No control vs. Intentional Control

The first step is to distinguish NC classes from IC classes. For the NC epochs the 2 seconds before the MI cue are extracted. The IC epochs are extracted between 1 and 3 seconds after the beginning of the MI cue. A total of 960 epochs are extracted for the calibration phase, 480 NC epochs and

480 IC epochs. The validation phase is tested on a total of 320 epochs, 160 NC epochs and 160 IC epochs. The dataset is balanced both in the calibration phase and in the validation phase. The accuracy results are reported in Figure 53 and Table 23. Accuracy results during the validation phase do not carry a SE since no cross-fold validation is done.

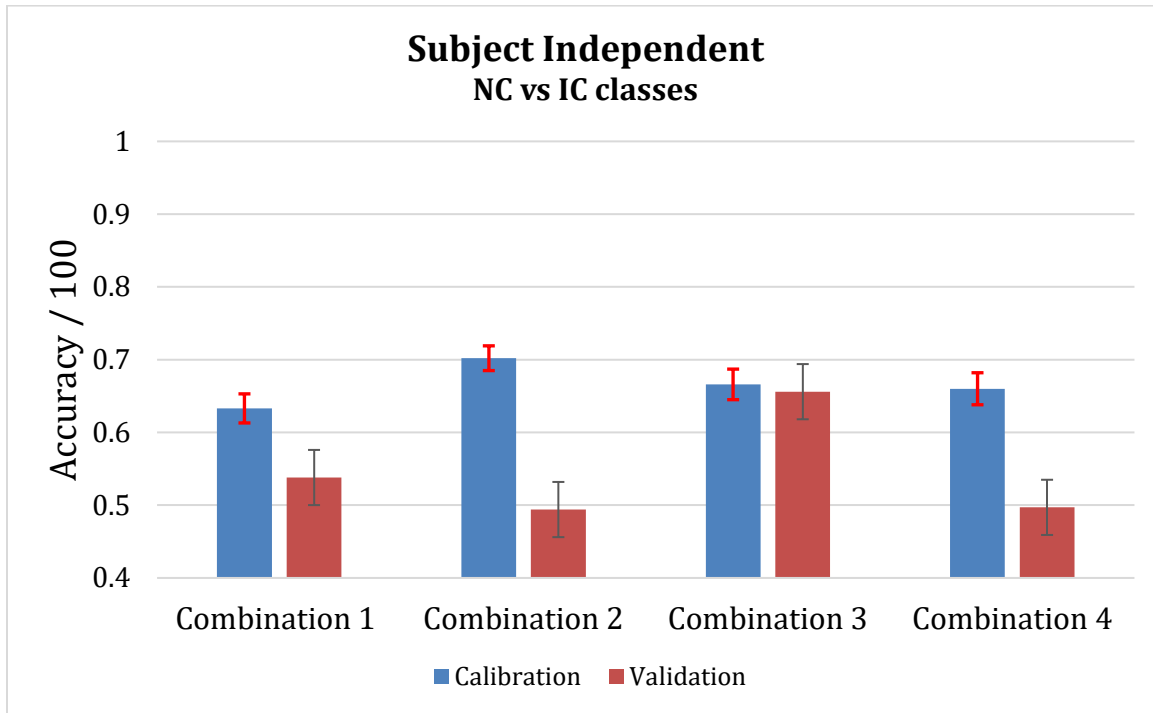


Figure 53: Classification performance of the subject independent BCI for the PoliTo^{BIO}Med Lab dataset between the IC and NC classes.

Table 23: Classification performance of the subject independent BCI for the PoliTo^{BIO}Med Lab dataset between the IC and NC classes.

Accuracy + Standard Error				
	Combination 1	Combination 2	Combination 3	Combination 4
Calibration	0.63 ± 0.02	0.70 ± 0.02	0.67 ± 0.02	0.66 ± 0.02
Validation	0.54	0.49	0.66	0.50

Analysis Intentional Control

The second step is to distinguish between IC classes. The epochs both for the testing window and the training window have a length of $L = 2.5s$ and they start at $I = 0.5s$. A total of 480 IC epochs

are extracted for the calibration phase. The validation phase is tested on a total of 160 epochs. The dataset is balanced both in the calibration phase and in the validation phase.

The accuracy results are reported in Figure 54 and Table 24. Accuracy results during the validation phase do not carry a SE since no cross-fold validation is done.

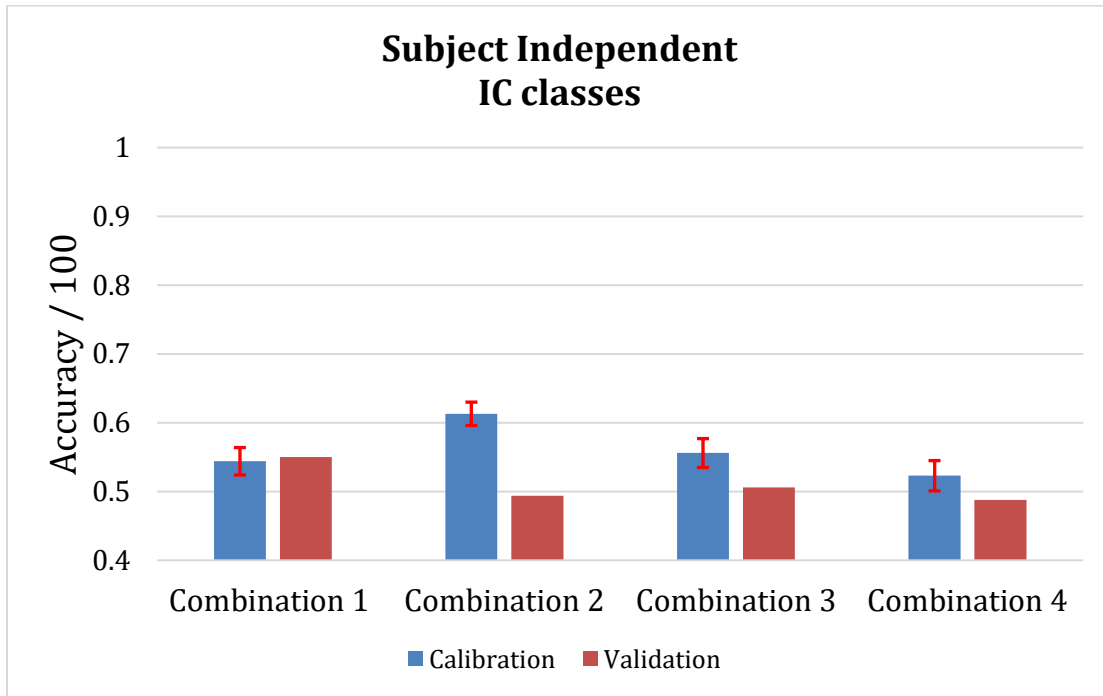


Figure 54: Classification performance of the subject independent BCI for the PoliTo^{BIO}Med Lab dataset between the IC classes.

Table 24: Classification performance of the subject independent BCI for the PoliTo^{BIO}Med Lab dataset between the IC classes.

Accuracy + Standard Error				
	Combination 1	Combination 2	Combination 3	Combination 4
Calibration	0.54 ± 0.02	0.61 ± 0.02	0.56 ± 0.02	0.52 ± 0.03
Validation	0.55	0.49	0.51	0.49

Discussions

The development of algorithms and protocols that allow asynchronous and subject-independent classification is a key step for the use of BCI in the assistive and rehabilitation fields. The aim of the present study was first to investigate an algorithm and protocol that would work in the synchronous and user-specific field on equal footing with the models studied in literature. Secondly, from the developed algorithm and experimental protocol the study tried to take an extra step to be able to use BCI in an asynchronous and subject independent way.

The algorithm has been built on Dataset 1 from BCI competition IV and it has been later adapted to the PoliTo^{BIO}Med Lab dataset with small adaptations.

The first part of the study focused on identifying the best pre-processing, feature extraction and classification techniques for a synchronous and user-specific BCI in the case of classification between the two *IC* classes. Looking at the results on Dataset 1, it has been seen that the best results are obtained using the CAR filter and CSP as pre-processing and feature extraction techniques and the SVM and LDA as classifiers. Statistical analysis reported that the techniques mentioned above achieve better results than the other techniques analyzed, such as the Power Band for feature extraction and The Naive Bayes for classification. No statistically significant differences were observed between using SVM or LDA. Therefore, the use of SVM has been chosen for the subsequent analyses so as not to repeat the later analyses with both classifiers.

Next, a comparison was made to understand which were the best training and testing windows. It has been seen that the best results were obtained when the training and testing window were entirely within the window in which the cue is provided. Better results are therefore obtained with longer windows located toward the end of the cue window rather than shorter windows located at the beginning.

The classification results both in comparing the two *IC* classes and the *NC* class against the *IC* class show high inter-subject variability. This is in line with results found in the literature [40]. The performance results obtained on the calibration data between *IC* classes achieved similar performance to the performance obtained on the same data in the literature [68]. In contrast, analyses done on the same data that distinguished between the *NC* class and *IC* classes during the calibration phase were not found in the literature.

During the validation phase done on Dataset 1, it was not possible to obtain an efficient classification in distinguishing between the class of *NC* and the class of *IC*. Therefore, it couldn't be accomplished an algorithm that worked satisfactorily with an asynchronous BCI. Only subject A obtained a Cohen's Kappa coefficient, κ other than 0, but much lower than the optimal value of $\kappa = 0.5$ [39]. Thus, it was not possible at this stage to obtain an algorithm that would work for an asynchronous BCI.

Regarding the subject-independent BCI studied on Dataset 1, performance results obtained in the calibration phase are in line with the literature [71]. The performance in the validation phase is worse than in the calibration phase. This is probably due to the high inter-subject variability and low numerosity of the training dataset [71].

The second part of the study focused on developing an experimental protocol and collecting and analyzing data related to the drafted protocol, the PoliTo^{BIO}Med Lab dataset.

The classification results are drastically worse between the two datasets when distinguishing between *IC* classes in both the users-specific and subject-independent BCI. The main reason is

probably the difference in the type of Motor Imagery task. While in Dataset 1 from BCI competition IV there is a distinction between hand and foot or between right and left hand, in the the PoliTo^{BIO}Med Lab dataset the distinction is between the opening and closing of the hand from the same limb. This confirms that it is a harder task to distinguish between motor tasks performed by the same limb particularly due to the low spatial resolution of EEG [48]. Certainly more invasive techniques, or techniques such as MEG, would be more effective in classifying motor tasks performed on the same limb, thanks to their higher spatial resolution, but would limit the usability of the instrument [35] [36].

The results of the algorithm distinguishing between the class of *NC* from the class of *IC* on the PoliTo^{BIO}Med Lab dataset are more in line with the results obtained from Dataset. This confirms the effectiveness of the developed algorithm in distinguishing between *NC* and *IC* even with different datasets. It reports its problems when the type of *IC* classes analyzed are motor tasks from the same limb.

The results obtained show the effectiveness of CSP, SVM, and LDA techniques for synchronous and user-specific BCI, but report their limitations when it comes to the development of asynchronous, subject-independent BCI that distinguish between movements of the same limb. Future research could focus on finding different pre-processing, feature extraction and classification techniques.

The study also highlighted the difficulty in handling the high inter-subject variability (in the case of independent subject BCI) and the high inter-session variability (in the case of validation for user-specific BCI). One possible solution could be the development of adaptive algorithms capable of adapting to new data by changing the parameters of supervised classifiers and feature extraction techniques to fit the new data [57] [48].

The study showed how using longer windows centered toward the end of the cue window improves classification. Therefore, it becomes necessary to explore new techniques to reduce the length of the window, as this introduces an inherent delay in the BCI system, compromising the immediacy of real-time use.

Regarding the subject-independent BCI, the numerosity of subjects used is very low; studies on subject-independent BCI use a much larger number of subjects [71]. Therefore, a key point to improve the development of independent subject BCI is to increase the number of subjects.

Further improvements can be made to the experimental protocol used. In fact, the quality of the results is given not only by the types of algorithms used but also by the quality of the data collected. The quality of the data is directly related to the type of experimental protocol used and how effectively it is perceived by the subjects of the study.

Reviewing the answers of the subjects' questionnaire the following points emerged:

1. The duration perception: Subjects A, C, and D found the experiment slightly or notably long, leading to discomfort and fatigue, with Subject D specifically noting pre-existing tiredness as a contributing factor.
2. Concentration challenges: Subjects B, C, and D reported difficulties in maintaining focus throughout the experiment, particularly in the validation phase for Subject B and towards the later stages for Subject C.

3. Screen brightness and visual fatigue: Subjects B and D noted issues with screen visibility. Subject B found the gray screen with white text hard to read, while Subject D mentioned eye strain due to screen brightness, leading to excessive blinking.
4. The perception of the MI task: Subjects A and D improved in their perception of imagined movement over time. Subjects B and C, however, struggled with understanding how to correctly perform the motor imagery task.
5. Perception of own performance: subjects generally believed they performed well, although they acknowledged some errors. Subject A felt confident about completing almost all tasks correctly, and Subject D estimated a low error rate (under 5%). Subjects B and C, however, expressed less certainty, indicating they might have made occasional errors.

Subjects' ability to concentrate is a key issue in collecting reliable and consistent data. The length of the experiment and visual discomfort can bring fatigue in subjects by reducing their ability to perform the required tasks. In addition, difficulty in performing the MI task correctly reduces the reliability of the data. Some future solutions could be:

1. Allow subjects to adjust or to modify the screen brightness and contrast.
2. Use a pilot study to optimize the duration of sessions and related breaks and to figure out what are the best instructions to give the subject to explain the MI task.

Further improvements can be made in the administration of the questionnaire. A quantitative scale could be used for the responses, so that not only qualitative responses, but also numerical indicators of the responses are available. These could be used to better understand the effectiveness of certain choices within the experimental protocol.

Appendices

Data Acquisition protocol

Introduction

The following protocol concerns the use of the *g.GAMMA*_{sys} EEG helmet with the *g.Scarabeo* electrode system in conjunction with the *g.HIamp* amplifier.

The data recording software analyzed and used in the following protocol is *gRecorder*.

The protocol has been developed during the present master thesis and the experimental sessions were performed at the PoliToBIOMed Lab of Politecnico di Torino, Turin, Italy.

The steps to be followed to configure the instrumentation and its software are described in the following chapters.

Amplifier configuration

1. Connect the front power supply (black cable) to power as in Figure 55.



Figure 55: Power supply.

2. Connect the front USB cable to the data recording computer as in the right side of Figure 56.



Figure 56: USB Cable.

3. Connect the blue "OUTPUT TO AMP" cable to the electrode's board and amplifier as shown in the left side of Figure 56. Connect the black cable to the board and amplifier as shown in Figure 57 and Figure 58;



Figure 57: Output to Amplifier

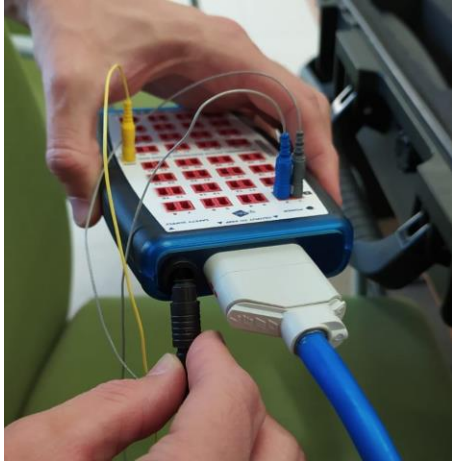


Figure 58: Electrode's Board. The ground electrode is yellow. The reference electrode is blue.

Electrode Cap Configuration

In order not to waste time once the subject is present, it would be advisable to ask the subject for the measurement of the circumference of the skull, in order to choose the right size of the helmet beforehand. Knowing which helmet is to be used (Small, Medium, or Large), insert the electrode holders in the appropriate positions of the electrode cap to avoid wasting time in the presence of the volunteer. The steps for the positioning of the electrode's cap are:

1. Measure the subject's head to choose which helmet to use (Small – Medium – Large).

The helmet/electrode cap has the following measures:

1. Small size: 50-54 cm;
2. Medium size: 54-58 cm;
3. Large size: 58-62 cm.

The skull dimension has not been asked beforehand during the experiment. It would be a good practice to keep in future experiments.

2. Once the helmet size has been chosen, insert the electrodes to be used in the CAP as shown in Figure 59.

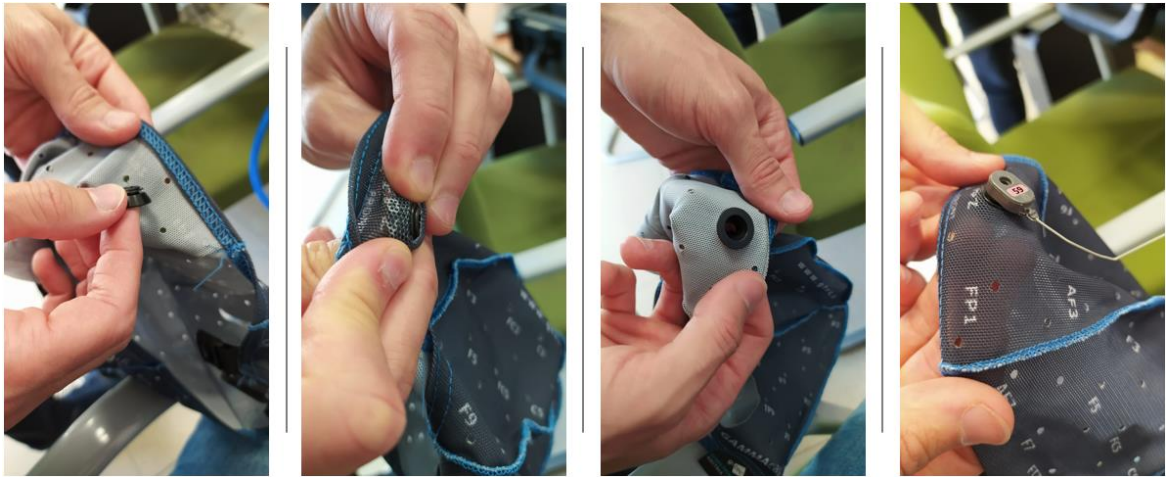


Figure 59: steps to insert electrodes in the electrode's cap.

The ground electrode (yellow one) is to be positioned in the AFz position of the 10-20 system, as shown in the gtec catalogue. The reference electrode (the blue one) is to be positioned pinching the right earlobe.



Figure 60: gtec product catalogue, it shows the positioning of the ground electrode over the scalp.

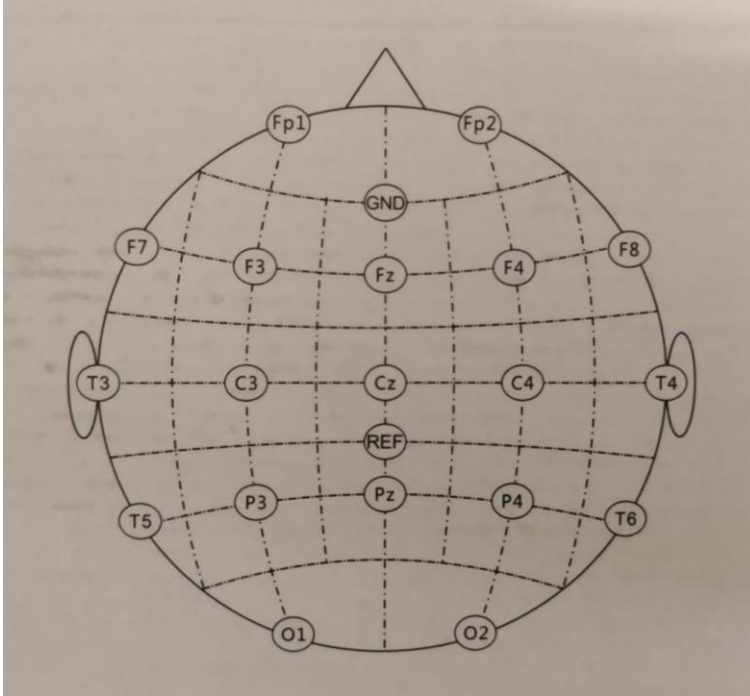


Figure 61: Example of electrode positioning in the 10-20 system within the openBCI settings. the openBCI positions are fixed and not changeable. As it can be seen the ground electrode is positioned in the same 10-20 position (AFz) as the ground electrode in the gtec catalogue.

3. Connect the electrodes to the electrode board shown in Figure 61 using a bandage to keep them tidy. By following Figure 62, connect the reference electrode (blue one) on the first channel of the board and the ground electrode (yellow one) in the in the appropriate yellow channel where it is written “GND”. Connect the rest of the electrodes to the other channels.



Figure 62: electrode positioning over the electrode board

4. Once the electrodes are placed on the helmet, place the cap on the person's head, checking that it fits properly. Move the helmet over the head using both hands gently. Do not pull at one end. Check that the Cz electrode is positioned in the centre of the head. Imagine a line between the left and right preaur and a second between the nasion andinion. The Cz electrode should be at the point where these two lines intersect. The subject can be asked to point to the centre of the head with their finger. Carefully insert the conductive gel into each electrode by making concentric movements from the base of the scalp upwards. Finally, place the reference electrode (blue) on the subject's ear, taking care to use the gel there too.

Software configuration

1. Insert the Green Dongle into the computer you intend to use. The dongle contains the license to use the g.tec software, without the dongle you cannot use the software;



Figure 63: Green dongle containing the license.

2. Open the gRecorder software on the lab's computer;
3. In Mode, switch from user mode to administration mode (there is no password).
4. Check that the g.HIamp amplifier is switched on and connected via cable to the computer. Select Settings → Select Hardware as in Figure 64.

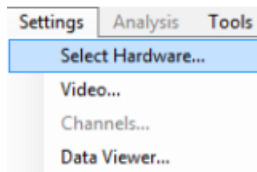


Figure 64: gRecorder window to select the settings of the experiment.

Move g.HIamp from Available Hardware to Selected Hardware using the right arrow button as in Figure 65. Click OK.

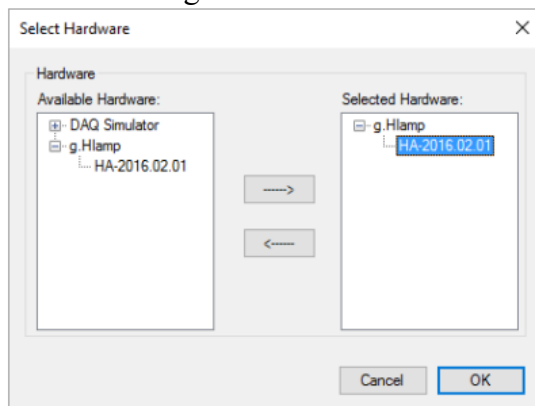


Figure 65: gRecorder window to select the hardware used in the experiment.

- Select Settings → g.HIamp as in Figure 66 to configure the amplifier and channels; All of the choices made here are saved on the data.

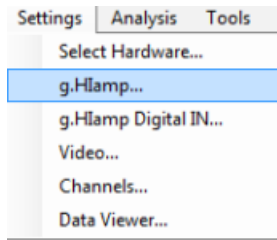


Figure 66: gRecorder window to select the settings of the experiment.

AMPLIFIER SETTINGS: Choose Sample Rate.

Hint: keep 512 Hz.

CHANNEL SETTINGS: Select the channels you are using on the board and choose whether to apply notch, bandpass, common average filters. Choose whether to use the bipolar option using channel 1 as the channel of reference.

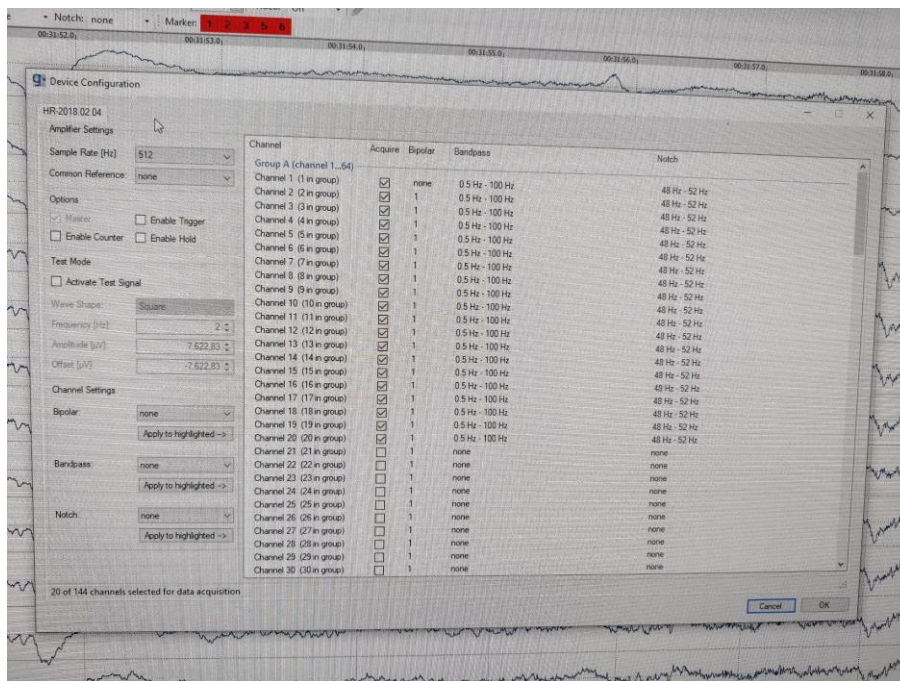


Figure 67: Example of the choices made in the Device configuration.

All of the choices made here, in paragraph 5, are saved on the data.

- Configure the gRecorder interface
Select Settings → Channels

Select the channels used and define their type (EEG, EMG etc.). it is possible to name the individual channels as their corresponding 10-20 system position.

7. At this point, the gRecorder interface should look like in Figure 68;

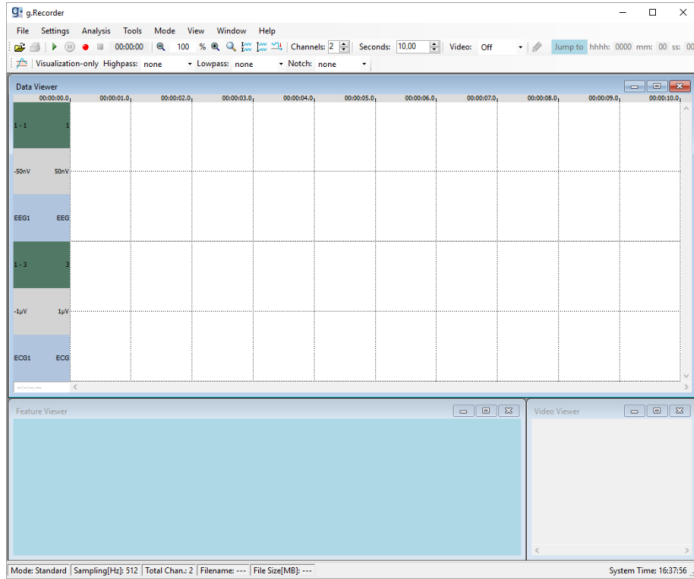


Figure 68: gRecorder interface.

If not all the chosen channels are displayed, check under Channels how many channels are selected. You can select how many channels to display from the Channels window;

8. Now you can start acquiring or viewing data by clicking “Start Data Viewing” or “Record”.

Pressing "Start Data Viewing", data are displayed without being saved on the hard disk.



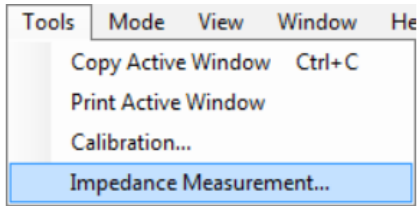
Figure 69: gRecorder’s software button to start the data viewing.

Pressing Record saves the data to the hard disk;



Figure 70: gRecorder’s software button to start the data recording.

9. Before starting the data acquisition, do an impedance measurement test to check if some of the channels are not well positioned. Select Tools → Impedance Measurement



When pressing start the software will start to measure the impedance of all the selected electrodes. The first channel will appear black as it is the one used as a reference to measure the impedance for all the other channels. The channel coloring indicates the impedance of each channel.

The ideal situation would be to have all the channels green (impedance $\leq 30 \text{ k}\Omega$). In a practical condition it is advisable to avoid red channels (impedance $\geq 100 \text{ k}\Omega$).

To stop the measure and close the window press “Close”.



Figure 71: Impedance measurement window on the gRecorder software.

10. Lastly, before data acquisition, it is good practice to check whether we can spot some artifacts in the signal such as eye blinking or mastication muscle artifacts.

The eye blinking artifact should be easily seen over the frontal electrode Fpz by asking the subject to blink their eyes at different rhythms.

EEG cleaning

At the end of the experiment, it is good practice to clean the instrumentation to prevent its deterioration. If left uncleaned, electrodes are keen to corrosion associated with repeated use, causing loss in signal quality.

Both the active electrode and its container can be washed with water and soap. It is advisable to use a pipe cleaner and a toothbrush to properly clean the electrodes from the gel.

Once cleaned and dried put the electrodes and their containers in the re-sealable transparent plastic bags. Each electrode should be in a bag together with its circled container.

The cap can be washed in water and soap as well. Before putting it back let it dry.

Experimental Instructions

In order to stick to the repeatability of the experiment, the following points must be explained to each subject, following the order below:

1. Explain the flexion/extension movement of the fingers of the right hand, introducing the concept of Imagination of the movement (or Motor Imagery - MI). Let the subject Imagine the intention of moving the right hand. Ask the subject to imagine the kinesthetic of the movement [88], by imagining the feeling in your body of opening and closing your hand;
2. Highlight the importance of avoiding muscular micro-activation as much as possible;
3. Show how the right forearm can be supported either by a pillow put on the subject's lap or on the chair armrest, to be comfortable and avoid unnecessary muscle activation during the experimental session. The volunteer is positioned in front of the laptop containing the stimulus.
4. Retry step number 1 with the forearm in the new position (i.e., right arm on a pillow or on the chair armrest);
5. Put the EEG cap on the subject. Ask to point the center of the head to better position the electrode Cz. Check with the subject that the EEG cap is not bothering him/her. If the cap is too tight or too large, change it for another measure;
6. Elucidate how the experiment is going to work. First, explain how the single trial works by showing on screen a printed image of the trial as in Figure 28 and Figure 29. Subsequently, explain the structure of the experiment (ME test and MI test followed by 4 runs) reminding them that there will be instructions on the screen to follow;
7. Explain the eye-blinking;
8. Check the impedance of the electrodes;
9. Before recording, look at the data through “Start Data Viewing” (Figure 69) and ask the subject to do some eye blinking. Check whether those eye blinks can be clearly spotted in the frontal electrode Fpz.
10. Start data recording with the data recording software gRecorder as in Figure 70.

Before starting the second session (i.e., validation phase) ask the subjects if there are any doubts regarding the continuation of the experiment. Remind the subject to wait at least 3 seconds between two consecutive self-performed movements. The duration of the imagined self-performed movement must be approximately the same length as the one in the calibration phase and in general no less than 2 seconds.

General principles of good experimentation

It is good to follow some expedients within the lab to acquire better quality signals. The environment should be as noise-free as possible in order to reduce artifacts.

Be aware not to keep the instrumentations too close to power sources to avoid interference.

The room temperature should be comfortable for the subject and the light not be too bright or too low.

Welcome the subject to a non-threatening, tidy environment and kindly guide him throughout the experiment. Let the subject sit in a comfortable position. All of this will help the subjects to avoid distraction and have a better focus on their task.

The experimenter should be calm and should explain the experiment to the subject always following the same steps. Following the fixed protocol helps with the repeatability of the experiment.

It is advisable to divide the experiment into sessions and runs, allowing the subjects to rest during those breaks and readjust their position, helping them to keep their vigilance.

Talking to the subjects during breaks can help to reduce drowsiness and a suitable moment to remind them to keep their head still and avoid movements and eye blinking as much as possible.

Drowsiness has to be reduced as much as possible as it might interfere with the signal quality and the success of the experiment. Following the tips above might help with this goal.

It's not advisable to give the subjects caffeine before the experiment as it might alter the EEG signal.

Following the same reasoning, it is better to avoid signal acquisition just after lunch or at least to ask the subject to avoid a heavy meal.

Since EEG experiments often require staring at a screen for a prolonged period reducing blinking, some subjects may experience eye discomfort and feel their eye dry. Suggesting glasses instead of lenses might help this [15].

List of Tables

Table 1: summary of the literature search over the models used in EEG-dependent BCI for movement classification.....	41
Table 2: summary of the literature search over the characteristics of experimental protocols for EEG-dependent BCI.	42
Table 3: Motor imagery classes performed by each subject in dataset 1 from BCI competition IV.	47
Table 4: Helmet size and age of each experimental subject of the dataset acquired within the PoliTo ^{BIO} Med Lab of Politecnico di Torino.	48
Table 5: Sequence of the runs in the calibration phase.....	57
Table 6: Single-run organization in the validation phase.	57
Table 7: Sequence of the runs in the validation phase.....	58
<i>Table 8: Combination of training and testing subjects for the subject independent BCI of Dataset 1 from BCI competition IV.</i>	<i>70</i>
Table 9: Combination of training and testing subjects for the subject independent BCI of the PoliTo ^{BIO} Med Lab dataset.	70
Table 10: Example of a confusion matrix for a 3-class classification problem with a balanced dataset.	79
<i>Table 11: Table showing the results of performance for a 10×5 cross fold validation during the calibration phase of Dataset 1 BCI competition IV. Combinations of different pre-processing and feature extraction techniques are looked at.</i>	<i>86</i>
<i>Table 12: Table showing the results of performance for a 10x5 cross fold validation during the calibration phase of Dataset 1 BCI competition IV. Combinations of different pre-processing and feature extraction techniques are looked at.</i>	<i>89</i>
Table 13: Table showing the results of performance for a 10×5 cross fold validation during the calibration phase of Dataset 1 BCI competition IV for subject A. Combinations of different epoch divisions are looked at.....	90
Table 14: Results of the Tukey HSD post hoc test on Table 13 data. Only results with $p < \alpha$ are reported.	91
Table 15: Table showing the results of performance for a 10×5 cross fold validation during the calibration phase of Dataset 1 BCI competition IV between the IC and NC classes.	93
Table 16: Cohen's Kappa coefficient κ results for the validation phase of Dataset 1 BCI competition IV between the IC and NC classes.....	94
Table 17: Confusion matrix of subject A during the validation phase of Dataset 1 BCI competition IV between the IC and NC classes. It is highlighted in green when the predicted class and the real class coincide. It is highlighted in red otherwise.....	94
Table 18: Classification performance of the subject-independent BCI for Dataset 1 BCI competition IV between the IC and NC classes.....	95

Table 19: Classification performance of the subject-independent BCI for Dataset 1 BCI competition IV between the IC classes.	96
Table 20: Table showing the results of performance for a 10x4 cross fold validation during the calibration phase of the PoliTo ^{BIO} Med Lab dataset. The table shows the ability of the algorithm to classify between the two classes of Intentional Control.	98
Table 21: Table showing the results of the Tukey HSD test on the 4 subjects of the PoliTo ^{BIO} Med Lab dataset during the calibration phase of the experiment.	99
Table 22: Table showing the results of performance for a 10x5 cross fold validation during the calibration phase of the PoliTo ^{BIO} Med Lab dataset between the IC and NC classes.	101
Table 23: Classification performance of the subject independent BCI for the PoliTo ^{BIO} Med Lab dataset between the IC and NC classes.	102
Table 24: Classification performance of the subject independent BCI for the PoliTo ^{BIO} Med Lab dataset between the IC classes.	103

List of Figures

Figure 1: Thesis workflow..... 6

Figure 2: Gray and white matter distribution in the brain (left side) and spinal cord (right side).
From “<https://www.hopkinsmedicine.org>”..... 7

Figure 3: The division of the brain into lobes, the main sulci, and the mapping of certain functions performed by the cortex. From Wolpaw (2012). 9

Figure 4: The motor homunculus derived by Wilder Penfield illustrating the effects of electrical stimulation of the cortex of human neurosurgical patients. Adapted from Nolte (2002). 10

Figure 5: Structure of a typical neuron. From: “www.training.seer.cancer.gov/brain/” 11

Figure 6: Phases of an action potential in relation to membrane voltage over time. From: “www.teachmephysiology.com” 12

Figure 7: The number of BCI publications over the years. The statistics were based on an electronic literature search on PubMed in which “Brain-Computer Interface” was the search keyword. The articles listed until December 4th have been accounted only. From “Progress in Brain Computer Interface: Challenges and opportunities” by Simanto Saha [14]. 15

Figure 8: General architecture of a Brain-Computer interface. From M. Rashid (2020) [20]. 16

Figure 9: The different layers between the cerebral cortex and the scalp. From “<https://www.hopkinsmedicine.org>”..... 19

Figure 10: EEG spectrum bandwidths. From “www.rafaelvallat.com”..... 20

Figure 11: The 10-20 system of the international federation for the standardization of the placements of EEG electrodes. From R. Shriram (2012) [31]...... 23

Figure 12: The standard 10-20, 10-10, and 10-5 electrode montages. The 21 black electrodes represent the 10-20 system. The 10-10 system is formed by the 21 black electrodes plus the 53 gray electrodes (74 electrodes in total). The 10-5 system is formed by the sum of the black, gray and white electrodes. From Wolpaw (2012) [10]. 24

Figure 13: An example of an Event-Related Potential (ERP) with 5 components, 3 positive ones, and 2 negative ones. From “www.wikipedia.org”..... 29

Figure 14: Example of a session structure. In this example each session is composed of 5 runs and each run is composed of 20 trials. Between runs there is a rest phase..... 30

Figure 15: Example of the division of a dataset into 80% training set, and 20 % testing set..... 31

Figure 16: Example of functional movements. Upper row from left to right we have a palmar grasp, pinch, and elbow flexion. From Ana. P. Costa [48] . Bottom row from left to right we have pronation, supination, palmar grasp, lateral grasp, and hand open. From P. Ofner [15]...... 33

Figure 17: Electrode positioning in the study by S. Romagosa, “Brain Computer Interface Treatment for Motor Rehabilitation of Upper Extremity of Stroke Patients-A Feasibility Study”. From S. Romagosa [21]. 34

Figure 18: Example of Bio signals recorded through EEG and EOG. EOG follows the standard placement of the left and right outer canthus of the eye (LOC and ROC) [53]. From M. Witkowski (2014) [11]...... 35

Figure 19: A diagram of how a BCI protocol works based on the two phases of calibration and validation. From Blankertz (2008) [54].	36
Figure 20: Example of a paradigm for motor execution for a synchronous BCI. From G. Pan (2018) [59].	38
Figure 21: Example of paradigms for motor attempt for a self-paced BCI. A) The paradigm for the calibration phase. B) The paradigm for the validation phase. From P. Ofner (2019) [15].	39
Figure 22: Paradigm structure of Dataset 1 BCI competition IV. The upper paradigm is related to the calibration part of the experiment while the lower paradigm is related to the validation part of the experiment. From M. Tangermann [6].	49
Figure 23: gRecorder software graphical user interface.	51
Figure 24: The g.tec parallel port used to connect the g.Hiamp amplifier to the stimulus computer.	52
Figure 25: Psychopy Builder Interface.	53
Figure 26: Psychopy Coder Interface.	53
Figure 27: Experimental protocol tasks: a) Hand open; b) Hand closed.	55
Figure 28: Calibration Phase Trial.	56
Figure 29: Validation phase trial.	58
Figure 30: Schematic representation of the synchronization process.	59
Figure 31: The voluntary eye-blinks recorded on the Fpz channel of subject A from the PoliTo ^{BIO} Med Lab dataset. Upper Figure: a picture of the whole length of the signal shows the three eye-blinking spikes at the beginning and at the end of the experiment. Bottom Figure: an enlarged portion of the signal showing the three eye-blinking spikes at the beginning of the experiment.	60
Figure 32: Electrode positioning within the extended 10-20 system/10-10 system. The electrodes colored in green have been used for the data acquisition related to this thesis. Modified from Zhang et al. [75].	61
Figure 33: Stimulus Vector for subject A of the PoliTo ^{BIO} Med Lab dataset during the calibration phase of the experiment. The x-axis shows the time axis in minutes. On the y-axis the value corresponding to the class: class 0 (no stimulus), class 1 (open hand), class 2 (closed hand).	64
Figure 34: EEG signal on the CP1 electrode for subject A of the PoliTo ^{BIO} Med Lab dataset during the calibration phase of the experiment. The signal is colored in blue during the NC phase (class 0), in green and red during the IC phase. When the signal is green the hand open stimulus is presented (class 1). When the signal is red the hand closed stimulus is presented (class 2).	65
Figure 35: Zoom in of Figure 34. The zoom is applied to a portion of the signal about one minute long between minute 6 and minute 7 of the experiment.	66
Figure 36: Pipeline of the processing steps used in the analysis of the data.	69
Figure 37: PSD of the signal of the FCz electrode of subject A during the calibration phase of the experiment.	72
Figure 38: Zoom in of Figure 37. The zoom is done on the x-axis in order to see the reduction of the signal's power around 50 Hz.	73

Figure 39: Zoom in of Figure 37. The zoom is done on the x-axis in order to see the reduction of the signal's power below 0.5 Hz.....	73
Figure 40: : Zoom in of Figure 37. The zoom is done on the x-axis in order to see the reduction of the signal's power above 100 Hz.....	74
Figure 41:Application of the three steps of Power band feature extraction over a signal epoch of subject A of dataset 1 of BCI competition IV. The channel in the figure is the Fcz channel.....	76
Figure 42: Application of CSP filter on a signal epoch of subject A of dataset I of BCI competition IV. On the left: the scatter plot of the first and last row of the unfiltered EEG signal for the 2 classes of Intentional Control. The distribution of sampling before the CSP filtering is shown. On the right: the scatter plot of the first and last row of the CSP filtered signal for the 2 classes of Intentional Control. The ellipses show the estimated covariance and the direction of the CSP projections. This figure shows how the variance of class1 is maximum in Xcsp row n.16 but minimum in Xcsp row n.1 while the variance of class 2 is opposite to class1. It is observed that the application of CSP significantly increases the separability of epochs of different classes.	77
Figure 43: Bar graph showing the results of performance for a 10×5 cross fold validation during the calibration phase of Dataset 1 BCI competition IV. The graph shows the ability of the algorithm to classify between the two classes of Intentional Control. 4 different cases are looked at: CAR+CSP, NO CAR + CSP, CAR + PB, NO CAR + PB. The graph shows the performance results for all subjects of the experiment.	86
Figure 44: Bar graph showing the results of performance for a 10x5 cross fold validation during the calibration phase of Dataset 1 BCI competition IV. The graph shows the ability of the algorithm to classify between the two classes of Intentional Control. 3 different classifiers are looked at: LDA, SVM and Naïve Bayes. The graph shows the performance results for all subjects of the experiment.	88
Figure 45: Classification accuracy + SE between the two IC classes. Subject A during the calibration phase of Dataset 1 BCI competition IV. The blue continuous line is the accuracy. The two dotted line represent the accuracy ± its SE. The red dotted line represents the random classification line.	92
Figure 46:Bar graph showing the results of performance for a 10×5 cross fold validation during the calibration phase of Dataset 1 BCI competition IV. The graph shows the ability of the algorithm to classify between the class of NC and the class of IC. All 4 subjects are looked at. 93	
Figure 47:Classification performance of the subject-independent BCI for Dataset 1 BCI competition IV between the IC and NC classes.....	95
Figure 48: Classification performance of the subject-independent BCI for Dataset 1 BCI competition IV between the IC classes.....	96
Figure 49: Bar graph showing the results of performance for a 10×4 cross fold validation during the calibration phase of the PoliTo ^{BIO} Med Lab dataset. The graph shows the ability of the algorithm to classify between the two classes of Intentional Control.	98

Figure 50: Tukey HSD test to compare the means of the accuracies between the subjects of the PoliTo ^{BIO} Med Lab dataset. The data correspond to the calibration phase of the experiment. The horizontal lines represent the means and confidence intervals.	99
Figure 51: Classification accuracy + SE between the two IC classes. Subject A during the calibration phase of the PoliTo ^{BIO} Med Lab dataset. The blue continuous line is the accuracy. The two dotted line represent the accuracy \pm its SE. The red dotted line represents the random classification line.	100
Figure 52: Bar graph showing the results of performance for a 10 \times 5 cross fold validation during the calibration phase of PoliTo ^{BIO} Med Lab dataset. The graph shows the ability of the algorithm to classify between the class of NC and the class of IC.....	101
Figure 53: Classification performance of the subject independent BCI for the PoliTo ^{BIO} Med Lab dataset between the IC and NC classes.	102
Figure 54: Classification performance of the subject independent BCI for the PoliTo ^{BIO} Med Lab dataset between the IC classes.	103
Figure 55: Power supply.	107
Figure 56: USB Cable.....	108
Figure 57: Output to Amplifier.....	108
Figure 58: Electrode's Board. The ground electrode is yellow. The reference electrode is blue.	109
Figure 59: steps to insert electrodes in the electrode's cap.....	110
Figure 60: gtec product catalogue, it shows the positioning of the ground electrode over the scalp.	111
Figure 61: Example of electrode positioning in the 10-20 system within the openBCI settings. the openBCI positions are fixed and not changeable. As it can be seen the ground electrode is positioned in the same 10-20 position (AFz) as the ground electrode in the gtec catalogue.....	112
Figure 62: electrode positioning over the electrode board.....	113
Figure 63: Green dongle containing the license.	114
Figure 64:gRecorder window to select the settings of the experiment.	114
Figure 65:gRecorder window to select the hardware used in the experiment.	114
Figure 66: gRecorder window to select the settings of the experiment.	115
Figure 67: Example of the choices made in the Device configuration.	115
Figure 68: gRecorder interface.	116
Figure 69: gRecorder's software button to start the data viewing.	116
Figure 70: gRecorder's software button to start the data recording.....	116
Figure 71: Impedance measurement window on the gRecorder software.	117

List of Abbreviations

ANOVA	Analysis of Variance
BCI	Brain Computer Interface
CNS	Central Nervous System
ECG	ElectroCardioGram
ECoG	ElectroCorticoGram
EEG	ElectroEncephaloGraphy
EMG	ElectroMyoGraphy
EOG	ElectroOculoGraphy
ERD	Event Related Desynchronization
ERP	Event Related Potential
ERS	Event Related Synchronization
FIR	Finite Impulse Response
HSD	Honest Significant Difference
IC	Intentional Control
ICA	Independent Component Analysis
IIR	Infinite Impulse Response
LFP	Local Field Potential
MA	Motor Attempt
ME	Motor Execution
MEAs	Micro-Electrode-Arrays
MEG	MagnetoEncephaloGraphy
MI	Motor Imagery
MRCP	Movement Related Cortical Potential
NC	No-Control
PCA	Principal Component Analysis
PNS	Pheripheral Nervous System
PSD	Power Spectral Density

SE	Standard Error
SCP	Slow Cortical Potential
VEP	Visually Evoked Potential

References

- [1] “<https://www.mondino.it/malattie-neuromuscolari>”.
- [2] “Ofori-Asenso, R. (2019). Global, regional, and national burden of traumatic brain injury and spinal cord injury, 1990-2016: a systematic analysis for the Global Burden of Disease Study 2016: *Lancet Neurol.* Quantum, 2022, 16.”.
- [3] “V. Hachinski et al., ‘Stroke: Working toward a prioritized world agenda,’ *Stroke*, vol. 41, no. 6, pp. 1084–1099, 2010, doi: 10.1161/STROKEAHA.110.586156”.
- [4] “Nicolas-Alonso LF, Gomez-Gil J. Brain Computer Interfaces, a Review. *Sensors*. 2012; 12(2):1211-1279. <https://doi.org/10.3390/s120201211>”.
- [5] “Kwon, O-Yeon, Min-Ho Lee, Cuntai Guan, and Seong-Whan Lee. ‘Subject-independent brain–computer interfaces based on deep convolutional neural networks.’ *IEEE transactions on neural networks and learning systems* 31, no. 10 (2019): 3839-3852.”.
- [6] “Tangermann, Michael, Klaus-Robert Müller, Ad Aertsen, Niels Birbaumer, Christoph Braun, Clemens Brunner, Robert Leeb et al. ‘Review of the BCI competition IV.’ *Frontiers in neuroscience* (2012): 55.”.
- [7] “www.hopkinsmedicine.org/health”.
- [8] “Penfield, Wilder, and Edwin Boldrey. ‘Somatic motor and sensory representation in the cerebral cortex of man as studied by electrical stimulation.’ *Brain* 60.4 (1937): 389-443.”.
- [9] “Catani M. A little man of some importance. *Brain*. 2017 Nov 1;140(11):3055-3061. doi: 10.1093/brain/awx270. PMID: 29088352; PMCID: PMC5841206.”.
- [10] “E. W. Wolpaw, J. R. and Wolpaw, *Brain-computer interfaces: principles and practice*. Oxford University Press., vol. 53, no. 9. 2012.”.
- [11] “Witkowski, Matthias, Mario Cortese, Marco Cempini, Jürgen Mellinger, Nicola Vitiello, and Surjo R. Soekadar. ‘Enhancing brain-machine interface (BMI) control of a hand exoskeleton using electrooculography (EOG).’ *Journal of neuroengineering and rehabilitation* 11, no. 1 (2014): 1-6.”.
- [12] “Soekadar SR, Witkowski M, Vitiello N, Birbaumer N. An EEG/EOG-based hybrid brain-neural computer interaction (BNCI) system to control an exoskeleton for the paralyzed hand. *Biomed Tech (Berl)*. 2014; doi: 10.1515/bmt-2014-0126 [in press].”.
- [13] “J J Vidal, *Toward Direct Brain-Computer Communication, Annual Review of Biophysics and Bioengineering* 1973 2:1, 157-180.”.
- [14] “Saha Simanto, Mamun Khondaker A., Ahmed Khawza, Mostafa Raqibul, Naik Ganesh R., Darvishi Sam, Khandoker Ahsan H., Baumert Mathias. *Progress in Brain Computer Interface: Challenges and Opportunities. Journal: Frontiers in Systems Neuroscience, Volume 15, Year 2021, DOI=10.3389/fnsys.2021.578875.*”, doi: 10.1109/TBME.2004.827072.
- [15] “Ofner P, Schwarz A, Pereira J, Wyss D, Wildburger R, Müller-Putz GR. Attempted Arm and Hand Movements can be Decoded from Low-Frequency EEG from Persons with Spinal Cord Injury. *Sci Rep*. 2019 May 9;9(1):7134. doi: 10.1038/s41598-019-43594-9. PMID: 31073142; PMCID: PMC6509331.”.
- [16] “B. Reuderink, A. Nijholt, and M. Poel, ‘Affective pacman: a frustrating game for brain-computer interface experiments,’ in *Intelligent Technologies for Interactive Entertainment*, A. Nijholt, D. Reidsma, and H. Hondorp, Eds., vol. 9 of *Lecture Notes of the Institute for*

- Computer Sciences, Social Informatics and Telecommunications Engineering, pp. 221–227, Springer, Berlin, Germany, 2009.”
- [17] “G. Pires, M. Torres, N. Casaleiro, U. Nunes, and M. Castelo-Branco, ‘Playing Tetris with non-invasive BCI,’ in Proceedings of the IEEE 1st International Conference on Serious Games and Applications for Health (SeGAH ’11), pp. 1–6, IEEE, Braga, Portugal, November 2011.”
- [18] “Aldayel, Mashael & Ykhlef, Mourad & Alnafjan, Abeer. (2020). Deep Learning for EEG-Based Preference Classification in Neuromarketing. Applied Sciences. 10. 1525. 10.3390/app10041525.”
- [19] “Zhao, Qinglin, Hong Peng, Bin Hu, Quanying Liu, Li Liu, YanBing Qi, and Lanlan Li. ‘Improving individual identification in security check with an EEG based biometric solution.’ In International Conference on Brain Informatics, pp. 145-155. Springer, Berlin, Heidelberg, 2010.”
- [20] “Rashid, M., Sulaiman, N., Musa, R. M., Fakhri, A., Bari, B. S., & Khatun, S. (2020). Current Status, Challenges, and Possible Solutions of EEG-Based Brain-Computer Interface: A Comprehensive Review. Frontiers in Neurorobotics. <https://doi.org/10.3389/fnbot.2020.00025>”
- [21] “Sebastián-Romagosa M, Cho W, Ortner R, Murovec N, Von Oertzen T, Kamada K, Allison BZ, Guger C. Brain Computer Interface Treatment for Motor Rehabilitation of Upper Extremity of Stroke Patients-A Feasibility Study. Front Neurosci. 2020 Oct 21;14:591435. doi: 10.3389/fnins.2020.591435. PMID: 33192277; PMCID: PMC7640937.”
- [22] “Willett, F.R., Avansino, D.T., Hochberg, L.R. et al. High-performance brain-to-text communication via handwriting. Nature 593, 249–254 (2021). <https://doi.org/10.1038/s41586-021-03506-2>”
- [23] “Marzbani H, Marateb HR, Mansourian M. Neurofeedback: A Comprehensive Review on System Design, Methodology and Clinical Applications. Basic Clin Neurosci. 2016 Apr;7(2):143-58. doi: 10.15412/J.BCN.03070208. PMID: 27303609; PMCID: PMC4892319.”
- [24] “T. J. La Vaque Ph.D. (1999) The History of EEG Hans Berger, Journal of Neurotherapy: Investigations in Neuromodulation, Neurofeedback and Applied Neuroscience, 3:2, 1-9, DOI: 10.1300/J184v03n02_01”
- [25] “Haas LF Hans Berger (1873–1941), Richard Caton (1842–1926), and electroencephalography Journal of Neurology, Neurosurgery & Psychiatry 2003;74:9.”
- [26] “Hari, MD, PhD, Riitta, and Aina Puce, PhD, MEG-EEG Primer, 1 (New York, 2017; online edn, Oxford Academic, 1 Mar. 2017), <https://doi.org/10.1093/med/9780190497774.001.0001>”
- [27] “Bouton CE, Shaikhouni A, Annetta NV, Bockbrader MA, Friedenberg DA, Nielson DM, Sharma G, Sederberg PB, Glenn BC, Mysiw WJ, Morgan AG, Deogaonkar M, Rezai AR. Restoring cortical control of functional movement in a human with quadriplegia. Nature. 2016 May 12;533(7602):247-50. doi: 10.1038/nature17435. Epub 2016 Apr 13. PMID: 27074513.”
- [28] “Mathewson, Kyle E., Tyler JL Harrison, and Sayeed AD Kizuk. ‘High and dry? Comparing active dry EEG electrodes to active and passive wet electrodes.’ Psychophysiology 54.1 (2017): 74-82. Wet vs dry (d 4-45)”

- [29] “Jeremy Frey. ‘Comparison of a consumer grade EEG amplifier with medical grade equipment in BCI applications’. Proceedings of the 6th International Brain-Computer Interface Meeting, organized by the BCI Society. DOI: 10.3217/978-3-85125-467-9-147”.
- [30] “Jasper, H.H. (1958) The Ten-Twenty Electrode System of the International Federation. *Electroencephalography and Clinical Neurophysiology*, 10, 371-375.”.
- [31] “Shriram, Revati & Sundhararajan, Dr & Daimiwal, Nivedita. (2012). EEG Based Cognitive Workload Assessment for Maximum Efficiency. *IOSR Journal of Electronics and Communication Engineering (IOSR-JECE)*.”.
- [32] “Laura Leuchs, Ph.D. Scientific Consultant (Brain Products). Choosing your reference – and why it matters. Brain Products Press Release - May 2019.”.
- [33] “Britton JW, Frey LC, Hopp JLet al., authors; St. Louis EK, Frey LC, editors. *Electroencephalography (EEG): An Introductory Text and Atlas of Normal and Abnormal Findings in Adults, Children, and Infants* [Internet]. Chicago: American Epilepsy Society; 2016. Appendix 2. Principles of Digital EEG.”.
- [34] “gRecorder user manual V5.16.00. Copyright 2007-2017, g.tec medical engineering GmbH.”.
- [35] “Kapeller, Christoph & Schneider, C & Kamada, Kyousuke & Ogawa, H & Kunii, Naoto & Ortner, Rupert & Prueckl, Robert & Guger, Christoph. (2014). Single trial detection of hand poses in human ECoG using CSP based feature extraction. 2014 36th Annual International Conference of the IEEE Engineering in Medicine and Biology Society, EMBC 2014. 2014. 4599-602. 10.1109/EMBC.2014.6944648.”.
- [36] “Luca Mesin, *Neuromuscular System Engineering*, 2019. ISBN: 9788892361881”.
- [37] “Fruitet, Joan & Clerc, Maureen. (2012). Investigating brief motor imagery for an ERD/ERS based BCI. Conference proceedings : ... Annual International Conference of the IEEE Engineering in Medicine and Biology Society. IEEE Engineering in Medicine and Biology Society. Conference. 2012. 2929-32. 10.1109/EMBC.2012.6346577.”.
- [38] “Pfurtscheller, Gert. ‘EEG event-related desynchronization (ERD) and synchronization (ERS).’ *Electroencephalography and Clinical Neurophysiology* 1.103 (1997): 26.”.
- [39] “Dyson, Matthew & Clerc, Maureen. (2013). An analysis of performance evaluation for motor-imagery based BCI. *Journal of neural engineering*. 10. 031001. 10.1088/1741-2560/10/3/031001.”.
- [40] “Lotte, Fabien, Marco Congedo, Anatole Lécuyer, Fabrice Lamarche, and Bruno Arnaldi. ‘A review of classification algorithms for EEG-based brain–computer interfaces.’ *Journal of neural engineering* 4, no. 2 (2007): R1.”.
- [41] “M. Tariq, L. Uhlenberg, P. Trivailo, K. S. Munir and M. Simic, ‘Mu-beta rhythm ERD/ERS quantification for foot motor execution and imagery tasks in BCI applications,’ 2017 8th IEEE International Conference on Cognitive Infocommunications (CogInfoCom), 2017, pp. 000091-000096, doi: 10.1109/CogInfoCom.2017.8268222.”.
- [42] “Jochumsen, Mads, Imran Khan Niazi, Natalie Mrachacz-Kersting, Dario Farina, and Kim Dremstrup. ‘Detection and classification of movement-related cortical potentials associated with task force and speed.’ *Journal of neural engineering* 10, no. 5 (2013): 056015.”.
- [43] “Niazi, Imran Khan, Ning Jiang, Olivier Tiberghien, Jørgen Feldbæk Nielsen, Kim Dremstrup, and Dario Farina. ‘Detection of movement intention from single-trial movement-related cortical potentials.’ *Journal of neural engineering* 8, no. 6 (2011): 066009.”.

- [44] “G. Pfurtscheller and C. Neuper, ‘Motor imagery and direct brain-computer communication,’ in *Proceedings of the IEEE*, vol. 89, no. 7, pp. 1123-1134, July 2001, doi: 10.1109/5.939829.”
- [45] “R. Beisteiner, P. Höllinger, G. Lindinger, W. Lang, and A. Berthoz, ‘Mental representations of movements. Brain potentials associated with imagination of hand movements,’ *Electroencephalogr. Clin. Neurophysiol.*, vol. 96, pp. 183–192, 1995.”
- [46] “Jeannerod, Marc. ‘Mental imagery in the motor context.’ *Neuropsychologia* 33, no. 11 (1995): 1419-1432.”
- [47] “J. Decety, D. Perani, M. Jeannerod, V. Bettinardi, B. Tadardy, R. Woods, J. Mazziotta, and F. Fazio, ‘Mapping motor representations with positron emission tomography,’ *Nature*, vol. 371, pp. 600–602, 1994.”
- [48] “Costa, A.P., Møller, J.S., Iversen, H.K. and Puthusserypady, S., 2018. An adaptive CSP filter to investigate user independence in a 3-class MI-BCI paradigm. *Computers in Biology and Medicine*, 103, pp.24-33.”
- [49] “Ang, Kai Keng, Zheng Yang Chin, Chuanchu Wang, Cuntai Guan, and Haihong Zhang. ‘Filter bank common spatial pattern algorithm on BCI competition IV datasets 2a and 2b.’ *Frontiers in neuroscience* 6 (2012): 39.”
- [50] “Zhang, Haihong, Cuntai Guan, Kai Keng Ang, Chuanchu Wang, and Zheng Yang Chin. ‘BCI competition IV–data set I: learning discriminative patterns for self-paced EEG-based motor imagery detection.’ *Frontiers in neuroscience* 6 (2012): 7.”
- [51] “Taheri, S., Ezoji, M. and Sakhaei, S.M., 2020. Convolutional neural network based features for motor imagery EEG signals classification in brain–computer interface system. *SN Applied Sciences*, 2(4), pp.1-12.”
- [52] “Lin, Ke, Andrea Cinetto, Yijun Wang, Xiaogang Chen, Shangkai Gao, and Xiaorong Gao. ‘An online hybrid BCI system based on SSVEP and EMG.’ *Journal of neural engineering* 13, no. 2 (2016): 026020.”
- [53] “Yetton, Benjamin & Niknazar, Mohammad & Duggan, Katherine & McDevitt, Elizabeth & Whitehurst, Lauren & Sattari, Negin & Mednick, Sara. (2015). Automatic Detection of Rapid Eye Movements (REMs): A machine learning approach. *Journal of Neuroscience Methods*. 259. 10.1016/j.jneumeth.2015.11.015.”
- [54] “Blankertz, Benjamin, et al. ‘Optimizing Spatial Filters for Robust EEG Single-Trial Analysis.’ *IEEE Signal Processing Magazine*, vol. 25, no. 1, 2008, pp. 41–56., doi:10.1109/msp.2008.4408441.”
- [55] “F. Lotte, ‘Signal processing approaches to minimize or suppress calibration time in oscillatory activitybased brain-computer interfaces,’ *Proc. IEEE*, vol. 103, no. 6, pp. 871–890, Jun. 2015, doi: 10.1109/JPROC.2015.2404941.”
- [56] “H. Ramoser, J. Müller-Gerking, and G. Pfurtscheller, ‘Optimal spatial filtering of single trial EEG during imagined hand movement,’ *IEEE Trans. Rehabil. Eng.*, vol. 8, no. 4, pp. 441–446, 2000, doi: 10.1109/86.895946.”
- [57] “Schlögl, Alois & Vidaurre, Carmen & Müller, Klaus-Robert. (2010). Adaptive Methods in BCI Research - An Introductory Tutorial. 10.1007/978-3-642-02091-9_18.”
- [58] “Blankertz, Benjamin, K-R. Muller, Dean J. Krusienski, Gerwin Schalk, Jonathan R. Wolpaw, Alois Schlogl, Gert Pfurtscheller, Jd R. Millan, Michael Schroder, and Niels Birbaumer. ‘The BCI competition III: Validating alternative approaches to actual BCI problems.’ *IEEE transactions on neural systems and rehabilitation engineering* 14, no. 2 (2006): 153-159.”

- [59] “Pan, Gang, Jia-Jun Li, Yu Qi, Hang Yu, Jun-Ming Zhu, Xiao-Xiang Zheng, Yue-Ming Wang, and Shao-Min Zhang. ‘Rapid decoding of hand gestures in electrocorticography using recurrent neural networks.’ *Frontiers in neuroscience* 12 (2018): 555.”
- [60] “Benabid, Alim Louis, Thomas Costecalde, Andrey Eliseyev, Guillaume Charvet, Alexandre Verney, Serpil Karakas, Michael Foerster et al. ‘An exoskeleton controlled by an epidural wireless brain–machine interface in a tetraplegic patient: a proof-of-concept demonstration.’ *The Lancet Neurology* 18, no. 12 (2019): 1112-1122.”
- [61] “Ajiboye, Abidemi Bolu, Francis R. Willett, Daniel R. Young, William D. Memberg, Brian A. Murphy, Jonathan P. Miller, Benjamin L. Walter et al. ‘Restoration of reaching and grasping in a person with tetraplegia through brain-controlled muscle stimulation: a proof-of-concept demonstration.’ *Lancet (London, England)* 389, no. 10081 (2017): 1821.”
- [62] “Zhang, Ce, and Azim Eskandarian. ‘A computationally efficient multiclass time-frequency common spatial pattern analysis on EEG motor imagery.’ In 2020 42nd Annual International Conference of the IEEE Engineering in Medicine & Biology Society (EMBC), pp. 514-518. IEEE, 2020.”
- [63] “Serdar Bascil, M., Ahmet Y. Tesneli, and Feyzullah Temurtas. ‘Multi-channel EEG signal feature extraction and pattern recognition on horizontal mental imagination task of 1-D cursor movement for brain computer interface.’ *Australasian physical & engineering sciences in medicine* 38, no. 2 (2015): 229-239.”
- [64] “Pfurtscheller, Gert, Patricia Linortner, Raimar Winkler, Gerd Korisek, and Gernot Müller-Putz. ‘Discrimination of motor imagery-induced EEG patterns in patients with complete spinal cord injury.’ *Computational intelligence and neuroscience* 2009 (2009).”
- [65] “Barachant, Alexandre, Stéphane Bonnet, Marco Congedo, and Christian Jutten. ‘Multiclass brain–computer interface classification by Riemannian geometry.’ *IEEE Transactions on Biomedical Engineering* 59, no. 4 (2011): 920-928.”
- [66] “Lu, Na, Tengfei Li, Xiaodong Ren, and Hongyu Miao. ‘A deep learning scheme for motor imagery classification based on restricted Boltzmann machines.’ *IEEE transactions on neural systems and rehabilitation engineering* 25, no. 6 (2016): 566-576.”
- [67] “Yi, Weibo, Shuang Qiu, Hongzhi Qi, Lixin Zhang, Baikun Wan, and Dong Ming. ‘EEG feature comparison and classification of simple and compound limb motor imagery.’ *Journal of neuroengineering and rehabilitation* 10, no. 1 (2013): 1-12.”
- [68] “<https://www.bbci.de/competition>”.
- [69] “<http://bnci-horizon-2020.eu/database/data-sets>”.
- [70] “Blankertz, Benjamin, Guido Dornhege, Matthias Krauledat, Klaus-Robert Müller, and Gabriel Curio. ‘The non-invasive Berlin brain–computer interface: fast acquisition of effective performance in untrained subjects.’ *NeuroImage* 37, no. 2 (2007): 539-550.”
- [71] “Kwon, O.Y., Lee, M.H., Guan, C. and Lee, S.W., 2019. Subject-independent brain–computer interfaces based on deep convolutional neural networks. *IEEE transactions on neural networks and learning systems*, 31(10), pp.3839-3852.”
- [72] “Peirce, J. W., Gray, J. R., Simpson, S., MacAskill, M. R., Höchenberger, R., Sogo, H., Kastman, E., Lindeløv, J. (2019). *PsychoPy2: experiments in behavior made easy*. *Behavior Research Methods*. 10.3758/s13428-018-01193-y”.
- [73] “<https://www.mathworks.com/>”.
- [74] “<https://www.python.org/>”.

- [75] “Zhang, Shenghuan & Mccane, Brendan & Shadli, Shabah & Mcnaughton, Neil. (2020). Trait depressivity prediction with EEG signals via LSBoost. 10.1109/IJCNN48605.2020.9207020.”
- [76] “Alotaiby, T., El-Samie, F.E.A., Alshebeili, S.A. et al. A review of channel selection algorithms for EEG signal processing. EURASIP J. Adv. Signal Process. 2015, 66 (2015). <https://doi.org/10.1186/s13634-015-0251-9>”.
- [77] “Peng, H., Long, F., & Ding, C. (2005). Feature selection based on mutual information: Criteria of max-dependency, max-relevance, and min-redundancy. IEEE Transactions on Pattern Analysis and Machine Intelligence, 27(8), 1226-1238”.
- [78] “Makeig, S., Jung, T. P., Bell, A. J., Ghahremani, D., & Sejnowski, T. J. (1997). Blind separation of auditory event-related brain responses into independent components. Proceedings of the National Academy of Sciences, 94(20), 10979-10984.”.
- [79] “Lotte, Fabien. (2014). A Tutorial on EEG Signal Processing Techniques for Mental State Recognition in Brain-Computer Interfaces. 10.1007/978-1-4471-6584-2_7.”.
- [80] “Y. Renard, F. Lotte, G. Gibert, M. Congedo, E. Maby, V. Delannoy, O. Bertrand, and A. Lécuyer, ‘Openvibe: An open-source software platform to design, test and use brain-computer interfaces in real and virtual environments,’ Presence: teleoperators and virtual environments, vol. 19, no. 1, 2010”.
- [81] “N. Brodu, ‘Multifractal feature vectors for brain-computer interfaces,’ in IJCNN, 2008, pp. 2883–2890.”.
- [82] “Nicolas Brodu, Fabien Lotte, Anatole Lécuyer. Comparative Study of Band-Power Extraction Techniques for Motor Imagery Classification. IEEE Symposium on Computational Intelligence, Cognitive Algorithms, Mind, and Brain (SSCI’2011 CCMB), Apr 2011, Paris, France. pp.1-6, [ff10.1109/CCMB.2011.5952105](https://doi.org/10.1109/CCMB.2011.5952105)[ff. ffinria-00609161](https://doi.org/10.1109/CCMB.2011.5952105)”.
- [83] “Schlögl, A., Kronegg, J., Huggins, J. E., & Mason, S. G. (2007). Evaluation criteria in BCI research. In Toward Brain-Computer Interfacing (1 ed., pp. 327-342). (Neural information processing series). MIT Press.”.
- [84] “J. Wolpaw, H. Ramoser, D. McFarland, and G. Pfurtscheller, ‘Eeg-based communication: improved accuracy by response verification,’ Rehabilitation Engineering, IEEE Transactions on, vol. 6, no. 3, pp. 326–333, 1998”.
- [85] “T. Nykopp, ‘Statistical modeling issues for the adaptive brain interface,’ Department of Electrical and Communications Engineering, Helsinki University of Technology, 2001.”.
- [86] “Allgaier, J.; Pryss, R. Cross-Validation Visualized: A Narrative Guide to Advanced Methods. Mach. Learn. Knowl. Extr. 2024, 6, 1378-1388. <https://doi.org/10.3390/make6020065>”.
- [87] S. Lamberto, *Statistica di base*, publisher: Piccin.
- [88] “Cho, Hohyun & Ahn, Minkyu & Kwon, Moonyoung & Jun, Sung. (2018). A Step-by-Step Tutorial for a Motor Imagery–Based BCI.”.

Acknowledgements

Me doy cuenta de que mi recorrido no ha sido lineal, y había comenzado este trabajo y este Máster con una idea sobre mí mismo, sobre mi visión del mundo y sobre mi futuro bastante distinta de lo que es ahora. Y por mucho que lo haya rechazado, sé el valor que tiene, aunque sea solo por lo que conlleva el cerrar algo, lo que significa poner un punto, el comenzar otra frase. Así que mis primeros agradecimientos van a aquellos que no pueden ver este cierre, alle due persone che mi hanno visto iniziare questo percorso e non sono riuscite a vederne la fine, mio padre e mia nonna.

Mi sono chiesto spesso cosa avrebbe pensato lui delle mie decisioni, di questa mia confusione e di questi miei cambi di direzione; come si immaginava il mio futuro? Forse attraverso il suo sguardo avrei avuto, lungo tutto il percorso, meno paura. Sé que habrías estado orgulloso de mi lucha por encontrarme, por re-encontrarnos todes. No te conocí cuando eras joven, pero te imagino así, como soy yo en este momento exacto de mi vida.

Grazie, nonna, per avermi insegnato, nonostante la tua testardaggine, che la mente non invecchia con gli anni e che l'elasticità dei nostri pensieri può rimanere giovane se ce ne prendiamo cura. Grazie per i momenti di pazza gioia quando ero piccolo.

Se sono riuscito a concludere questo capitolo devo ringraziare soprattutto mia madre e mio fratello. Siete stati due colonne portanti che mi hanno permesso di non perdermi e mi avete insegnato il valore di ciò che chiamiamo casa. Grazie, mamma, perché so che sono ciò che sono principalmente grazie a te. Vedo nelle mie parole e nei miei movimenti la tua luce. Grazie, Giacomo, per esserci sempre. Anche se a volte può sembrare di no, io lo vedo. Sono profondamente orgoglioso di te, e, a volte, ti stimo così tanto che mi sembri tu quello più grande.

Aunque se haya un poco interrumpido la relación en el último periodo, quiero agradecer a mi tío, que ha sido en diversos momentos de mi vida un ejemplo. Me has enseñado mucho. e per questo te ne sarò sempre grato.

Grazie, Amore. Non so da dove iniziare queste frasi dedicate a te. In pochi mesi ho imparato cosa voglia dire amare una donna. Credo che non sia tanto il tempo che scorre a definire l'evoluzione della vita, quanto piuttosto i singoli momenti e le persone che incontriamo. Dire che tu sei stata uno di questi momenti o una di queste persone è riduttivo. Sei stato un uragano che ha smosso ogni mia cellula, che ha girato mille pagine della mia esistenza. Mi hai fatto riosservare tutto da capo, come un racconto che riinizia. Sei l'infinito in un'istante, in ogni istante. Ed è grazie soprattutto a te se sono riuscito a fare questo piccolo sprint finale.

Grazie ad Alessandro, Alessandro, Alessandro e Federico. A voi che mi siete sempre stati vicini. A voi che mi sarete sempre vicini. Siete la mia famiglia non di sangue. Mi avete visto crescere ed evolvere e ci siete sempre stati in ogni momento, in ogni transizione, in ogni cosa bella e brutta... dalle spiagge di Magaluf alle 11 di sera (vorrei dire 4 del mattino, ma non è questo il caso) ai nostri discorsi infiniti davanti ad un Bang. Ho imparato da voi il valore della parola amicizia.

Grazie a Silviu, Alessandro, Alessio e Francesco. Grazie per ogni pezzo di pista graffiato insieme, per ogni vetta scalata, per ogni patatina rubata. Ho imparato da voi l'autenticità del saper sognare. E, anche se non sarò da me in campagna, non vedo l'ora di essere davanti ad un fuoco con voi, un Agricola sul tavolo e un mini Silviu che rincorre un mini Gabri, giocando a chi arriva per primo. E scusatemi se vi ringrazio solo una volta.

Grazie alle mie tarantoline, a Lorena, Marta, Alessandra e Belén. Mi avete dato molto più di quello che potrebbe dare un'amicizia. Mi avete insegnato ben più del teatro; con voi ho davvero compreso il significato della parola cura, individuale e collettiva. Non vedo l'ora di poter continuare a viaggiare, ricercare e a sviscerare il mondo insieme a voi.

Grazie a Lorenzo, a te che mi conosci da sempre e mi ricordi ogni volta l'incanto del giocare. Sei forse l'unica persona con cui riesco ancora a giocare, non come fanno gli adulti, ma per davvero, come quando eravamo piccoli.

Grazie a Fabrizio. Grazie per avermi accompagnato lungo tutto questo percorso politecnico, per essere stato ben più di una spalla su cui disperare o gioire prima di ogni esame e difficoltà. Grazie per non avermi mai fatto sentire solo in mezzo a quelle mura.

Grazie a Paolo e Fra, mi avete insegnato a guardare il mondo in obliquo, a tuffarmi nelle sue sfumature, a perdermi, ad annoiarmi nei suoi silenzi.

Infine, grazie alla professoressa Agostini e all'ing. Ghislieri che mi hanno seguito in questo percorso di tesi. Grazie per la vostra gentilezza e sensibilità. Grazie per la vostra umana professionalità. Grazie per avermi dato la possibilità di inciampare.